Description and phylogenetic relationships of a new species of *Torvoneustes* (Crocodylomorpha, Thalattosuchia) from the Kimmeridgian of Switzerland

Léa C Girard [Corresp., 1, 2] , **Sophie De sousa oliveira** [2] , **Irena Raselli** [1, 3] , **Jeremy E Martin** [4] , **Jérémy Anquetin** [1, 3]

[1] Department of Geosciences, University of Fribourg, Fribourg, Fribourg, Switzerland

[2] Géosciences Rennes, Université Rennes I, Rennes, Bretagne, France

[3] Jurassica Museum, Porrentruy, Jura, Switzerland

[4] Laboratoire de géologie de Lyon, terre, planète, environnement, UMR CNRS 5276 (CNRS, ENS, université Lyon 1), Ecole Normale Supérieure de Lyon, Lyon, Rhône-Alpes, France

Corresponding Author: Léa C Girard
Email address: lea.girard@unifr.ch

Metriorhynchids are marine crocodylomorphs found across Jurassic and Lower Cretaceous deposits of Europe and Central and South America. Despite being one of the oldest fossil families named in paleontology, the phylogenetic relationships within Metriorhynchidae have been subject to many revisions over the past fifteen years. Herein, we describe a new metriorhynchid from the Kimmeridgian of Porrentruy, Switzerland. The material consists of a relatively complete, disarticulated skeleton preserving pieces of the skull, including the frontal, prefrontals, right postorbital, nasals, maxillae, right premaxillae and nearly the entire mandible, and many remains of the axial and appendicular skeleton such as cervical, dorsal, and caudal vertebrae, ribs, the left ischium, the right femur, and the right fibula. This new specimen is referred to the new species *Torvoneustes jurensis* sp. nov. as part of the large-bodied macrophagous tribe Geosaurini. *Torvoneustes jurensis* presents a unique combination of cranial and dental characters including a smooth cranium, a unique frontal shape, acute ziphodont teeth, an enamel ornamentation made of numerous apicobasal ridges shifting to small ridges forming an anastomosed pattern toward the apex of the crown and an enamel ornamentation touching the carina. The description of this new species allows to take a new look at the currently proposed evolutionary trends within the genus *Torvoneustes* and provides new information on the evolution of this clade.

1 Description and phylogenetic relationships of a new
2 species of *Torvoneustes* (Crocodylomorpha,
3 Thalattosuchia) from the Kimmeridgian of Switzerland.

5 Léa C. Girard[1,2], Sophie De sousa oliveira[2], Irena Raselli[3,1], Jeremy E. Martin[4], Jérémy
6 Anquetin[3,1]

8 [1] Department of Geosciences, University of Fribourg, 1700 Fribourg, Switzerland
9 [2] Université de Rennes 1, Rennes 35000, France
10 [3] Jurassica Museum, 2900 Porrentruy, Switzerland
11 [4] Laboratoire de géologie de Lyon, terre, planète, environnement, UMR CNRS 5276 (CNRS,
12 ENS, université Lyon 1), École normale supérieure de Lyon, 69364 Lyon cedex 07, France

14 Corresponding Author:
15 Léa Girard[1,2]
16 Chemin du Musée 6, 1700 Fribourg, Switzerland
17 Email address: lea.girard@unifr.ch

19 Abstract

20 Metriorhynchids are marine crocodylomorphs found across Jurassic and Lower Cretaceous
21 deposits of Europe and Central and South America. Despite being one of the oldest fossil
22 families named in paleontology, the phylogenetic relationships within Metriorhynchidae have
23 been subject to many revisions over the past fifteen years. Herein, we describe a new
24 metriorhynchid from the Kimmeridgian of Porrentruy, Switzerland. The material consists of a
25 relatively complete, disarticulated skeleton preserving pieces of the skull, including the frontal,
26 prefrontals, right postorbital, nasals, maxillae, right premaxillae and nearly the entire mandible,
27 and many remains of the axial and appendicular skeleton such as cervical, dorsal, and caudal
28 vertebrae, ribs, the left ischium, the right femur, and the right fibula. This new specimen is
29 referred to the new species *Torvoneustes jurensis* sp. nov. as part of the large-bodied
30 macrophagous tribe Geosaurini. *Torvoneustes jurensis* presents a unique combination of cranial
31 and dental characters including a smooth cranium, a unique frontal shape, acute ziphodont teeth,
32 an enamel ornamentation made of numerous apicobasal ridges shifting to small ridges forming
33 an anastomosed pattern toward the apex of the crown and an enamel ornamentation touching the
34 carina. The description of this new species allows to take a new look at the currently proposed
35 evolutionary trends within the genus *Torvoneustes* and provides new information on the
36 evolution of this clade.

38 Introduction

39 Thalattosuchia Fraas, 1901 is a clade of mostly marine crocodylomorphs that lived from the
40 Early Jurassic to the Early Cretaceous and had a near global distribution from the eastern
41 margins of the Tethys, the opening Atlantic Ocean, down to the coasts of South America, China
42 and north of Africa (Fraas, 1901, 1902; Andrews, 1913; Gasparini & Iturralde-Vinent, 2001;
43 Fara *et al.*¸2002; Frey *et al.*, 2002; Buchy *et al.*, 2006b; Chiarenza *et al.*, 2015; Herrera *et al.*,
44 2015b; Johnson *et al.*, 2020b; Young *et al.*, 2020a; Wilberg *et al.*, 2022). Thalattosuchians are
45 subdivided into the more coastal Teleosauroidea Geoffroy Saint-Hilaire, 1831, and the fully
46 aquatic Metriorhynchoidea Fitzinger, 1843. Among archosaurs, Metriorhynchidae show many
47 skeletal, soft tissue and neuroanatomical features that suggest they were suited for a pelagic
48 lifestyle, including: limbs transformed into flippers with a great reduction of the forelimbs and a
49 simplification of the pelvic girdle; lengthening of the body; loss of osteoderms; a smooth skin; a
50 hypocercal tail; a slender and lighter skull; hypertrophied salt glands; orbits placed laterally and
51 overhung by the prefrontals; loss of the mandibular fenestra (Fraas, 1902; Andrews, 1913;
52 Vignaud, 1995; Frey *et al.*, 2002; Gandola *et al.*, 2006; Pierce *et al.*, 2009; Young & Andrade,
53 2009; Young *et al.*, 2010, 2020a, 2020b; Herrera *et al.*, 2013a, 2015; Foffa *et al.*, 2018b; Sachs *et
54 al.*, 2021; Spindler *et al.*, 2021; LeMort *et al.*, 2022; Schwab *et al.*, 2022).
55 Metriorhynchids include two subclades. Metriorhynchinae Lydekker, 1889 are usually
56 characterized by a slender body, an elongated snout, and a higher count of poorly ornamented
57 teeth (Parrilla-Bel *et al.*, 2013; Sachs *et al.*, 2021). In contrast, Geosaurinae Lydekker, 1889 are
58 more robust macrophagous predators with shorter snouts and a reduced number of large, often
59 ornamented, ziphodont teeth (Young *et al.*, 2012b, 2015). During the Middle Jurassic, each of
60 these groups saw the emergence of the more derived tribes Rhacheosaurini and Geosaurini,
61 respectively (Young *et al.*, 2013a, 2013b, Foffa & Young, 2014b, Foffa *et al.*, 2017). The
62 diversity of metriorhynchids has long been underestimated, but intensives revisions in the last
63 two decades and the description new material significantly improved the knowledge of the group
64 and its inner phylogenetic relationship (Frey *et al.*, 2002; Wilkinson *et al.*, 2008; Pierce *et al.*,
65 2009; Young & Andrade, 2009; Andrade *et al.*, 2010; Wilberg, 2012; Young *et al.*, 2010, 2020a,
66 2020b; Cau & Fanti, 2011).
67 Compared to their counterparts in England or Germany, the Late Jurassic metriorhynchid fossil
68 record of Switzerland is relatively poor. Most of the fossils of Swiss thalattosuchians belongs to
69 teleosauroids (Krebs, 1967; Guignard & Weidmann, 1977; Rieppel, 1981) with rare occurrence
70 of metriorhynchoids (Schaefer *et al.*, 2018; Abel *et al,* 2020; Young *et al.*, 2020b). In addition to
71 the specimen described herein, several specimens of Thalattosuchia have been excavated in the
72 canton of Jura in the past 20 years. They are mainly represented by isolated teeth, but a few well
73 preserved teleosaurid skulls and skeletons are known (Schaefer, 2012; Schaefer *et al.*, 2018).
74 Unidentified remains of metriorhynchids have been found in the canton of Jura in the form of a
75 nasal, frontal, femur and vertebrae, as well as a single tooth of *Dakosaurus* Quenstedt, 1856
76 (Schaefer *et al.*, 2018). A metriorhynchid anterior rostrum is also known from the lower
77 Tithonian of Bern representing an indeterminate Rhacheosaurini (Rieppel, 1979, Young *et al.*,
78 2020b). Here we describe a new specimen from the upper Kimmeridgian of the canton of Jura,

79 Switzerland (Fig. 1). It consists of a relatively complete, associated skeleton with many cranial
80 and postcranial bones preserved. This specimen is identified herein as a new species of the genus
81 *Torvoneustes* Andrade, *et al*, 2010 and located in the phylogenetic context of Metriorhynchidae.
82 This material also allows a reassessment of the evolutionary trends previously proposed for the
83 genus.
84

Materials & Methods

86 *Material*

87 MJSN BSY008-465 is a disarticulated metriorhynchid skeleton (Fig. 2). The specimen was
88 initially collected by the Pal A16 on a large block of limestone. Bones were prepared directly on
89 the surface and kept on pedestals of rock. This initial phase of preparation, especially the acid
90 preparation, was poorly controlled and resulted in damages of the more fragile bony elements
91 such as some cranial and mandibular elements. More recently, all bones were completely
92 removed from the block to facilitate scientific study. The preserved remains of MJSN BS008-
93 465 include cranial and mandibular elements as well as material from the axial and appendicular
94 skeleton. Many elements are fragmented and show evidence of deformation.
95 The preserved elements of the cranium include the frontal, prefrontals, right postorbital, nasals,
96 maxillae, right premaxillae. The mandible is almost complete and preserve both angulars,
97 surangulars, articulars, splenials, and dentaries. Many isolated teeth are also preserved. The
98 postcranial elements include cervical, dorsal, and caudal vertebrae, ribs, the left ischium, the
99 right femur, and the right fibula. Numerous bone fragments are not identifiable.
100

101 *Geological setting*

102 Between 2000 and 2011, controlled paleontological excavations were conducted by the Pal A16
103 before the construction of the A16 Transjurane highway in the canton of Jura (Fig. 1). They
104 revealed the presence of several rich fossiliferous horizons of marls and limestones, as well as
105 many dinosaurs tracksites in the Ajoie region around the city of Porrentruy (Marty *et al.*, 2003).
106 During the Late Jurassic, this region was part of a carbonate platform with diversified shallow
107 depositional environments such as lagoons, reefs, channels and littoral zones forming layers rich
108 in marine fossils (Colombié & Strasser, 2005; Comment *et al.*, 2015).
109 MJSN BSY008-465 was found in 2008 on the hardground level 4000 of the Lower *Virgula*
110 Marls (Fig. 3) in the locality Courtedoux-Bois de Sylleux, Switzerland (Fig. 1). The Lower
111 *Virgula* Marls belong to the Chevenez Member of the Reuchenette Formation. They date to the
112 late Kimmeridgian and correspond to the end of the *Mutabilis* ammonite zone and beginning of
113 the *Eudoxus* ammonite zone (Comment *et al.*, 2015). These marls are notably characterized by
114 the abundance of the small oyster *Nanogyra virgula* Koppka, 2015, which gives them their
115 name. The hardground level 4000 is rich in invertebrates, notably encrusted and benthic bivalves
116 and brachiopods. Vertebrates are mostly represented by isolated material, with the exception of
117 the metriorhynchid MJSN BSY008-465 described herein, a partial teleosauroid skeleton
118 provisionally referred to *Steneosaurus* cf. *bouchardi* Sauvage, 1872, now combined as

119 *Proexochokefalos* cf. *bouchardi* (Schaefer *et al.*, 2018; Johnson *et al.*, 2020b), and a relatively
120 complete shell of the thalassochelydian turtle *Thalassemys bruntrutana* Puntener, Anquetin, and
121 Billon-Bruyat, 2015 (Püntener *et al.*, 2015).
122
123 *Phylogenetic analyses*
124 The phylogenetic analyses were conducted using the data matrix and procedure of Young *et al.*
125 (2020a), which were derived from Young *et al.* (2020b). The original matrix includes 179 taxa
126 coded for 574 characters. The outgroup is *Batrachotomus kupferzellensi*s Gower, 1999. The
127 matrix was modified with Mesquite 3.61 (Maddison & Maddison, 2019) to include MJSN
128 BSY008-465 as a new operational taxonomic unit (see Supplementary material 1). The latter was
129 scored for 204 characters. The analytical procedure strictly follows the one described by Young
130 *et al.* (2020a). The parsimony analyses were conducted using TNT 1.5 (No taxon limit)
131 (Goloboff *et al.*, 2008; Goloboff & Catalano, 2016) with the RAM increased to 900 Mb. The
132 analysis used the scripts provided by Young *et al.* (2020a) and consisted of an unweighted
133 analysis followed by seven different extended implied weighting analyses (k=1, 3, 7, 10, 15, 20
134 and 50). The main script (EIW.run) runs an initial "new technology" search (xmult:hits 10
135 replications 100 rss css xss fuse 5 gfuse 10 ratchet 20 drift 20; sec:drift 10 rounds 10 fuse 3;
136 ratchet:numsubs 40 nogiveup; drift:numsubs 40 nogiveup) holding 20,000 trees per analysis,
137 then runs a "traditional methods" search (bbreak:TBR) on the saved trees. The script then
138 computes the descriptive statistics, the strict consensus tree, the majority rule consensus tree, and
139 the maximum agreement subtree (for more details, see Young *et al.*, 2020a).
140 The Bayesian analysis was conducted using MrBayes3.2.7 (Ronquist *et al.*, 2012), again
141 following the procedure described by Young *et al.* (2020a). The sampling model is a Markov
142 Chain Monte Carlo with only variable characters scored and a Gama distribution (Mkv+G
143 model). Five independent analyses are run, each with 10 chains for 10 million generations with a
144 sampling every 5000 generations and a burn-in of 40% (for more details, see Young *et al.*,
145 2020a). At the end of the analysis, the consensus tree is saved.
146
147 *Imaging*
148 Each element of the cranium of MJSN BSY008-465 was individually scanned with a portable
149 surface scanner (Artec Space Spider). The scans were treated with the software Artec Studio 13
150 to produce textured 3D models. The elements were assembled in Blender 2.8 in order to
151 reconstruct the skull of MJSN-BSY008-465 in 3D (De Sousa Oliveira *et al.*, in press). This
152 technique helped the description of the specimen and highlighted lost contacts between the
153 bones. The 3D models of each individual element, as well as the reconstructed skull and
154 mandible are made openly available in De Sousa Oliveira *et al.* (in press) and in Supplementary
155 material 2.
156 The microscopic observation and detailed photographs of the teeth of MJSN BSY008-465 were
157 realized with a digital microscope (Keyence VHX-970F).
158

159 *Institutional abbreviations*
160 BSPG, Bayerische Staatssammlung für Paläontologie und Geologie, Munich, Germany;
161 CAMSM, Sedgwick Museum, Cambridge, UK; IGM, Colección Nacional de Paleontología,
162 Instituto de Geología, México, Mexico; MANCH, Manchester Museum, Manchester, UK;
163 NHMUK, Natural History Museum, London, UK; NHMW, Naturhistorisches Museum Wien,
164 Vienna, Austria; MHNG, Muséum d'Histoire Naturelle, Genève, Switzerland; MJML, Museum
165 of Jurassic Marine Life, Dorset, UK; MJSN, Jurassica Museum (formerly Musée Jurassien des
166 Sciences Naturelles), Porrentruy, Switzerland; NKMB, Naturkunde Museum Bamberg,
167 Bamberg, Germany; MUDE, Museo del Desierto, Saltillo, Mexico; OUMNH, Oxford University
168 Museum of Natural History, Oxford, UK; SMNS, Staatliches Museum für Naturkunde Stuttgart,
169 Baden-Württemberg, Germany; YORYM, Yorkshire Museum, York, UK.
170
171 The electronic version of this article in Portable Document Format (PDF) will represent a
172 published work according to the International Commission on Zoological Nomenclature (ICZN),
173 and hence the new names contained in the electronic version are effectively published under that
174 Code from the electronic edition alone. This published work and the nomenclatural acts it
175 contains have been registered in ZooBank, the online registration system for the ICZN. The
176 ZooBank LSIDs (Life Science Identifiers) can be resolved and the associated information viewed
177 through any standard web browser by appending the LSID to the prefix http://zoobank.org/. The
178 LSID for this publication is: act:5DEFCF6F-D7EF-4711-9CB6-A7219F612ECB. The online
179 version of this work is archived and available from the following digital repositories: PeerJ,
180 PubMed Central SCIE and CLOCKSS.
181

Results

183 *Systematic paleontology*
184 CROCODYLOMORPHA Hay, 1930
185 THALATTOSUCHIA Fraas, 1901
186 METRIORHYNCHIDAE Fitzinger, 1843
187 GEOSAURINAE Lydekker, 1889
188 GEOSAURINI Lydekker, 1889
189 *Torvoneustes* Andrade, Young, Desojo & Brusatte, 2010
190
191 Diagnosis. see in Young *et al*., 2013b
192 Type species. *Dakosaurus carpenteri* Wilkinson, Young and Benton., 2008
193 Included valid species. *Torvoneustes coryphaeus* Young, Andrade, Etches and Beatty, 2013b;
194 *Torvoneustes mexicanus* Wieland, 1910; *Torvoneustes jurensis* sp. nov.
195 Occurrence. Kimmeridgian of Mexico (Barrientos-Lara *et al.*, 2016); Kimmeridgian of Dorset,
196 UK (Grange & Benton, 1996; Wilkinson *et al.*, 2008, Young *et al.* 2013b); middle Oxfordian to
197 Tithonian of Oxfordshire, UK (Young, 2014); middle Oxfordian of Yorkshire (Foffa *et al.*,

198   2018a); late Kimmeridgian of canton of Jura, Switzerland (Schaefer *et al.*, 2018); upper
199   Valanginian of Moravian-Silesian Region, Czech Republic (Madzia *et al.*, 2021).
200
201   *Torvoneustes jurensis* sp. nov.
202   urn:lsid:zoobank.org:act:5DEFCF6F-D7EF-4711-9CB6-A7219F612ECB
203   Figs 2 and 4–16
204
205   Diagnosis. *Torvoneustes jurensis* sp. nov. is identified as a member of *Torvoneustes* by the
206   following combination of characters: robust teeth lingually curved, conical crown, bicarinate
207   with a prominent keel; enamel ornamentation made of conspicuous subparallel apico-basal
208   ridges on the basal two thirds of the crown shifting to short, low-relief ridges forming an
209   anastomosed pattern on the apex; carinae formed by a keel and true microscopic denticles
210   forming a continuous row on the distal and mesial carinae; enamel ornamentation extending up
211   to the carinae near the crown apex; inflexion point on the lateral margin of the prefrontals
212   directed posterolaterally in dorsal view, at an angle of approximately 70° from the
213   anteroposterior axis of the skull; acute angle (close to 60°) between the posteromedial and the
214   lateral processes of the frontal. *Torvoneustes jurensis* differs from the other species of
215   *Torvoneustes* by the following combination of characters: presence of a distinct angle between
216   the anteromedial and the lateral processes of the frontal; lack of cranium ornamentation aside
217   from faint ornamentation on the anterior part of the maxilla. *Torvoneustes jurensis* also differs
218   from *To. carpenteri* in: lacking "finger-like" projections on the posterior margin of the
219   prefrontal; having an angle of 142° in average between the anterior and lateral processes of the
220   frontal; and having a long anteromedial process of the frontal reaching the same level as the
221   anterior margin of the prefrontals (shorter process in *To. carpenteri*). *Torvoneustes jurensis* is
222   also clearly distinct from *To. coryphaeus* in having: a tooth enamel ornamentation extending up
223   to the carinae; prefrontals with a rounded distal margin (forming an acute angle in *To.*
224   *coryphaeus*); and a supraorbital notch of 90° (45° in *To. coryphaeus*). The slender morphology,
225   acuteness, and great number of teeth of *Torvoneustes jurensis* nov. sp. differs from both *To.*
226   *coryphaeus* and *To. carpenteri*. *Torvoneustes jurensis* differs from *To. mexicanus* in having
227   irregular denticle basal length (120–200µm, mean: 160µm) and distribution (density up to 40
228   denticles/5mm in the upper middle part of the crown and down to 30 denticles/5mm in the base
229   and apex) on the carinae (regular basal length of 142 µm and density of 30 denticles/5mm in *To.*
230   *mexicanus*).
231   Etymology. The species is named after the Jura, which corresponds to both the mountain range
232   and the Swiss canton where the holotype was found. The complete name could therefore be
233   translated from Latin as "savage swimmer from Jura".
234   Holotype. MJSN BSY008-465, a relatively complete disarticulated skeleton including the
235   frontal, prefrontals, right postorbital, nasals, maxillae, right premaxillae, angulars, surangulars,
236   articulars, splenials, dentaries, several isolated teeth, cervical, dorsal, and caudal vertebrae, ribs,
237   the left ischium, the right femur, and the right fibula (Fig. 2 and Fig. 4–16).

238 Type horizon and locality. Courtedoux-Bois de Sylleux, Ajoie, canton of Jura, Switzerland (Fig.
239 1). Lower *Virgula* Marls, Chevenez Member, Reuchenette Formation, late Kimmeridgian
240 (Eudoxus ammonite zone), Late Jurassic (Fig. 3; Comment *et al.*, 2015).
241
242   **DESCRIPTION**
243
244 **Cranium**
245 Cranial elements are disarticulated except for the frontal preserving its contact with the left
246 prefrontal. The preserved elements of the cranium are exclusively part of the skull roof and
247 snout. Many pieces are broken, incomplete, and/or deformed. As a result, the general shape and
248 size of most of the skull fenestrae and apertures, such as the preorbital fossae, orbits, and
249 supratemporal fenestrae cannot be clearly determined. Based on the skull reconstruction (Fig. 4),
250 the skull total length is estimated at 88 cm, and the rostrum length (nasals and maxillae) is about
251 49 cm (55.7% of the total skull length), corresponding to the mesorostrine condition as defined
252 by Young *et al.* (2010). The skull width-to-length ratio is 0.28. The supratemporal fenestrae are
253 greatly enlarged and the orbits are facing laterally (Fig. 4).
254
255 *Premaxillae*
256 An incomplete right premaxilla is preserved. Its anterior part is severely damaged and the
257 posterior part, including the contact with the maxilla, is missing. The premaxilla seemingly
258 suffered deformation as the location of the alveoli relative to the narial opening seems unnatural,
259 looking more laterally placed than it should. The external nares aperture is partly conserved,
260 oblong, moderate in width and formed entirely by the premaxilla (Fig. 5d, 5e). A complete
261 alveolus, likely P2, is visible in ventral view. In dorsal view, the external surface of the bone is
262 smooth except for a few superficial pits. The bone thickens on the external edge of the narial
263 opening and close to the alveolus, but it thins posteriorly. The alveolar orientation suggests a
264 tooth implantation directed anteroventrally (Fig. 4c).
265
266 *Maxillae*
267 Both maxillae are preserved. The right maxilla is almost complete, only missing its anteriormost
268 part and the posterior end of the tooth row (Fig. 6). This element is heavily fractured and
269 deformed, especially in its anterior part where the bone was broken in several parts and glued
270 back together. This anterior part is deformed as the alveoli show extreme anteroposterior
271 orientation that does not seems natural compared to the alveoli posterior to this major break. The
272 remaining matrix prevents the observation of the medial side of the right maxilla. The left
273 maxilla is incomplete and broken in four parts. Some of the fragments are severely damaged.
274 Both maxillae contact with a posteromedial bone fragment which is probably formed by the
275 palatine. As preserved, the right maxilla is 49.8 cm long. In ventral view, it widens in its
276 posterior region. In lateral and dorsal view, the bone surface is smooth with only pitting
277 ornamentation on its anterior half (Fig. 6). Shallow grooves extend a few millimeters posterior to

278 some of the foramina but are barely visible and can only be spotted on the 3D model (see
279 Supplementary material 2). Most other members of the Geosaurini subclade with known
280 maxillae present conspicuous surface bone ornamentation made of grooves and ridges, often
281 with a unique pattern (Young *et al.*, 2013b). *Plesiosuchus manselii* and *To. coryphaeus* both have
282 maxillae ornamented with grooves and raised ridges, while *Dakosaurus maximus* has additional
283 pits to this ornamentation pattern (Young *et al.*, 2012a; Young *et al.*, 2013b). The incomplete
284 maxilla of cf. *Torvoneustes* (MANCH L6459) shows a similar pattern to *To. coryphaeus* with
285 moderate to strong grooves and a raised edge aligned with the sagittal axis of the skull but lack
286 posteroventral foramina (Young, 2014). *Torvoneustes carpenteri* has a pattern of pits and
287 grooves on the lateral edge of its maxilla (Grange & Benton, 1996; Wilkinson *et al.*, 2008). In
288 contrast, MJSN BSY008-465 has an ornamentation pattern closer to the one seen in *Geosaurus*
289 *giganteus*, or *Purranisaurus potens* (Young & Andrade, 2009; Young *et al.*, 2013b, Herrera *et*
290 *al.*, 2015a).
291 The alveoli are set on a slightly more dorsal plane than the palatal surface of the maxilla. The
292 medial margin of the palatal plate of the right maxilla bears a longitudinal furrow that likely
293 corresponds to the maxillary palatal groove. Each maxilla preserves at least 15 alveoli, which is
294 more than the estimated number of 14 (with 11 strictly preserved alveoli) for *To. carpenteri*
295 (Grange & Benton, 1996; Wilkinson *et al.*, 2008; Young *et al.*, 2013b) and less than the
296 estimated alveolar count of 17-19 for *To. coryphaeus* (Young *et al.*, 2013b). However, there is at
297 least one or two missing alveoli on MJSN BSY008-465 considering the dentary alveolar count.
298 None of the specimens referred to the genus *Torvoneustes* preserves a complete maxilla,
299 therefore this character should be treated carefully (see Discussion). Among derived Geosaurini,
300 maxillary alveolar count is usually estimated to be lower than 16 (Table 1; Wilkinson *et al.*,
301 2008; Young & Andrade, 2009; Young *et al.*, 2012b). The alveoli are large, overall
302 homogeneous in size, slightly anteriorly oriented and subcircular with a slightly longer
303 anteroposterior axis than their mediolateral axis, which differentiates MJSN BSY008-465 from
304 the members of the informal 'E-clade' taxa whose members show the opposite condition with
305 alveoli wider than long (Abel *et al.*, 2020). The interalveolar space is homogeneously narrow,
306 being less than a quarter the length of the adjacent alveoli. Tooth enlargement and interalveolar
307 space reduction are characteristics shared among several members of the Geosaurini subclade
308 (Herrera *et al.*, 2015b) like *Dakosaurus, Plesiosuchus* (Young *et al.*, 2012b), *P. potens* (Herrera
309 *et al.*, 2015a) some members of the 'E-clade' (Abel *et al.*, 2020) and *Torvoneustes* (Grange &
310 Benton, 1996; Wilkinson *et al.*, 2008; Young *et al.*, 2013b; Young, 2014). The maxillary sutural
311 surfaces with the nasal and premaxilla are visible in lateral and dorsal views. In medial view, the
312 maxilla is concave to accommodate the nasal cavity and thicker around the tooth row. A notch
313 between the 5th and 6th alveoli (Fig. 6a) on the right maxilla is a reception pit but is the only one
314 on the fossil and therefore does not support a tooth-on-tooth vertical interlocking as seen in
315 *Dakosaurus* (Young *et al.*, 2012a) or *Tyrannoneustes lythrodectikos* (Foffa & Young, 2014). In
316 addition, there is no evidence for a maxillary overbite as seen in *Geosaurus giganteus* (Young &

317   Andrade, 2009). It is likely that the tooth occlusion of MJSN BSY008-465 follows the same
318   interdigitated pattern as in *To. mexicanus* (Barrientos-Lara *et al.*, 2016).
319
320   *Nasal*
321   Both nasals are present as symmetrical, unfused elements (Fig 5a, 5b). The right nasal is the best
322   preserved, most complete and less deformed of the two. The nasals are flattened by taphonomy,
323   the left one more so than the right one. The anterior process of the right nasal is curved upward
324   due to postmortem deformation. The posterior part of the right nasal has been fractured then
325   glued back but is not perfectly aligned. This same part is lost in the left nasal. The anterior part
326   of the left nasal is broken and bent laterally. The bone surface is smooth. Only a few elliptical
327   pits are present along the anterolateral parts (Fig. 5a, 5b). This ornamentation pattern differs
328   from the one seen in *To. coryphaeus* (Young *et al.*, 2013b), *Pl. manselii, D. maximus* (Young *et*
329   *al.*, 2012b), and cf. *Torvoneustes* (MANCH L6459) (Young, 2014). However, it is consistent
330   with other species of Geosaurini with smooth and pitted nasals such as *To. carpenteri* (Grange
331   and Benton, 1996), *G. grandis, G. giganteus* (Young & Andrade, 2009), and *Dakosaurus*
332   *andiniensis* (Pol & Gasparini, 2009). The end of the dorsoposterior process, which should
333   contact the lacrimal, is lost in both nasals. Overall, the nasals are triangular in shape, with the
334   anterior part being elongate and acute. This shape is found in most metriorhynchoids (Andrews,
335   1913; Lepage *et al.*, 2008) including rhacheosaurines such as *Cricosaurus* Wagner, 1858 (Fraas,
336   1902.; Herrera et al., 2013; Parrilla-Bel & Canudo, 2015, Sachs *et al.*, 2019; 2021), derived
337   geosaurins like *Dakosaurus, Plesiosuchus, Torvoneustes, Purranisaurus* (Wilkinson *et al.*, 2008;
338   Pol & Gasparini, 2009; Young *et al.*, 2012b, 2013b; Herrera et al., 2015a) and basal
339   metriorhynchoid such as *Pelagosaurus typus* Bronn, 1841 (Pierce & Benton, 2010). Based on the
340   skull reconstruction (Fig. 4), the nasals do not reach the premaxillae anteriorly. The
341   posteromedial, posterolateral, and anterolateral sutural surfaces of the nasal with the frontal, the
342   prefrontal, and the maxilla, respectively, are well preserved. On the median edge, a subtle angle
343   marks the limit between the nasal-frontal and the median nasal sutures. The two nasals would
344   contact on the midline of the skull, the medial concavity of the nasals in dorsal aspect suggests
345   the presence of the longitudinal depression at their contact, a metriorhynchoid apomorphy
346   (Young *et al.*, 2012).
347
348   *Prefrontal*
349   Both prefrontals are preserved, but the anterior parts and the descending processes are missing.
350   The left prefrontal is still connected with the frontal (Fig. 7) while the right one is found apart
351   (Fig. 5c). The right prefrontal seemingly suffered more damage than the left one, with the bone
352   surface being partially flaked off and the bone flattened and stretched. It has also been broken
353   and glued back together. The left prefrontal shows little deformation but is raised in its anterior
354   part above the level of the frontal during taphonomy. The posterior part of the descending
355   process on both prefrontals is barely preserved as a thin, concave structure. In dorsal view, the
356   prefrontal is large, laterally extended, and it partially overhangs the orbit (Fig. 4a), a feature

357 common within Metriorhynchidae (Fraas, 1902; Andrews, 1913; Herrera *et al.*, 2015a; Young *et*
358 *al.*, 2010). The bone surface is smooth with numerous round or elliptical pits, as in *P. potens*
359 (Herrera *et al.*, 2015a), more densely distributed on the anteromedial part (Fig. 5c, 7). As in most
360 metriorhynchids, the posterolateral corner of the prefrontal is rounded in MJSN BSY008-465
361 (Andrews, 1913; Lepage *et al.*, 2008), which differs from the geosaurines *To. coryphaeus*
362 (Young *et al.*, 2013b) and *D. maximus* (Young *et al.*, 2012a, Pol & Gasparini, 2009) in which the
363 posterolateral corner is angular. The inflection point of this corner is directed posteriorly and
364 forms with the midline of the skull an angle of about 70°, which is found in other Geosaurinae
365 such as *To. carpenteri, D. maximus* and *D. andiniensis*. A posteriorly directed inflection point of
366 the prefrontal of 70° or less is an apomorphy of the tribe Geosaurini (Cau & Fanti, 2011). If they
367 share a similar shape, the posterior edge of the prefrontals in MJSN BSY0008-465 lacks the
368 "finger-like" projections described in *To. carpenteri* (Young *et al.*, 2013b).
369
370 *Frontal*
371 The frontal is mostly complete but somewhat flattened during taphonomy (Fig. 7). It consists of
372 a single unpaired element without external sign of a medial suture. Only the anterior most part of
373 the anteromedial process and portions of both intratemporal flanges are missing. The
374 medioventral part of the left lateral process is extended in posteromedial direction (Fig. 7).
375 Remaining matrix prevents the observation of the ventral side of the frontal. The anteromedial
376 process of the frontal is broad, triangular in shape and extends anteriorly between the nasals.
377 Considering the nasals geometry and preserved sutural contacts (Fig. 4), it is likely that the
378 anterior process of the frontal ended in an acute tip, almost reaching the level of the anterior
379 margin of the prefrontals as seen in cf. *Torvoneustes* (MANCH L6459) and *To. coryphaeus*
380 (Young *et al.*, 2013b; Young, 2014). This differs from the shorter process of *To. carpenteri*
381 (Grange & Benton, 1996; Wilkinson *et al.*, 2008), but the crushing of the specimen might
382 prevent an unbiased assessment of this character. Posteriorly, the frontal has two posterolateral
383 processes forming the anterior margin of each supratemporal fenestrae, and a posteromedial
384 process forming the anterior part of the intertemporal bar. The opening between the posterior and
385 the lateral processes form an angle of approximately 60°, which is commonly found among
386 geosaurines whereas metriorhynchines typically show an angle of about 90° (Wilkinson *et al.*,
387 2008). The posterior process is straight with a constant width of 23 mm and contact the parietal,
388 forming a M-shaped, strongly digitated suture (Fig. 7). The intratemporal flanges (*sensu* Buchy,
389 2008) extend ventrally from the posterior and lateral processes. They form a triangular area with
390 faint pitting inside the anterior corner of the supratemporal fenestrae. The anterior outline of the
391 supratemporal fossa suggests that it was longer than wide and ovoid in shape, which is a
392 common feature among geosaurines (Buchy, 2008). The supratemporal fenestrae extend far
393 anteriorly and almost reach the level of the interorbital minimal distance (Fig. 7). This condition
394 is seen in both *To. carpenteri* and *To. coryphaeus* as well as within *G. grandis* (Foffa and Young,
395 2014, fig. 9). In dorsal view, the external surface of the frontal is smooth with occasional pitting
396 on the center of the bone, mostly concentrated on the anterior part of the posterior process. This

397   differs from the ornamented frontal of *To. coryphaeus* (Young *et al.*, 2013b), as well as from the
398   anteroposteriorly aligned grooves and ridges observed in the frontal of cf. *Torvoneustes*
399   (MANCH L6459; Young, 2014). In contrast, it resembles the description of *To. carpenteri*
400   (Grange & Benton, 1996; Wilkinson *et al.*, 2008). In *To. carpenteri* and *To. coryphaeus,* the
401   anterior and lateral processes of the frontal form an almost straight line or a slight concavity
402   (Young *et al.*, 2013b), whereas in MJSN BSY008-465 there is a clear angle of 142° between the
403   processes, measured on the better preserved left side (Fig. 7b). The inflection point is probably
404   located at the meeting point between the frontal, nasal and prefrontal.
405
406   *Postorbital*
407   Only the part forming the anterolateral margin of the supratemporal fossa of the right postorbital
408   is preserved (Fig. 8a-c). It is broken around its middle and was glued back together. The
409   ventrolateral part, which should make a major contribution to the postorbital bar, is missing. The
410   posterior portion of the postorbital curves slightly laterally but this is probably the result of
411   postmortem deformation. Two processes are distinguishable on what is preserved of the
412   postorbital. The anterior process is anteromedially oriented in dorsal view, making most of the
413   curve of the lateral edge of the supratemporal fossa, and was in contact with the posterolateral
414   process of the frontal. The posterior process is almost straight, slightly posteromedially oriented,
415   and was in contact with the squamosal. The contact with the lateral process of the frontal is V-
416   shaped, as described in several other metriorhynchids like *Ty. lithrodectikos* (Andrews, 1913;
417   Foffa and Young, 2014). In the posterior part, the postorbital becomes a thin raised ridge that
418   forms the anterior part of the postorbital-squamosal ridge. Posteriorly, the postorbital-squamosal
419   suture is not readily visible but a change in the bone texture on the medial surface of the bone
420   could match with a similar change on the anterior part of the right squamosal. In medial view, a
421   deep incision in the postorbital marks the contact with the frontal (Fig. 8b), which agrees with
422   observations made on complete skulls of other Metriorhynchidae (Andrews, 1913; Young *et al.*,
423   2013b). This contact marks the point where the postorbital extends medioventrally to take part in
424   the intratemporal flange. Based on the skull reconstruction, the postorbital likely extended
425   further laterally than the prefrontal, resulting in an enlarged supratemporal fossa as usually seen
426   in metriorhynchids (Wilkinson *et al.*, 2008; Foffa & Young, 2014). The bone surface is
427   unornamented except for one elliptical foramen on the anterior process. There might be another
428   foramen at the corner of the "V-shaped" suture but it is hard to discern due to poor bone
429   preservation.
430
431   *Squamosal*
432   Both squamosals are present but only their dorsal portion is preserved. The descending process,
433   which participated to the occipital region, is lost. The right squamosal is the better preserved than
434   the left. In dorsal view, the medial part of the right squamosal is concave (Fig 8f), forming a
435   characteristic "L-shape" (Andrews, 1913; Foffa & Young, 2014; Pol & Gasparini, 2009). The
436   anterior part was in contact with the postorbital. This suture is not readily visible, but a change in

437 bone texture could match with the one seen on the postorbital (see above). A marked ridge
438 separates the squamosal in a medial and a lateral half. This ridge forms the posterior part of the
439 postorbital-squamosal ridge, whose postorbital-squamosal contact would be an area of muscle
440 attachment (Holliday & Witmer, 2007, 2009; Young *et al.*, 2013b). This ridge is present in all
441 Metriorhynchidae but significantly lower among Metriorhynchinae compared to Geosaurinae
442 (Andrews, 1913; Lepage *et al.*, 2008; Pol & Gasparini, 2009; Young *et al.*, 2012b; 2013b; Young
443 & Andrade, 2009). The median process of the squamosal forms the posterolateral corner of the
444 supratemporal fossa and was probably in contact with the lateral process of the parietal, this
445 contact however is not preserved. The posterior edge of the lateral process curves slightly
446 upwards. The lateral part if the squamosal is a vertical descending surface forming the squamosal
447 flat surface. This structure has been described in many metriorhynchids (Pol & Gasparini, 2009;
448 Herrera *et al.*, 2013, 2015a; Parrilla-Bel *et al.*, 2013) and is not as well expressed as the one
449 described for *To. coryphaeus* (Young *et al.*, 2013b) but does resemble the one seen in *D.*
450 *andiniensis* and *Cricosaurus araucaniensis* (Pol & Gasparini, 2009). There is a foramen in the
451 middle of the squamosal on both medial and lateral sides. In ventral view, the squamosal
452 presents several concavities, identical on both elements that may correspond to portions of the
453 cranioquadrate canal and otic aperture, but they cannot be identified with certainty due to poor
454 preservation.
455
456 *Parietal*
457 The parietal is a single unpaired element, as usual in crocodylomorphs (Fig. 8d, 8e; Pol &
458 Gasparini, 2009; Leardi *et al.*, 2017). The medial part of the parietal is well preserved, whereas
459 its lateral processes are lost. Like the squamosal, only the dorsal part is preserved. The parts that
460 should connect ventrally with the prootic and the laterosphenoid are missing. Upon discovery,
461 the parietal and frontal were still articulated with one another (Fig. 2), but this contact was lost
462 during extraction and preparation. Anteriorly, the parietal is of equal width with the posterior
463 process of the frontal. It then gradually narrows posteriorly to an extreme degree until it only
464 appears as a raised sagittal ridge (Fig. 4, 8e). This narrowing is more pronounced in MJSN
465 BSY008-465 than in *To. coryphaeus* (Young *et al.*, 2013b) and is at least as strong as in *To.*
466 *carpenteri* (Grange & Benton, 1996), if not more. The anterior process of the parietal forms the
467 posterior part of the intertemporal bar. Ventrally, the parietal widens to form the posteromedial
468 corner of the supratemporal fossae. When complete, the parietal would be "T-shaped" in dorsal
469 view with widely extended lateral processes as in other metriorhynchids (Andrews, 1913; Young
470 *et al.* 2013b; LeMort *et al.*, 2022). In lateral view, the anterior process of the parietal slopes
471 down posteriorly, starting from the point where the ridge is thinnest. From this point, the ridge
472 widens again and forms a triangular area facing dorsally as in other Metriorhynchidae (Herrera *et*
473 *al.*, 2015a). The contact with the supraoccipital is not preserved. In ventral view, the posterior
474 part of the parietal is hollow and has one or two foramina on its deepest point.
475
476 **Mandible**

477   Both mandibular rami are preserved (Fig. 4b). They are relatively complete, but some parts are
478   fractured, eroded, and deformed. Some elements of the mandible are not articulated anymore.
479   The mandible is represented by several main parts: two ensembles made of the angular,
480   surangular, articular and prearticular; the disarticulated splenials; and the dentaries (preserved in
481   several pieces). The coronoids are lost. The notable absence of a mandibular fenestra is an
482   apomorphy of the Metriorhynchidae (Fraas, 1902; Andrews, 1913; Vignaud, 1995; Young *et al.*,
483   2010). The total length of the mandible is about 815 mm with the anterior end missing. The
484   general shape of the mandible is similar to the one described for *Ty. lythrodectikos* and
485   Geosaurini with the coronoid process located higher than the plan of the tooth row and lower
486   than the retroarticular process, indicating an increase in gape (Young *et al.*, 2012a, 2012b, 2013a,
487   Foffa & Young 2014).
488
489   *Dentary*
490   Both dentaries are preserved but not equally well. The left dentary is almost complete but broken
491   into three parts (Fig. 9), only missing its anteriormost portion. The right dentary is broken into
492   two pieces but is highly damaged and deformed. Its ventral and medial parts are completely lost,
493   whereas the posterior part is crushed and deformed. The latter now lies more dorsally and
494   medially compared to the anterior part. The damages are partly due to taphonomic conditions,
495   but also to the poorly controlled acid treatment of the fossil. The left dentary is about 45 cm long,
496   4.5 cm high and 2.6 cm wide. The right dentary preserves two teeth, including one on its most
497   deformed part with the alveolus deformed and projected inward (Fig. 4b). The left dentary
498   preserves one tooth in the middle of the rostrum (Fig. 9). In dorsal view, the dentary is a long and
499   thick bone. It narrows posteriorly where it was in contact with the angular and surangular. The
500   dentary widens anteriorly starting from the posteriormost alveolus, which is smaller than the one
501   immediately in front. The anterior part of the dentary, including the three anteriormost visible
502   alveoli, shortly curves inward, this bending of the dentary seems natural. There are at least 16
503   clearly identifiable alveoli, potentially 17, that are overall homogeneous in size. The alveoli are
504   enlarged, subcircular, and slightly longer than wide. The three anteriormost alveoli are larger
505   than the others and lie slightly more dorsally. Overall, the more anterior are the alveoli the more
506   anterodorsally they are oriented. The remaining tooth on the left dentary is anterodorsally
507   directed while the one on the undeformed part of the right dentary is dorsally oriented. As in the
508   maxillae, the interalveolar space is uniform and greatly reduced, being less than half of the
509   anteroposterior length of the adjacent alveoli (see above). In lateral view, the lateral margin of
510   the alveoli lies slightly lower than the medial margin except for the three anteriormost alveoli
511   where the lateral and medial margins are on the same plane (Fig. 9b, d). The surangular-dentary
512   groove is visible (Fig, 9b), and does not end anteriorly with an enlarged foramen as it does in
513   *Dakosaurus* (Pol & Gasparini, 2009). A pitting pattern is present on the lateral and ventral
514   surfaces of the dentaries. However, there is no heavy grooving as described in *To. carpenteri*
515   (Wilkinson *et al.*, 2008). At least eight alveoli are adjacent to the symphysis. This count is higher
516   than the four observed in *Dakosaurus maximus* (Young *et al.*, 2012b) but close to estimated

517   height in the indeterminate Geosaurini (SMNS 80149) from the informal E-clade (Abel *et al.*,
518   2020; Young *et al.*, 2020a) and *Geosaurus* (Young *et al.*, 2012b); as well as the nine of *Pl.*
519   *manselii* (Young *et al.*, 2012b), but lower than the 10-13 of the early Geosaurini *Ty.*
520   *lythrodectikos* (Young *et al.*, 2013a; Waskow *et al.*, 2018). No reception pits for maxillary teeth
521   are observed on the dentaries, indicating that there was no overbite creating a scissor-like
522   occlusion mechanism like in *G. giganteus* nor any tooth-on-tooth interlocking as seen in *D.*
523   *maximus* (Young *et al.*, 2012a; Young & Andrade, 2009).
524
525   *Splenial*
526   The left splenial is better preserved than the right one. The two splenials have been flattened and
527   both their anterior and posterior ends are broken off. The left splenial is about 37 cm long. In
528   dorsal view, each splenial is narrow on its anterior and posterior ends and thicker in the middle.
529   The lateral edge is straight, but the medial edge is slightly convex (Fig. 10c). The lateral aspect
530   of the splenial is overall concave, with raised ridges forming the sutural contacts with the angular
531   and dentary ventrally, and with the dentary and surangular dorsally (Fig. 10a). Anteriorly, the
532   splenial likely reaches the fifth or sixth alveoli, but this observation might be obscured by the
533   poor preservation of the specimen in this area. In *Pl. manselii* (Young *et al.*, 2012b), the splenial
534   anteriorly reaches alveoli six anteriorly and alveoli seven or eight in *Ty. lythrodectikos* (Foffa &
535   Young, 2014; Waskow *et al.*, 2018) and in Rhacheosaurini such as *Cricosaurus bambergensis* or
536   *C. albersdoerferi* it is clearly posterior to the 10th alveoli (Sachs *et al.*, 2019, 2021; LCG,
537   pers.obs). The medial surface of the splenial is slightly convex. The ventral edge of the bone is
538   thicker and participates to the ventral edge of the mandible itself. The bone surface is smooth. On
539   the medial surface, a foramen is visible posterior to the thickened part of the bone. The splenials
540   would contact one another along the symphysis and the remains of the contact is visible on the
541   anterior third of the splenial, marked by a rougher surface of the bone (Fig. 10b, 10d).
542
543   *Angular and surangular*
544   The angular and surangular are preserved on both sides. They are missing their anterior part and
545   show signs of crushing, erosion, and deformation, especially on the left mandibular ramus. The
546   angular and surangular are strongly sutured along their entire length. They respectively form the
547   ventral and dorsal halves of the posterior part of the mandibular ramus (Fig. 11). In lateral view,
548   the surangular-dentary groove is well expressed. This groove is present in all Metriorhynchidae,
549   albeit not always visible due to deformation, and it is especially deep in the members of the
550   Geosaurini tribe (Pol & Gasparini, 2009; Young & Andrade, 2009; Young *et al.*, 2012b, 2013b).
551   This groove is associated with the passage of the mandibular nerve (Holliday and Witmer, 2007;
552   Young & Andrade, 2009; George & Holliday, 2013) and its posterior end is marked by a
553   foramen. Two other smaller foramina, more or less aligned with the one on the surangular-
554   dentary groove, are found on the posterior part of the surangular, following the upward curve of
555   the bone. The dorsal margin of the surangular rises slightly posteriorly before sloping down after
556   reaching the coronoid process. The coronoid process is located on the anterodorsal half of the

557 surangular. The coronoid process is higher than the tooth row, but lower than the retroarticular
558 process. In dorsal view, the coronoid process narrows posteriorly and forms a ridge. In medial
559 view, the surangular medial ridge for the coronoid is visible. The medial surface of the angular
560 and surangular is concave, especially on their anterior part where they would form the lateral
561 wall of the Meckelian groove and contact the splenial and the coronoid. The large foramen that
562 connects with the surangular-dentary groove in the lateral surface of the ramus is present below
563 the coronoid process. The angular is thicker than the surangular and forms the ventral margin of
564 the mandible. The posterior part of the angular curves upward towards the retroarticular process
565 at an angle of approximately 30° with the ventral surface of the angular. Posteriorly, the angular
566 extends beyond and rises higher than the glenoid fossa to form the ventral part of the
567 retroarticular process as on other Geosaurini (Young *et al.*, 2012b; Herrera *et al.*, 2015).
568
569 *Prearticular*
570 Only the right prearticular is well preserved. The prearticular is absent in many crocodylomorphs
571 (Iordansky, 1973; Ruebenstahl *et al*., 2022) but is present in metriorhynchoids as well as in a few
572 teleosaurids such as *Machimosaurus* (Andrews, 1913; Martin & Vincent, 2013; Young *et al.*,
573 2014a; Martin *et al.*, 2015) Its presence is therefore considered a symplesiomorphy of
574 Thalattosuchia (Andrews, 1913; Martin *et al.*, 2015). The prearticular is a triangular-shaped bone
575 only visible in medial view of the ramus (Fig. 11a, 11b). It contacts the angular ventrally, the
576 surangular laterally, and the articular posterodorsally.
577
578 *Articular*
579 The articular is well preserved only on the right mandibular ramus. It contacts the prearticular
580 anteroventrally, the angular posteroventrally, and the surangular laterally. The articular projects
581 far medially. The glenoid fossa, which accommodates the articular condyle of the quadrate, is
582 deep and rounded, and is oriented anterodorsally. The glenoid fossa is divided in two concavities
583 by a low ridge similar to the condition in *To. coryphaeus* and *Ty. lithrodectikos* (*Young et al.*,
584 2013b; Foffa & Young, 2014) but different to what is seen in *Pl. manselii* where there is no
585 separation (Young *et al.*, 2012b). The glenoid fossa is separated from the retroarticular process
586 by a raised ridge similar to the one seen in *To. coryphaeus, Ty lithrodectikos* or
587 "*Metriorhynchus*" *brachyrhynchus* which forms "ridge-and-concavity" morphology to
588 accommodate the "sulcus-and-condyle" of the quadrate (Andrews, 1913; Young *et al.*, 2012b,
589 2013b; Foffa & Young, 2014). The dorsal surface of the retroarticular process is a triangular
590 smooth posterodorsally oriented concavity, which curves medially in dorsal view. The
591 retroarticular process extends laterally beyond the glenoid fossa and slopes downward in medial
592 view. The medial end of the bone is a rugose surface. This overall matches the usual
593 metriorhynchid condition (Andrews, 1913; Young *et al.*, 2012b, 2013b; Foffa & Young, 2014).
594 The tip of the retroarticular process is broken off, but it would rise higher than the rest of the
595 articular.
596

597 **Dentition**
598 At least fifteen isolated teeth were found closely associated with the skeleton MJSN BSY008-
599 465. Nine of these isolated teeth are complete, or almost complete, and preserve both the crown
600 and the root. Three additional teeth are still in place on the dentaries and two more on the left
601 maxilla (see above).
602
603 *Teeth*
604 Based on macroscopic observation, the teeth correspond to the typical metriorhynchid
605 morphology. They are caniniform, conical, and single-cusped (Massare, 1987; Vignaud, 1997).
606 The teeth are large, robust and bicarinate with the carinae on the anteroposterior axis running
607 continuously from the crown base to the apex. There is no basal constriction of the crown, but
608 the crown-root junction is clearly visible from color and texture (Fig. 12). The length of each
609 tooth roots is at least twice the height of each crown. In cross section, the base of the crown is
610 sub-circular to ovoid with the labial face thicker than the lingual one. The tooth roots are ovoid
611 in cross-section. Closer to the apex, the mediolateral compression of the teeth is increasing. Most
612 tooth crowns are over 20 mm high, but the tooth height is not uniform. The average crown height
613 is 21.94 mm with a standard deviation of 4.38. These measures includes all of the 15 teeth. It is
614 to be noted that some of them have their apex broken but not enough to significantly affect the
615 crown height. The shortest tooth crown is 13.23 mm high and the highest is 29.28 mm. The
616 average width at the tooth base is 10 mm (standard deviation 0.9) for a length of 11.36 in average
617 (standard deviation 0.87). The average difference between the width and the length is 1.36 mm
618 (standard deviation 0.93), but the minimal value is 0.3 mm and the maximal value is 3.67 mm
619 with no correlation to the crown height. The teeth are curved lingually and posteriorly. The
620 morphology of the alveoli and the teeth still in place, especially the anterior ones, indicate that
621 teeth were implanted slightly forward in the jaws. Crowns are heavily ornamented with long
622 longitudinal subparallel ridges on at least the basal two thirds of the crown. Ridges are denser on
623 the lingual face than on the labial one. On the apex, the ornamentation becomes low, short ridges
624 forming an anastomosed pattern of drop-shaped ornaments (Figs. 12, 13). This distinctive
625 ornamentation pattern has only been described in other *Torvoneustes* species (Andrade *et al.*,
626 2010; Young *et al.*, 2013b; Barrientos-Lara *et al.*, 2016; Foffa *et al.*, 2018a, Young *et al.*, 2019;)
627 as well as in the machimosaurids *Machimosaurus* von Meyer, 1837 and *Lemmysuchus*
628 *obtusidens* Andrews, 1909 (Johnson *et al.*, 2017). As seen in *To. carpenteri, To. mexicanus* and
629 isolated *Torvoneustes* teeth (Andrade *et al.*, 2010; Young *et al.*, 2013b, 2014, 2019; Barrientos-
630 Lara *et al.*, 2016; Foffa *et al.*, 2018a; Madzia *et al.*, 2021) , the enamel ridges on the upper part
631 of the teeth shift and bend toward the carinae. The carina is well developed, as in other
632 *Torvoneustes* specimens. The developed keel and the shift of enamel ridges toward the carinae
633 are both autapomorphies of *Torvoneustes* (Andrade *et al.*, 2010; Young *et al.*, 2013b, 2014,
634 2019; Barrientos-Lara *et al.*, 2016; Foffa *et al.*, 2018a; Madzia *et al.*, 2021). On the basal two
635 thirds of the crown, the carinae are serrated with no involvement of the enamel ornamentation.
636 On the apical third of the crown, there is a clear shift in the enamel ornamentation pattern, and

637 the enamel ridges bend toward the carinae and touch the serrated keel (Fig. 13a). The serration is
638 present from the base of the carinae to the apex and is high, especially on the apical half of the
639 crown. Both of these features are also found in *Torvoneustes* (Andrade *et al.*, 2010; Young *et al.*,
640 2013b, 2014, 2019; Barrientos-Lara *et al.*, 2016; Foffa *et al.*, 2018a; Madzia *et al.*, 2021). The
641 serration is only faintly visible on macroscopic observation. The tooth apex is sharp, similar to
642 what is described for *Torvoneustes mexicanus* and different from the blunter tooth tips of *To.*
643 *carpenteri*, *To. coryphaeus* and *Torvoneustes* teeth from the UK (Wilkinson *et al.*, 2008;
644 Andrade *et al.*, 2010; Young *et al.*, 2013b, 2019; Barrientos-Lara *et al.*, 2016; Foffa *et al.* 2018a;
645 Madzia *et al.*, 2021). In an unpublished work on isolated thalattosuchian teeth from the Pal A16
646 collection, Schaefer (2012) already noted the resemblance of the teeth of MJSN BSY008-465
647 with the ones of *To. carpenteri*, while pointing out the greater sharpness of the former.
648 Observed with optic aids, the serration of the carinae is formed by a continuous row of poorly
649 isomorphic, isolated denticles weakly affecting the keel height (poorly developed incipient
650 denticles). This serration corresponds to the microziphodont condition as defined by Andrade *et*
651 *al.* (2010) with the denticles all smaller than 300 μm in height and length. The denticles base
652 length varies between 120 and 200 μm with an average of 160 μm (Fig. 13), differing from the
653 regular and 142-μm-long (average) denticles of *To. mexicanus* (Barrientos-Lara *et al.*, 2016;
654 Table 1). The denticle density (number of denticles/5mm, following Andrade *et al.*, 2010) ranges
655 from 31 to 40 depending on the area on the teeth with an average of 35, which is higher than the
656 average measured on *To. mexicanus* (Barrientos-Lara *et al.*, 2016) and *G. grandis*, but
657 corresponds to the number found on *Geosaurus* indet. (SMNS 81834; Andrade *et al.*, 2010;
658 Table 1). The denticle density increases in the middle of the tooth crown and decreases at the
659 apex, making the denticles more densely packed and narrower on the part where the carina is the
660 highest. At the apex, the enamel ornamentation joins the carina (Fig. 13a, 13b), similar to the
661 condition in *To. carpenteri* and *To. mexicanus* (Andrade *et al.*, 2010; Barrientos-Lara *et al.*,
662 2016) and contrary to what is observed in *To. coryphaeus* (Young *et al.*, 2013b; Foffa *et al.*,
663 2017). The denticles are harder to discern in this region. This false-ziphodont condition (Prasad
664 & de Lapparent de Broin, 2002) is found in *Torvoneustes* but also in *Machimosaurus* (Andrade
665 *et al.*, 2010; Young *et al.*, 2014b). However, the combination of true and false ziphodonty, as
666 defined by Andrade *et al.*, 2010, is only known in *To. carpenteri, To. mexicanus,* and
667 *Torvoneustes* sp. (OUMNH J.50061 and OUMNH J.50079-J.50085; Young *et al.*, 2013b, 2019;
668 Barrientos-Lara *et al.*, 2016). The base of the carina around the upper middle of the tooth shows
669 structures resembling the "inflated base" seen in *To. carpenteri* (Fig. 13b; Andrade *et al.*, 2010).
670 MJSN BSY008-465 does not present the faceted teeth of *Ieldraan* and *Geosaurus* (Young *et al.*,
671 2013a; Foffa *et al.*, 2017), nor the macroscopic denticles of *Dakosaurus* (Andrade *et al.*, 2010;
672 Pol & Gasparini, 2009), nor the characteristic flanges on the side of the carinae seen in
673 *Plesiosuchus* (Owen, 1883; Young *et al.*, 2012b; Table 1).
674
675 *Tooth count*

676   The holotype of *To. carpenteri* (BRSMG Ce17365) is the only other specimen referred to
677   *Torvoneustes* that has a maxilla as complete as MJSN BSY008-465 (Grange & Benton, 1996;
678   Wilkinson *et al.*, 2008). The paratype of *To. carpenteri* (BRSMG Cd7203) preserves a dentary,
679   yet just a few fragments and not a complete piece, in contrast to MJSN BSY008-465. On the
680   right maxilla of MJSN BSY008-465, there are at least 15 preserved alveoli (13 on the left one)
681   while there are at least 16 to 17 alveoli on the left dentary and possibly 17 alveoli on the more
682   poorly preserved right dentary. The dentary tooth count is usually lower than the maxillary
683   count. This might indicate at the very least one to two missing alveoli on the right maxilla.
684   Metriorhynchids bear three teeth on the premaxilla (Andrews, 1913; Wilkinson *et a*l., 2008;
685   Young & Andrade, 2009). Therefore, this would indicate a dental formula for MJSN BSY008-
686   465 of three premaxillae teeth, 16 to 18 maxillary teeth and 16 to 17 dentary teeth (3+16-18/16-
687   17) for a minimal count, but it is likely that the maxillary tooth count could be even higher. It is
688   therefore closer to the 3+17-19/15-17 estimated for *To. coryphaeus* than the 3+14/14 formula
689   estimated for *To. carpenteri* (Young *et al.*, 2013b; Table 1). However, it must be noted that no
690   *Torvoneustes* species was found with complete maxillae. Moreover, the skull of *To. carpenteri*
691   (BRSMG Ce17365) is damaged, so the estimated tooth count might be underestimated,
692   especially considering that, in *To. coryphaeus*, the maxillary tooth row reaches beyond the
693   anterior margin of the orbit. This is also observed in other geosaurines such as *D. andiniensis, G.*
694   *giganteus* and potentially *Pl. manselii* (Young *et al.*, 2013b). Comparison with *To. carpenteri*
695   and MJSN BSY008-465 are limited because the contour of the orbits is completely lost in both.
696
697   *Tooth wear*
698   In addition to postmortem fractures, the teeth of MJSN BSY008-465 present signs of
699   macroscopic wear. Several teeth have their apex broken resulting in a flattened and smoothed tip.
700   This type of wear was described in *To. coryphaeus* as an indication of repeated impact against
701   hard surfaces. Some teeth also present signs of enamel spalling wear, mainly represented by
702   triangular facets of broken enamel on the labial face. This type of wear was interpreted as
703   resulting from tooth-food abrasion and was also described in *To. coryphaeus*, *To. carpenteri* and
704   *D. maximus* (Grange & Benton, 1996; Andrade *et al.*, 2010; Young *et al.*, 2012a, 2012b, 2013b).
705
706   **Postcranial elements**
707   From the postcranial skeleton, many vertebrae and ribs are preserved as well as a few elements
708   of the pelvis and hindlimbs. Despite the number of postcranial elements, no osteoderms were
709   found. The absence of osteoderms is an apomorphy of Metriorhynchidae (Fraas, 1902; Andrews,
710   1913; Young *et al.*, 2010).
711
712   *Vertebrae*
713   MJSN BSY008-465 was found with 22 of its vertebrae including three cervicals, nine dorsals
714   and 10 caudals (Fig. 14). The atlas-axis complex is missing as well as the sacral vertebrae. The
715   vertebrae suffered different level of damage and deformation. Some show stretching, with the

716 centrum deflected from its natural, vertical plane and the apophyses not aligned anymore, or
717 crushing with no preferential direction of deformation. This is mainly the case in the dorsal
718 vertebrae. All vertebrae are amphicoelous, as in all metriorhynchids (Fraas, 1902; Pierce &
719 Benton, 2006; Cau & Fanti, 2011; Young *et al.*, 2013a; Parrilla-Bel & Canudo, 2015). The
720 concavity is shallow and similarly developed in the anterior and posterior articular surfaces.
721
722 *Cervical vertebrae*
723 Three post-axis cervical vertebrae are preserved. The number of post-axis cervical vertebrae is
724 considered to be five among Metriorhynchidae, with the fifth cervical closely resembling the first
725 dorsal (Fraas, 1902; Wilkinson *et al.*, 2008; Young *et al.*, 2013a; Parrilla-Bel & Canudo, 2015;
726 Sachs *et al.*, 2021). The cervical vertebrae of *To. jurensis* look similar to one another, we can
727 therefore assume that the preserved vertebrae are all mid cervicals. Two of them are well
728 preserved, including one complete (Fig 14a, 14b). The centrum is subcircular to ovoid, with the
729 length of the vertebra subequal to the centrum height and width, which is typical for geosaurines
730 (Parrilla-Bel & Canudo, 2015). The neural spine is shorter than the centrum height. As in all
731 thalattosuchians, the cervical vertebrae are amphicoelous (Fraas, 1902; Wilkinson *et al.*, 2008;
732 Pierce & Benton, 2006; Cau & Fanti, 2011; Young *et al.*, 2013a; Parrilla-Bel & Canudo, 2015;
733 LeMort *et al.*, 2022). The parapophysis is low on the centrum, ventrally directed, without
734 reaching lower than the ventral margin of the centrum (Fig. 14). A low parapophysis not
735 associated with the neural arch is what characterizes cervical vertebrae in metriorhynchids
736 (Andrews, 1913; Young *et al.*, 2013a; Parrilla-Bel & Canudo, 2015). The parapophysis ends with
737 a concave articular facet. This facet articulates with the cervical rib. The diapophysis is also low,
738 starting just above the neural arch-centrum suture, and ventrally oriented, reaching below the
739 suture. The neurocentral sutures are not closed. On the ventral margin, at the edges of the
740 articulation surfaces of the centrum, discrete ridges are a sign of muscle attachments (Parrilla-Bel
741 & Canudo, 2015). There is a deep concavity between the parapophysis and diapophysis. This
742 strong constriction has also been noted in *Maledictosuchus riclaensis* (Parrilla-Bel & Canudo,
743 2015). In ventral view, there are two shallow concavities between the parapophyseal processes
744 and the centrum ventral margin, creating a medial keel also described on the cervical vertebrae of
745 *D. maximus* and *Ma. riclaensis* (Fraas, 1902; Parrilla-Bel & Canudo, 2015). The ventral margin
746 of the centrum is concave in lateral view. The parapophyses project below this margin in the
747 middle of the centrum, but they do not extend more ventrally than the ventral margin of the
748 articular facets. The zygapophyses are well developed, separated, and extended beyond the
749 centrum. The postzygapophyses are wider than the prezygapophyses, but the latter extend further
750 from the centrum. The articular surfaces of the zygapophyses are ovoid and flat. The morphology
751 of the cervical vertebrae is consistent with the ones described for *To. carpenteri*, *Ma. riclaensis*
752 and other metriorhynchids (Fraas, 1902; Andrews, 1913; Wilkinson *et al.*, 2008; Young *et al.*,
753 2013a; Parrilla-Bel & Canudo, 2015; LeMort *et al.*, 2022).
754
755 *Dorsal vertebrae*

756 At least nine dorsal vertebrae are preserved, none of them with a complete neural spine nor
757 complete diapophyseal processes. All of them are deformed to some extent. In metriorhynchids,
758 the first dorsal vertebra is the one where the parapophysis is no longer on the centrum but on the
759 neural arch (Young *et al.*, 2013a; Parrilla-Bel & Canudo, 2015). The dorsal vertebrae of MJSN
760 BSY008-465 follow the trend observed by Fraas (1902) with a constriction of the middle of the
761 centrum giving it an hourglass shape. The centrum is higher than wide. Its length is subequal to
762 its height. The vertebrae are amphicoelous, with both articular faces overall equally concave,
763 unlike what had been noted in *Ty. lythrodectikos* and *To. carpenteri* (Wilkinson *et al.*, 2008;
764 Young *et al.*, 2013a; Parrilla-Bel & Canudo, 2013). On the neural arch, the spine extends
765 vertically in the posterior half of the centrum length. The parapophysis joins the diapophysis on
766 the neural arch to form the anterior extension, like a little step, of the transverse apophysis, as
767 typically observed within Metriorhynchidae (Fig.14c, 14d; Andrews, 1913, fig. 62; Parrilla-Bel
768 & Canudo, 2015). The transverse apophysis extends greatly beyond the centrum on each side. It
769 is overall straight with a slight ventral concavity. The zygapophyses are well developed, but not
770 as much as the ones on the cervical vertebrae. As in *Ty. lythrodectikos* and the E-clade member
771 PSHME PH1, they project slightly beyond the centrum (Parrilla-Bel & Canudo, 2015; Abel *et*
772 *al.*, 2020). Among the dorsal vertebrae of MJSN BSY008-465, some of them show unfused
773 suture between the centrum and neural arch, indicating a specimen which did not achieved full
774 maturity (a sub-adult; Brochu, 1996, Herrera *et al.*, 2013). As seen on the cervical vertebra, on
775 the ventral margin of the caudal vertebra the edges of the articulation surfaces of the centrum,
776 discrete ridges are a sign of muscle attachments.
777
778 *Caudal vertebrae*
779 In MJSN BSY008-465, only ten caudal vertebrae are preserved. The number of caudal vertebrae
780 can differ greatly between metriorhynchid species but it is usually over 30 (Fraas, 1902;
781 Andrews, 1913; Parrilla-Bel & Canudo, 2015; De sousa oliveira, in press). The size and shape of
782 the preserved vertebrae vary greatly, which suggests that they originate from different parts of
783 the tail (Fig. 14e–h). However, none of them can be associated with the bend of the tail fluke.
784 Three vertebrae with reduced apophysis are associated with the anterior part of the tail (Fig. 14e,
785 14f). These caudal vertebrae are hourglass shaped, but the constriction is not as strong as in the
786 cervical and dorsal vertebrae. Their centrum presents a ventral keel. The centrum length of the
787 vertebrae is subequal to their width. The neural spine is overall rectangular in shape and oriented
788 posterodorsally. The general shape of the caudal vertebra of MJSN BSY008-465 is similar to *To.*
789 *carpenteri* and E-clade member PSHME PH1 (Wilkinson *et al*., 2008; Abel *et al.,* 2020). The
790 other caudal vertebrae do not all preserve the neural spine. These vertebrae are greatly reduced
791 for some of them, and are interpreted as more posterior in the caudal series. The zygapophyses
792 are not preserved. The articular surfaces of the centra are rounded and slightly concave. On the
793 caudal vertebrae, the suture between the centrum and neural arch is closed.
794
795 **Ribs**

796
797   *Cervical ribs*
798   Three cervical ribs are identified. They form short, slender ribs directed posteriorly with an acute
799   end (Fig. 15a-c). The external face forms a ridge starting from the tuberculum and capitulum.
800   The medial face is concave. In cross section, the cervical ribs are roughly triangular at mid-shaft.
801   In lateral view, the ribs are "V-shaped". This correspond to the typical condition in
802   Metriorhynchidae (Andrews, 1913; Wilkinson *et al.*, 2008; Abel *et al.*, 2020)
803
804   *Dorsal ribs*
805   There are 15 preserved, but incomplete, dorsal ribs from MJSN BSY008-465. The dorsal ribs are
806   long and slender, ovoid or round in cross section (Fig. 15d, 15e). They are arched, having a flat
807   medial surface, whereas the lateral surface is rounded. There is a ridge on the posterior surface
808   running down from the tubercular (diapophyseal process). The proximal two thirds are flat on the
809   medial side. In its distal third in lateral view, the rib narrows to form a ridge. On the medial side
810   this part shows a sutural surface. This shift might mark the limit between the vertebrocostal part
811   to the intercostal part of the rib, but no intercostal is sufficiently preserved to give a better
812   description. Tuberculum and capitulum are not preserved in available ribs. The ribs overall
813   resemble the dorsal ribs of *To. carpenteri* and other metriorhynchids (von Arthaber, 1906;
814   Andrews, 1913; Wilkinson *et al.*, 2008, Herrera *et al.*, 2013, fig. 7N).
815
816   *Chevron*
817   At least one chevron is preserved, probably from the posterior part of the tail considering its
818   small size (Fig. 15f, 15g). In lateral view it is Y-shaped, and in dorsal view it presents two lateral
819   and one medial branches, which corresponds to what has been described in other
820   Metriorhynchidae (Andrews, 1913; Sachs *et al.*, 2019, 2021).
821
822   **Appendicular skeleton**
823
824   *Ischium*
825   The left ischium is badly preserved, lacking a major portion of its ventral part where the bone
826   would widen the most (Fig. 16c). The proximal part is also missing, as well as the anterior
827   process it should be bearing (Andrews, 1913; Wilkinson *et al.*, 2008; Herrera *et al.*, 2013; Young
828   *et al.*, 2013b). Like in other metriorhynchids, the neck of the ischium is narrow and thick,
829   measuring 2.5 cm wide. The ischium widens and flattens distally in an overall triangular wing
830   with a thickness of about two millimeters only. The partly preserved wing is similar to the classic
831   metriorhynchid morphology as seen in *To. carpenteri, C. araucanensis* (Andrews, 1913;
832   Wilkinson *et al.*, 2008; Herrera *et al,* 2013; LeMort *et al.*, 2022). The surface of the wing is
833   covered by striations corresponding to muscular attachment marks on both sides but better
834   expressed on the lateral one.
835

Femur

836 *Femur*
837 The right femur of MJSN BSY008-465 lacks both proximal and distal ends (Fig. 16a, b). It has
838 the sigmoidal shape typically found in Thalattosuchia (Andrews, 1913; Wilkinson *et al.,* 2008;
839 Herrera *et al.*, 2013; Young *et al.*, 2013b; Sachs *et al*., 2021) but with the curves not as
840 pronounced as in *Enaliosuchus macrospondylus* Koken, 1883 or *Ty. lythrodectikos* (Young *et al.*,
841 2013b; Sachs *et al*., 2020). The bone is about 24 cm long and 3 cm wide, a similar size to *Ty.*
842 *lythrodectikos* (Young *et al.*, 2013b). It is slightly narrower in the middle than at the ends. The
843 medial side is almost flat, whereas the lateral side is convex. The bone flattens toward the distal
844 end. As in *Ty. lythrodectikos* and *C. araucanensis,* the femur widens toward the distal end
845 (Herrera *et al.*, 2013; Young *et al.*, 2013b; Sachs *et al*., 2021). The proximal end, despite the
846 damages it suffered, shows on both sides the rugose surface for muscle attachment commonly
847 found in metriorhynchids (Andrews, 1913; Lepage *et al.*, 2008; Wilkinson *et al.*, 2008; Herrera
848 *et al.*, 2013; Young *et al.*, 2013b).
849
850 *Fibula*
851 The right fibula is a slender bone about a third of the preserved femur length (Fig. 16d), the same
852 proportion as found in *Ty. lythrodectikos, C. suevicus* and *C. araucanensis* (Andrews, 1913;
853 Herrera *et al.*, 2013; Young *et al.*, 2013b). This ratio is affected by the missing ends of the femur,
854 as well as the missing part of the fibula. The hindlimb proportion in metriorhynchids are often
855 measured with the femur and tibia. The tibia length being 30 to 40% of the femoral length is the
856 general trend found among metriorhynchids while a ratio below 30% is distinctive of derived
857 metriorhychins (Andrews, 1913; Wilkinson *et al*., 2008; Young & Andrade, 2009; Cau & Fanti,
858 2011; Young *et al.*, 2013b; Foffa *et al.*, 2019). The distal end of the fibula is not preserved. The
859 proximal end is damaged but shows a single convex condyle as usual in Metriorhynchidae
860 (Andrews, 1913; Herrera *et* al., 2013; Sachs *et al.*, 2019, 2021). The inner side is flatter than the
861 outer one, like what is seen in the femur. The bone is one centimeter wide at mid length and
862 enlarged toward both ends, being 2 cm wide at the proximal end.
863
864 **Phylogenetic analysis**
865 Following the methodological protocol of Young *et al.* (2020b), the eight parsimony analyses
866 resulted in eight strict consensus topologies with lengths ranking from 2417 steps for the
867 unweighted analysis to 2033 steps for the weakly downweighted topologies (k=20 and k=50; see
868 Table 2). The complete eight strict consensus trees are provided in Supplementary material 3,
869 while descriptive statistics for each of these trees are presented in Table 2. Focusing on the
870 internal relationships of Geosaurinae, four distinct topologies are recovered (Fig. 17). They all
871 have a similar structure, except for the position of *Tyrannoneustes lythrodectikos*, *Ieldraan*
872 *melkshamensis*, *Geosaurus lapparenti*, "*Metriorhynchus*" *westermanni*, and "*Metriorhynchus*"
873 *casamiquelai*.
874 In all of the strict consensus trees, *Torvoneustes jurensis* is included in a polytomous clade with
875 all terminal taxa assigned to *Torvoneustes* (Fig. 17). This clade forms a polytomy with the E-

876   clade and *Purranisaurus potens*. In the unweighted analysis, this group made of *Torvoneustes*,
877   the E-clade and *P. potens* forms a polytomy with *Ty. lythrodectikos* and a clade consisting of
878   Geosaurina + Plesiosuchina (Fig. 17a). These taxa form together the Geosaurini. In the strongly
879   downweighted analyses (k = 1 and k = 3), "*M.*" *westermanni* and "*M.*" *casamiquelai* assume
880   more basal positions outside of geosaurines (Fig. 17b). *Tyrannoneustes lythrodectikos* is sister
881   group to the E-clade, which corresponds to the 'subclade T' of Foffa *et al.* (2018a). Within
882   Geosaurina, *I. melkshamensis* and *G. lapparenti* switch positions. The moderately downweighted
883   analyses (k = 7 and k = 10) result in a topology overall consistent with that of the strongly
884   downweighted analyses, except that "*M.*" *westermanni* and "*M.*" *casamiquelai* regain a basal
885   position among geosaurines (Fig. 17c). In the moderately to weakly downweighted analyses (k =
886   15, k = 20 and k = 50), *I. melkshamensis* and *G. lapparenti* switch back to the positions they
887   have in the strict consensus of the unweighted analysis (Fig. 17d). Overall, the results of our
888   parsimony analyses are consistent with those of Young *et al.* (2020b) and Abel *et al.* (2020),
889   except our strict consensus for the unweighted analysis that is less well resolved (subclade T
890   only recovered by the weighted analyses).
891   To improve the resolution of relationships, unstable taxa were pruned a posteriori from the
892   consensus trees to produce a maximum agreement subtree for each of the parsimony analysis
893   (see Material and methods). For the unweighted analysis, a total of 13 OTUs, including eight
894   geosaurines ("*Metriorhynchus*" *brachyrhynchus*, *Tyrannoneustes lythrodectikos*, *Geosaurus*
895   *lapparenti*, *Purranisaurus potens*, Druegendorf merged, English rostrum, *Torvoneustes* sp.,
896   *Torvoneustes mexicanus*), are pruned from the original set of 180 OTUs. In contrast, 33 OTUs,
897   including 12 geosaurines ("*Metriorhynchus*" *brachyrhynchus*, *Neptunidraco ammoniticus*,
898   *Purranisaurus potens*, Druegendorf merged, English rostrum, Mr. Passmore's specimen,
899   Chouquet cf. *hastifer*, *Torvoneustes* sp., *Torvoneustes mexicanus*, *Geosaurus grandis*, *Geosaurus*
900   *giganteus*, and *Ieldraan melkshamensis* or *Geosaurus lapparenti*), are pruned for the weighted
901   analyses. The four new topologies obtained for relationships within Geosaurinae are presented in
902   Figure 18 and the complete pruned consensus trees are available in Supplementary material 4.
903   All maximum agreement subtrees suggest that *Torvoneustes* sp. and *Torvoneustes mexicanus* are
904   unstable taxa. This is probably the result of the partial nature of these terminals represented by
905   single specimens consisting of an incomplete occipital region and a portion of rostrum,
906   respectively. The pruning of these taxa reveals the internal relationships of the *Torvoneustes*
907   clade. *Torvoneustes coryphaeus* is recovered as the most basal taxon in a sister group
908   relationship with a clade consisting of cf. *Torvoneustes* and *To. jurensis* + *To. carpenteri* (Fig.
909   18). From a more general perspective, the internal relationships of the E-clade and Geosaurina
910   are also identified as unstable.
911   The Bayesian analysis results in a resolved, but poorly supported tree (Fig. 19). *Torvoneustes*
912   *jurensis* is resolved as the sister taxon of *To. carpenteri*. These two species form the most
913   derived clade within the clade *Torvoneustes*. *Torvoneustes mexicanus* is found as the sister taxon
914   of *To. jurensis* + *To. carpenteri*, whereas *To. coryphaeus* appears as the most basal unit. Most
915   nodes in the *Torvoneustes* clade and the E-clade are weakly supported. The Bayesian topology

916 for Geosaurini is similar to the one obtained by Young *et al.* (2020b), with only two exceptions:
917 1) the position of cf. *Torvoneustes* and *Torvoneustes* sp. are switched; 2) *To. mexicanus* and *To.*
918 *carpenteri* are no longer sister taxa. In our analysis, the node supports within subclade T is
919 slightly lower, which can be explained by the inclusion of *To. jurensis* as a new terminal. the
920 complete maximum compatibility is are available in Supplementary material 5.
921 The different phylogenetic analyses performed as part of the present study all consistently find
922 *To. jurensis* (MJSN BSY008-465) nested within a *Torvoneustes* clade, supporting our
923 identification. Both the Bayesian analysis and the maximum agreement subtrees of the
924 parsimony analyses support a close relationship between *To. jurensis* and *To. carpenteri*.
925
926 ## Discussion
927 **MJSN BSY008-465 assigned to Geosaurinae**
928 The absence of mandibular fenestrae, the orbits facing laterally and overhung by the prefrontals,
929 and the absence of osteoderms (despite the preservation of numerous postcranial remains)
930 unambiguously place MJSN BSY008-465 among Metriorhynchidae (Fraas, 1901, 1902;
931 Andrews, 1913; Young *et al.*, 2010). In this section, we discuss the assignment of this specimen
932 to Geosaurinae.
933 The dental characteristics of the Late Jurassic metriorhynchids allow to discriminate the
934 Geosaurini from the Metriorhynchinae. The latter usually have smooth to faintly ornamented
935 teeth, uncarinated or with low, non-serrated carinae, whereas Geosaurini have smooth to heavily
936 ornamented teeth with high, serrated carinae (Table 1). The presence of prominent serrated
937 carinae appears to be restricted to the Geosaurini tribe (Andrade *et al.*, 2010; Young *et al.* 2011).
938 Metriorhynchids genera can even be identified based on teeth only and within Geosaurini, teeth
939 can be used for species identification, (Young & Andrade, 2009; Andrade *et al.*, 2010; Schaefer,
940 2012; Young *et al.*, 2013a, 2013b; Barrientos-Lara *et al.*, 2016; Foffa *et al.*, 2017, 2018a;
941 Schaefer *et al.*, 2018; Madzia *et al.*, 2021). MJSN BSY008-465 shares with *Torvoneustes* the
942 presence of conspicuous apicobasal ridges on the first two-thirds of the crown shifting to an
943 anastomosed pattern on the apex, as well as the bending of the enamel ridges toward the carinae.
944 The teeth of some Metriorhynchinae (*Cricosaurus* spp., *Maledictosuchus nuyivijanan*) resemble
945 those of *Torvoneustes* with conspicuous apicobasal ridges on the first two-thirds of the crown,
946 but in their case the apex is smooth and the carinae are low and non-serrated (Sachs *et al.*, 2019;
947 Table 1).
948 Derived geosaurines, such as *Plesiosuchus*, *Dakosaurus*, *Torvoneustes*, *Geosaurus*,
949 *Purranisaurus* and the E-clade, show an extreme reduction in interalveolar space associated with
950 a reduction of the tooth count and a moderate enlargement of the teeth (Young *et al.*, 2012b,
951 2013a, 2013b; Herrera *et al.*, 2015a; Abel *et al.*, 2020). Metriorhynchines, including those with a
952 low tooth count such as *'Cricosaurus' saltillensis* (see below), have large and variable
953 interalveolar spaces (Buchy *et al.*, 2013; Young *et al.*, 2020a; Herrera *et al.*, 2021a, 2021b). The
954 only exception is *Gracilineustes leedsi* in which reduced interalveolar spaces are associated with
955 a high tooth count (+30 per maxilla; Young *et al.*, 2013b). MJSN BSY008-465 has reduced

956   interalveolar spaces associated with moderately enlarged teeth, which corresponds to the
957   condition in derived geosaurines. In addition, the teeth of MJSN BSY008-465 are on average
958   larger than the typical height observed for metriorhynchine teeth, which are usually shorter than
959   two centimeters (Wilkinson *et al.*, 2008; Herrera *et al.*, 2021b).
960   The tooth count is often used to differentiate geosaurines from metriorhynchines (Young *et al.*,
961   2013), but it should be noted that the absolute tooth count is known only in a limited number of
962   species (Table 1). Geosaurini are usually considered to have 16 or less teeth per maxilla (Cau &
963   Fanti, 2011). With this in mind, the estimated tooth count for MJSN BSY008-465 (17–18 or
964   more, see above) may seem high for a Geosaurini, especially when some non-rhacheosaurin
965   metriorhynchines, such as *"C." saltillensis* and *"C." macrospondylus*, present comparable tooth
966   counts (Table 1; Buchy *et al.*, 2013; Aiglstorfer *et al.*, 2020). However, this relatively low tooth
967   count in some rhacheosaurins seems to be linked to a pronounced shortening of the skull. On the
968   other hand, it appears that the tooth count is poorly estimated in *Torvoneustes* because no
969   complete maxilla is known, and some species have a comparable tooth count as MJSN BSY008-
970   465. For example, *To. coryphaeus* is estimated to have up to 19 alveoli per maxilla (Young *et al.*,
971   2013b), which also falls into the range of other geosaurines such as Chouquet's
972   *"Metriorhynchus"* cf. *hastifer* and its at least 20 maxillary teeth (Lepage *et al.*, 2008). Therefore,
973   the tooth count for *Torvoneustes* is maybe underestimated for the moment based on the available
974   material. It is also possible that the tendency toward the great reduction in the number of teeth is
975   restricted to the clade uniting Geosaurina, Dakosaurina, and Plesiosuchina. In any case, it
976   appears that tooth count, as a tool for identification, should be handled with care, especially
977   when based on estimations.
978   MJSN BSY008-465 shares with Geosaurinae the presence of an acute angle of about 60°
979   between the medial and lateral processes of the frontal. This angle is closer to 90° in most
980   Metriorhynchinae, to the exception of *Cricosaurus* and *Maledictosuchus* in which this angle is
981   around 45-50° (Wilkinson *et al.*, 2008; Cau & Fanti, 2011; Buchy *et al.*, 2013, Parrilla-Bel *et al.*,
982   2013; Foffa & Young, 2014). The new specimen described herein shares several additional
983   cranial and mandibular features with the macrophagous predators of the Geosaurini tribe: an
984   inflection point of the prefrontals relative to the skull midline of 70° or less; a high glenoid fossa
985   and retroarticular process; a strongly expressed surangular-dentary groove (Young & Andrade,
986   2009; Young *et al.*, 2012b, 2013b; Foffa & Young, 2014). In addition to some dental
987   characteristics discussed above, MJSN BSY008-465 also has some cranial features that may
988   recall the metriorhynchine *Cricosaurus*. MJSN BSY008-465 notably has a smooth and
989   unornamented cranial surface, but this is also the case of *D. andiniensis* and *P. potens* (Pol &
990   Gasparini, 2009; Herrera *et al.*, 2015a). The frontal of MJSN BSY008-465 differs in shape from
991   that of other geosaurines and somewhat resembles that of *"C." saltillensis* (Buchy *et al.*, 2013),
992   but there is a great diversity of frontal shapes among metriorhynchids (Foffa & Young, 2014, fig.
993   10; Herrera, 2015). Despite these few similarities, MJSN BSY008-465 lacks some cranial
994   characters that are typical of *Cricosaurus*, such as the presence of a bony septum on the
995   premaxillary and the presence of reception pits on the maxilla (as seen in *C. bambergensis* and

996   *C. albersdoerferi*; Sachs *et al.*, 2019, 2021). Therefore, the craniomandibular characters, like the
997   dental characters, indicate that MJSN BSY008-465 should be assigned to Geosaurinae and
998   suggest that the resemblances with *Cricosaurus* are only superficial.
999   The total body length of MJSN BSY008-465 is estimated to be around four meters (De Sousa
1000   Oliveira *et al.*, in press), which exceeds the sizes typically measured and estimated for
1001   *Rhacheosaurus* (157 cm), *Cricosaurus* (200 cm), and *Geosaurus* (270 cm), but falls in the range
1002   of large-bodied geosaurines such as *Suchodus durobrivensis* Lydekker, 1890 (410 cm), *D.*
1003   *andiniensis* (430 cm); *To. coryphaeus* (370 cm) and *To. carpenteri* (400-470 cm) (Young *et al.*,
1004   2010, 2019). Because this specimen is one of the few metriorhynchids found with a significant
1005   part of its postcranium (see also Sachs *et al.*, 2019; LeMort *et al.*, 2022), some remarks relative
1006   to the assignment of the specimen should be made also on this part of the skeleton.
1007   Geosaurinae (*Neptunidraco ammoniticus*, "*M.*" *brachyrhynchus*, *Ty. lythrodectikos*, *To.*
1008   *carpenteri*, *Geo. lapparenti*, *D. maximus*) and MJSN BSY008-465 share a centrum length
1009   subequal to centrum width on cervical vertebrae, whereas in other Metriorhynchidae
1010   (*Thalattosuchus superciliosus*, *Rhacheosaurus gracilis*, *C. araucanensis*, *C. suevicus*, *C.*
1011   *bambergensis*, *C. albersdoerferi*) the centrum is shorter than wide (see character 423 of the
1012   phylogenetic matrix; Parrilla-Bel & Canudo, 2015). In MJSN BSY008-465, the neural length
1013   spine of the dorsal vertebrae is about half the length of the centrum and its dorsal margin is
1014   rounded. This is markedly different from *C. suevicus* and *C. albersdoerferi* in which the neural
1015   spine of the dorsal vertebrae is wide and rectangular with a flat dorsal margin and subequal in
1016   length to the length of the centrum (Sachs *et al.*, 2021). The centrum of the dorsal vertebrae is
1017   also distinctly longer than high in *C. albersdoerferi* and Cretaceous metriorhynchids (Sachs *et*
1018   *al.*, 2020, 2021), whereas the centrum length is subequal to its height in MJSN BSY008-465 as
1019   in E-clade member PSHME PH1 and *N. ammoniticus* (Cau & Fanti, 2011; Abel *et al.,* 2020).
1020   In metriorhynchids there is a drastic reduction of the length of the tibia and fibula compared to
1021   the femur (Fraas, 1902; Andrews, 1913; Foffa *et al.*, 2019). The tibia of MJSN BSY008-465 is
1022   not preserved, but the fibula is usually subequal or slightly longer than the tibia in
1023   metriorhynchids and can therefore be used as a proxy (Sachs *et al.*, 2019). As preserved,
1024   knowing that each bone is missing parts of the articular heads, the fibula of MJSN BSY008-465
1025   is about 30% of the femoral length, which corresponds to the proportions usually observed in
1026   metriorhynchids. Members of the tribe Rhacheosaurini appear to be an exception because their
1027   tibia is less than 30% of the femur length (Andrews, 1913; Wilkinson *et al.*, 2008; Young &
1028   Andrade, 2009; Cau & Fanti, 2011; Foffa *et al.*, 2019). However, this character (see #518 in the
1029   phylogenetic matrix; Supplementary data in Foffa *et al.*, 2019) can only be scored in a small
1030   number of metriorhynchids, and its repartition should be further investigated, especially in
1031   derived geosaurines such as *Dakosaurus*. Although not as diagnostic as the dental and cranial
1032   characters, the postcranial characters of MJSN BSY008-465 tend to suggest an affinity of this
1033   specimen with geosaurines rather than with non-metriorhynchine metriorhynchid and to exclude
1034   a relationship with rhacheosaurins such as *Cricosaurus*.
1035

Taxonomic diversity in the geosaurine genus *Torvoneustes*

The genus *Torvoneustes* is a member of Geosaurinae and is currently represented by three valid species: the type species *To. carpenteri* from the upper Kimmeridgian, a skull heavily crushed and not described in many details, and some postcranial remains from a second specimen (Grange & Benton, 1996; Wilkinson *et al.*, 2008; Andrade *et al.*, 2010); *To. coryphaeus* from the lower Kimmeridgian, a 3D preserved skull missing the anterior part of the rostrum (Young *et al.*, 2013b); and *To. mexicanus,* likely from the Kimmeridgian, represented by a piece of a rostrum (Barrientos-Lara *et al.*, 2016). Other specimens were referred to the genus and include several isolated teeth form the Oxfordian (BRSMG Cd5591, Cd5592; CAMSM J.13305J, 13309, J.13310, YORYM:2016.306–2016.309; OUMNH J.52428, J.47587a, J.47560; Foffa *et al.*, 2018a); three specimens referred to *Torvoneustes sp.*, MJML K1707 from the Upper Kimmeridgian; OUMNH J.50061 and OUMNH J.50079-J.50085 from the lower Tithonian (Young *et al.*, 2019); cf. *Torvoneustes* (MANCH L6459) from the middle Oxfordian (Young, 2014), and *Torvoneustes*? (NHMW 2020/0025/0001) an isolated tooth crown from the upper Valanginian. All specimens are from England, except *To. mexicanus* and *Torvoneustes*?, which are from Mexico and Czech Republic respectively (Table 1).

Based on the three valid species, the genus *Torvoneustes* is defined by the following characteristics (Wilkinson *et al.*, 2008; Andrade *et al.*, 2010; Young *et al.*, 2013b; Barrientos-Lara *et al.*, 2016): great reduction of the interalveolar space; acute angle (around 60°) between the medial and lateral processes of the frontal; inflexion point on the lateral margin of the prefrontals directed posterolaterally at an angle of ~70° from the anteroposterior axis of the skull; circular to subcircular tooth cross section; carina formed by a keel and a contiguous row of poorly defined microscopic denticles difficult to observe even under SEM observation; conspicuous enamel ornamentation consisting of subparallel apicobasal ridges on the first two thirds of the crown shifting to short, low relief tubercles on the apex. The new specimen described herein closely follows this definition, but also presents significant differences with each of the recognized species.

The frontal of MJSN BSY008-465 is shaped differently than those of *To. carpenteri* and *To. coryphaeus*. In *To. carpenteri*, the frontal is shorter than in *To. coryphaeus* and MJSN BSY008-465. *Torvoneustes coryphaeus* has an ornamented frontal while in *To. carpenteri* and MJSN BSY008-465 the frontal is smooth. Finally, MJSN BSY008-465 is characterized by a clear angle between the anterior and posterolateral processes of the frontal, at the meeting point of the frontal, nasals and prefrontals. In the aforementioned two species, there is no visible angle and the processes are aligned in an almost straight line. Variation in shape of the frontals in the genus *Torvoneustes* is not well known, as only two described specimens preserve this element in addition to the new material described herein. Within metriorhynchids, we can note the great interspecific variation in the shape of the frontal (Foffa & Young, 2014). For example in *Cricosaurus*, there is a great variation of the frontal shape, as seen in *C. araucanensis* (Herrera, 2015).

1075 MJSN BSY008-465 cannot be compared with *Torvoneustes* sp. (MJML K1707). The latter
1076 consists of an incomplete occipital region and this part is completely lost in our specimen.
1077 However, MJSN BSY008-465 can be distinguished from all other English specimens.
1078 *Torvoneustes jurensis* differs from the type species *To. carpenteri* based on the following
1079 characters: smooth maxillae without grooves; anterior process of the frontal reaching the anterior
1080 margin of the prefrontals; posterolateral edges of the prefrontals lacking "finger-like"
1081 projections; teeth slenderer, more curved, and with a sharp apex. MJSN BSY008-465 also differs
1082 from *To. coryphaeus* in having: a smooth skull; rounded posterolateral edges of the prefrontals
1083 (no acute angle); slender teeth with sharp apex; tooth ornamentation touching the carina in the
1084 upper part of the crown. Isolated *Torvoneustes* sp. teeth from the UK (BRSMG Cd5591,
1085 Cd5592; CAMSM J.13305J, 13309, J.13310, YORYM:2016.306–2016.309; OUMNH J.52428,
1086 J.47587a, J.47560, J.50061, J.50079-J.50085) preserve tooth crowns and roots very similar to *To.*
1087 *carpenteri*, As noted above, MJSN BSY008-465 has slender teeth. Finally, MJSN BSY008-465
1088 is different from cf. *Torvoneustes* MANCH L6459 by its smooth cranium.
1089 *Torvoneustes mexicanus* is only known by a single specimen that consists of a fragment of snout
1090 with preserved teeth. The species diagnosis is based only on the teeth with the following
1091 characters: conical, lingually curved, bicarinate, and more slender than in other *Torvoneustes*
1092 species; sharp apex; microziphodont condition with well-defined isomorphic denticles; crown
1093 enamel ornamentation consisting of apicobasally aligned ridges on the basal two-thirds of the
1094 crown and shifting to short drop-shaped tubercles meeting the carina on the apex (Barrientos-
1095 Lara *et al.*, 2016). On macroscopic observation, the teeth of MJSN BSY008-465 and *To.*
1096 *mexicanus* are very similar, but they differ on microscopic features. The denticles of *To.*
1097 *mexicanus* are well defined, regular in shape, size and distribution with a denticle basal length of
1098 about 142 µm and a denticle density (#denticles/5mm) of 30 (Barrientos-Lara *et al.*, 2016). The
1099 crown height seems to range between 1 and 2.5 cm. In MJSN BSY008-465, the basal length and
1100 distribution of denticles are irregular; on the tooth total length, the base of the denticles can vary
1101 from 120 to 200 µm in length with an average of 160 µm measured on four different teeth;
1102 denticles are also more densely packed in the upper middle of the tooth with a density reaching
1103 40 while they can drop to 30 on the basal most part of the carina and the tooth apex. These
1104 observations are homogenous on the four observed teeth. It is to be noted however that denticles
1105 are sometimes hard to discern, because of their shape and size but also due to areas where they
1106 are worn or where the carina is broken. We compared these results with measurements based on
1107 formerly published SEM photographs of teeth of *To. carpenteri* (Young *et al.*, 2013a). In this
1108 species, the denticle basal length varies between 120 and 220 µm, with most measured denticles
1109 having a basal length between 160 and 200 µm. Unfortunately, denticle density cannot be
1110 determined. Again based on published SEM photographs (Madzia *et al.*, 2021), the denticles of
1111 *Torvoneustes*? (NHMW 2020/0025/0002) range in size from 200 to 270 µm in basal length and
1112 have a density of 19.
1113 Previous studies showed that the denticle density is variable between geosaurines species such as
1114 *Dakosaurus* and *Geosaurus* (Andrade *et al.*, 2010). Measurements took in the middle of the

1115 carina gives the following densities for the microziphodont specimens: 28.1 in *Geosaurus* indet.
1116 (NHM R.486), and 33.3 for the mesial carina and 41.7 for the distal carina in *G. grandis*. These
1117 results suggest possible interspecific variations in denticles density for a same tooth morphotype
1118 among geosaurines and that these variations should not be overlooked for systematic purposes
1119 (Andrade *et al.*, 2010). In this study however, the density of denticles is only measured on one
1120 tooth. The intraspecific and the individual variation, which were documented in other studies on
1121 crocodylomorphs teeth (Prasad & de Lapparent de Broin, 2002), were not explored in this case.
1122 However, the observations on MJSN BSY008-465, in addition to previous studies on
1123 metriorhynchid teeth, support the idea that microscopic dental characteristics in metriorhynchids
1124 have a potential to be used in systematics and should be further investigated.
1125 From the above discussion and considering that *To. mexicanus* is only known by a very
1126 incomplete specimen of uncertain stratigraphical origin, it seems reasonable to conclude that
1127 MJSN BSY008-465 represents a different species (Table 3), which we name *Torvoneustes*
1128 *jurensis*. Future discoveries of more complete fossil specimens of *To. mexicanus* will allow a
1129 better understanding of the differences between these species.
1130
1131 **Macroevolution trends in *Torvoneustes***
1132 Young *et al.* (2013b, 2019) discussed macroevolutionary trends in the genus *Torvoneustes*, we
1133 here include the new taxon *To. jurensis* within these putative trends and discuss how its addition
1134 strengthens or contradicts them. The first potential trend noted by Young *et al.* (2013b, 2019) is a
1135 reduction of the maxillary tooth count with time from "relatively high" in cf. *Torvoneustes*
1136 (MANCH L6459; Young *et al.*, 2019) and 17–19 in *To. coryphaeus* (Young *et al.*, 2013b), to 14
1137 in *To. carpenteri* (Wilkinson *et al.*, 2008). However, it should be noted that no complete maxilla
1138 is known for any specimen referred to *Torvoneustes*, so these tooth counts represent estimations
1139 (see above). Another trend noted in *Torvoneustes* is a decrease in dermocranial external
1140 ornamentation, with the upper Kimmeridgian *To. carpenteri* having a smoother skull than the
1141 older representatives *To. coryphaeus* and cf. *Torvoneustes* MANCH L6459 (Grange & Benton,
1142 1996; Wilkinson *et al.*, 2008; Young *et al.*, 2013b; Young, 2014).
1143 Concerning the tooth morphology, the following macroevolutionary trends were proposed:
1144 increasing enamel ornamentation; blunter crown apices; tooth crown losing the lingual curvature;
1145 and crown cross section becoming subconical (Young *et al.*, 2019). These trends are interpreted
1146 to be linked to an increasingly durophagous diet (Young *et al.*, 2013b; 2019; Foffa *et al.*, 2018b).
1147 *Torvoneustes coryphaeus*, *To. carpenteri*, *Torvoneustes?* (NHMW 2020/0025/0001) and
1148 *Torvoneustes* sp. (OUMNH J.50061 and OUMNH J.50079-J.50085) fit relatively well into this
1149 proposed evolutionary trend. However, that is not the case of *To. mexicanus* which has more
1150 slender teeth than *To. coryphaeus* and *To. carpenteri,* as well as more curved teeth than the latter.
1151 The teeth of *To. mexicanus* are also sharper than those of *To. coryphaeus, To. carpenteri* and
1152 *Torvoneustes* sp. OUMNH J.50061 and OUMNH J.50079-J.50085.
1153 The acquisition of false serration (false ziphodont dentition; Prasad & de Lapparent de Broin,
1154 2002; Young & Andrade, 2009; Andrade *et al.*, 2010) is another macroevolutionary trend

1155 proposed for *Torvoneustes* (Young *et al.*, 2019). *Torvoneustes coryphaeus* is the only species
1156 lacking the false ziphodont dentition and is also the oldest specimen whose teeth are known
1157 (Table 3). The other specimens preserving teeth (*To. carpenteri*; *Torvoneustes* sp., OUMNH
1158 J.50061 and OUMNH J.50079-J.50085; *Torvoneustes*?, NHMW 2020/0025/0001; *To.*
1159 *mexicanus*) all present the false ziphodont condition. Therefore, the authors propose the
1160 acquisition of the false ziphodont condition in all species younger than *To. coryphaeus* (Young *et*
1161 *al.*, 2019).
1162 The discovery of the occipital region of a *Torvoneustes* specimen of great size from the
1163 Tithonian of England led Young *et al.* (2019) to propose an increase of body size as a possible
1164 evolutionary trend within *Torvoneustes*. This specimen is estimated to be around 6 meters long
1165 while other *Torvoneustes* specimens are estimated to be between 3.70 and 4.70 meters long
1166 (Young *et al.*, 2011, 2019). And finally, Young *et al.* (2019) also suggested that the increase in
1167 length of the suborbital fenestrae leading to an enlarged pterygoid musculature and the
1168 ventralization of basioccipital tuberosities would be another evolutionary trend of *Torvoneustes*.
1169 However, because this part of the cranium is not preserved in *To. jurensis*, this trend will not be
1170 further discussed below.
1171 *Torvoneustes jurensis* fits relatively well with some of the aforementioned macroevolutionary
1172 trends. First, *To. jurensis* is younger than *To. coryphaeus* and indeed presents the false ziphodont
1173 condition on its teeth. However, it should be noted that in the current state of knowledge the
1174 distribution of this character does not per se corresponds to an evolutionary trend, especially
1175 considering the observation of this character among Oxfordian isolated teeth (Foffa *et al.*,
1176 2018a), older than *To. coryphaeus*. Therefore, false ziphodont condition may be a synapomorphy
1177 uniting *Torvoneustes* species but lost in *To. coryphaeus*.
1178 *Torvoneustes jurensis*, which is from the early late Kimmeridgian, has an even smoother cranium
1179 than *To. carpenteri*. Dermocranial ornamentation appears early during ontogeny in
1180 crocodylomorphs, usually developing in specimens with a skull longer than 200 mm (de
1181 Buffrénil, 1982; de Buffrénil *et al.*, 2015). This indicates that the smooth cranium of *To. jurensis*
1182 is not linked to its ontogenic stage and fits into the evolutionary trend proposed by Young *et al.*
1183 (2019). Within Thalattosuchia, the trend toward smoother dermocranial bones is believed to
1184 improve hydrodynamic efficiency (Young *et al.*, 2013b) and overall follows the idea that pelagic
1185 species have less ornamented skulls than semi-aquatic one (comparing metriorhynchids and
1186 pelagic teleosauroids to non-pelagic teleosauroids for example; Clarac *et al.*, 2017, Foffa *et al.*,
1187 2019). This trend is also present in *Dakosaurus* with *D. andiniensis*, the geologically younger
1188 species, showing smoother cranial bones than *D. maximus* (Pol & Gasparini, 2009; Young *et al.*,
1189 2012a). However, the functional role of bone ornamentation remains controversial in
1190 crocodylomorphs (de Buffrénil *et al.*, 2015). Clarac *et al.* (2017) presented evidence that the
1191 evolution of ornamentation in pseudosuchians is influenced by both natural selection and
1192 Brownian motion. The study shows that heavy ornamentation is present in pseudosuchians with
1193 semi-pelagic lifestyle and linked to basking for animals with low mobility, these results are
1194 backed by findings from Pochat-Cottilloux *et al.* (2022). Therefore, the loss of ornamentation in

1195   Thalattosuchia may rather be linked to an increasingly pelagic lifestyle than directly to
1196   hydrodynamic efficiency. The reduction of ornamentation of the cranium and osteoderms was
1197   also observed by Foffa *et al*. (2019) in teleosauroids and similarly linked it to adaptation to
1198   pelagic lifestyle.
1199   The description of *To. jurensis* contradicts some aspects of the other proposed evolutionary
1200   trends. *Torvoneustes jurensis* presents slenderer and sharper teeth than the other *Torvoneustes*
1201   species, except *To. mexicanus*. In their description, Barrientos-Lara *et al*. (2016) raised the
1202   question of whether the slender and sharp teeth of *To. mexicanus* could be linked to ontogeny,
1203   but the lack of data to characterize ontogenic changes within *Torvoneustes* teeth led them to
1204   consider the differences between *To. mexicanus* and other *Torvoneustes* as a specific
1205   characteristic. The teeth of *To. jurensis* are very similar to those of *To. mexicanus*. However, the
1206   skull length of the holotype of *To. jurensis* is similar to that of the holotype of *To. carpenteri*.
1207   Their body length is estimated to be close to 4.0 m for *To. jurensis* and between 4.0 and 4.70 m
1208   for *To. carpenteri* (Grange & Benton, 1996; Wilkinson *et al.*, 2008; Young *et al.*, 2011; De
1209   Sousa Oliveira *et al.*, in press). Therefore, ontogeny cannot explain the differences in tooth
1210   morphology between these species. The sharp and slender teeth of *To. jurensis* and *To.*
1211   *mexicanus* may instead represent a diverging tooth morphotype within the genus. It might
1212   indicate that *To. mexicanus* and *To. jurensis* are less specialized than species with more robust
1213   teeth. They might be opportunist feeders with durophagous tendencies. This would be consistent
1214   with the Kimmeridgian environment of the Jura platform: *Torvoneustes jurensis* was found in a
1215   carbonate platform environment where remains of teleosauroids (*Sericodon jugleri* Von Meyer,
1216   1845; *Proexochokefalos* cf. *bouchardi* and another durophagous genus *Machimosaurus hugii*
1217   Meyer, 1837) are abundant, as well as many coastal marine turtles (Thalassochelydia Anquetin,
1218   Püntener and Joyce, 2017) and fishes with hard scale (e.g., *Scheenstia* sp., Figure 20).
1219   The maxillary tooth count of *To. jurensis* is estimated to be at least 16 or 17, but is probably
1220   higher. Therefore, it seems like the reduction of maxillary tooth count is not a homogenous trend
1221   in the genus. However, it should be stressed once more that no definitive maxillary tooth count is
1222   known at the moment for any specimen referred to *Torvoneustes*. It is then possibly too early to
1223   conclude on any trend for this character.
1224   Regarding the increase in body size, it should be noted that crocodilians continue to grow well
1225   into adulthood (Sebens, 1987; Grigg & Kirshner, 2015) and that only a handful of specimens are
1226   known for *Torvoneustes*. In these circumstances, any conclusion on size evolutionary trends
1227   must therefore be taken with care. As noted above, the holotype specimens of *To. carpenteri* and
1228   *To. jurensis* are roughly of comparable total length, which could agree with the proposed
1229   evolutionary trend as the two species are roughly of the same age. However, many isolated teeth
1230   showing similar characteristics as those of MJSN BSY008-465 were found in the same
1231   stratigraphical layers during the excavation on the A16 highway, along with teeth of *Sericodon, ,*
1232   *Proexochokefalos, Machimosaurus* and *Dakosaurus* (Schaefer, 2012; Schaefer *et al.*, 2018) :
1233   teeth with sub-circular to ovoid cross-section, bicarinate with micro-ziphodont condition, enamel
1234   ornamentation composed of sub parallel apicobasal ridges on the basal two thirds of the crown

1235   shifting into low relief drop-shaped ridges forming an "anastomosed pattern" on the remaining
1236   upper third of the crown. These teeth show a great variation of height and base length (Schaefer,
1237   2012; LCG, pers. obs.). One of these teeth in particular (MJSN TCH007-91) shows a base length
1238   31% longer than the largest tooth associated with MJSN BSY008-465. The great variation in
1239   crown size of isolated teeth indicates that specimens of various sizes (and potentially ages)
1240   visited the area, including specimens significantly larger than MJSN BSY008-465. Considering
1241   there is only a few *Torvoneustes* specimens known between the middle Oxfordian and the
1242   Tithonian, it seems premature to consider size increase as an evolutionary trend in *Torvoneustes*
1243   for the moment.
1244
1245
1246

Conclusions

1248   The holotype of *Torvoneustes jurensis* is the most complete skeleton of the genus and the first
1249   specimen to preserve both extensive cranial and postcranial material. This new species is distinct
1250   from the other species on the basis of cranial morphology, dental characters, and geographic
1251   distribution. The phylogenetic analysis tends to confirm these observations. The distinction
1252   between *To. jurensis* and *To. mexicanus* remains difficult due to the fragmentary nature of the
1253   Mexican specimen. While future discovery of more specimens of *To. mexicanus* might help to
1254   get a better understanding of the differences between these two taxa, the dental characters allow
1255   us to discriminate them as two distinct species. It is interesting to note also that the genera
1256   *Cricosaurus* and *Dakosaurus* are as well found in the Kimmeridgian deposits of Europe, Mexico
1257   and South America, but that they are represented by different species in each of these
1258   geographically distant areas (Buchy *et al.*, 2006b, 2013; Pol & Gasparini, 2009; Young *et al.*,
1259   2012b; Herrera, 2015; Herrera *et al.*, 2021a). In addition, it seems that the Late Jurassic marine
1260   reptiles of the Mexican Gulf are represented by species that differ from the coeval European and
1261   South American fauna, with the notable exception of one specimen of *Ophtalmosaurus* (Buchy
1262   *et al.*, 2006a; Buchy, 2007).
1263
1264

Acknowledgements

1266   The authors would like to thank the Paleontology A16 team for the discovery and initial surface
1267   preparation of the specimen, Renaud Roch (Jurassica Museum) for his skillful complete
1268   extraction of the bones from the matrix, and Davit Vasilyan (Jurassica Museum) for the
1269   acquisition of the images from the digital microscope. We would also like to thank Corentin
1270   Jouault (Muséum National d'Histoire Naturelle) for his help with setting up Bayesian analysis
1271   and Mark Young (University of Edinburgh) for giving access to the character matrix and TNT
1272   script as well as for editing the manuscript. We thank the reviewers Pascal Abel (University of
1273   Tuebingen), Sven Sachs (Naturkunde-Museum Bielefeld) and Davide Foffa (Virginia Tech) for
1274   their comments that helped improve the quality of the manuscript, and Kenneth De Baets

1275 (University of Warsaw) for editing the second draft of the manuscript. We also thank the Willi
1276 Hennig Society for making TNT freely available.

1277
1278
1279
1280

References

1282 Abel, P., Sachs, S., Young, M.T., 2020. Metriorhynchid crocodylomorphs from the lower
1283 Kimmeridgian of Southern Germany: evidence for a new large-bodied geosaurin lineage in
1284 Europe. Alcheringa: An Australasian Journal of Palaeontology 44(2), p. 312- 326.
1285 Aiglstorfer, M., Havlik, P., & Herrera, Y., 2020. The first metriorhynchoid crocodyliform
1286 from the Aalenian (Middle Jurassic) of Germany, with implications for the evolution of
1287 Metriorhynchoidea. Zoological Journal of the Linnean Society 188(2), p. 522-551.
1288 Andrade, M.B., Young, M.T., Desojo, J.B., Brusatte, S.L., 2010. The evolution of
1289 extreme hypercarnivory in Metriorhynchidae (Mesoeucrocodylia: Thalattosuchia) based on
1290 evidence from microscopic denticle morphology. Journal of Vertebrate Paleontology 30(5), p.
1291 1451-1465.
1292 Andrews, C.W., 1909. On some new steneosaurs from the Oxford Clay of Peterborough.
1293 Annals and Magazine of Natural History 3, p. 299-308.
1294 Andrews, C.W., 1913. A descriptive catalogue of marine reptiles of the oxford clay.
1295 Based on the Leeds collection in The British Museum (Natural History), London. Part II.
1296 Anquetin, J., Püntener, C., Joyce, W.G., 2017. A Review of the Fossil Record of Turtles
1297 of the Clade Thalassochelydia, Bulletin of the Peabody Museum of Natural History 58(2), p.
1298 317-369
1299 Barrientos-Lara, J.I., Herrera, Y., Fernández, M.S., Alvarado-Ortega, J., 2016.
1300 Occurrence of *Torvoneustes* (Crocodylomorpha, Metriorhynchidae) in marine Jurassic deposits
1301 of Oaxaca, Mexico. Revista Brasileira de Paleontologia 19(3), p. 415-424.
1302 Brochu, C.A., 1996. Closure of neurocentral sutures during crocodilian ontogeny:
1303 Implications for maturity assessment in fossil archosaurs. Journal of Vertebrate Paleontology 16,
1304 p. 49–62.
1305 Buchy, M.-C., 2008. New occurrence of the genus *Dakosaurus* (Reptilia, Thalattosuchia)
1306 in the Upper Jurassic of north-eastern Mexico, with comments upon skull architecture of
1307 Dakosaurus and Geosaurus. Neues Jahrbuch für Geologie und Paläontologie - Abhandlungen
1308 249(1), p.1-8.
1309 Buchy, M.-C., 2007. Mesozoic marine reptiles from northeast Mexico: description,
1310 systematics, assemblages and palaeobiogeography. Unpublished PhD thesis, University of
1311 Karlsruhe
1312 Buchy, M.-C., Frey, E., Stinnesbeck, W., López, J.G., 2006a. An annotated catalogue of
1313 the Upper Jurassic (Kimmeridgian and Tithonian) marine reptiles in the collections of the

1314 Universidad Autónoma de Nuevo León, Facultad de Ciencias de la Tiersra, Linares, Mexico.
1315 ORYCTOS 6.
1316   Buchy, M.-C., Vignaud, P., Frey, E., Stinnesbeck, W., González, A.H.G., 2006b. A new
1317 thalattosuchian crocodyliform from the Tithonian (Upper Jurassic) of northeastern Mexico.
1318 Comptes Rendus Palevol 5, p. 785–794.
1319   Buchy, M.-C., Young, M.T., Andrade, M.B., 2013. A new specimen of *Cricosaurus*
1320 *saltillensis* (Crocodylomorpha: Metriorhynchidae) from the Upper Jurassic of Mexico: evidence
1321 for craniofacial convergence within Metriorhynchidae. ORYCTOS 10, p. 9-21
1322   Cau, A., Fanti, F., 2011. The oldest known metriorhynchid crocodylian from the Middle
1323 Jurassic of North-eastern Italy: *Neptunidraco ammoniticus* gen. et sp. nov. Gondwana Research
1324 19, p. 550–565.
1325   Chiarenza, A.A., Foffa, D., Young, M.T., Insacco, G., Cau, A., Carnevale, G.,
1326 Catanzariti, R., 2015. The youngest record of metriorhynchid crocodylomorphs, with
1327 implications for the extinction of Thalattosuchia. Cretaceous Research 9.
1328   Clarac, F., De Buffrénil, V., Brochu, C., Cubo, J., 2017. The evolution of bone
1329 ornamentation in Pseudosuchia: morphological constraints versus ecological adaptation.
1330 Biological Journal of the Linnean Society 121, p. 395–408.
1331 https://doi.org/10.1093/biolinnean/blw034
1332   Colombié, C., Strasser, A., 2005. Facies, cycles, and controls on the evolution of a keep-
1333 up carbonate platform (Kimmeridgian, Swiss Jura): Evolution of a keep-up carbonate platform.
1334 Sedimentology 52, p. 1207–1227. https://doi.org/10.1111/j.1365-3091.2005.00736.x
1335   Comment, G., Lefort, A., Koppka, J., Hantzpergue, P., 2015. Le Kimméridgien D'Ajoie
1336 (Jura, Suisse) : Lithostratigraphie Et Biostratigraphie De La Formation De Reuchenette.
1337 https://doi.org/10.5281/ZENODO.34341
1338   de Buffrenil, V., 1982. Morphogenesis of bone ornamentation in extant and extinct
1339 crocodilians. Zoomorphology 99, p. 155–166.
1340   de Buffrénil, V., Clarac, F., Fau, M., Martin, S., Martin, B., Pellé, E., Laurin, M., 2015.
1341 Differentiation and growth of bone ornamentation in vertebrates: A comparative histological
1342 study among the Crocodylomorpha: Development of Bone Ornamentation In The
1343 Crocodylomorpha. Journal of Morphology 276, p. 425–445. https://doi.org/10.1002/jmor.20351
1344   De sousa oliveira, S., Girard, L., Raselli, I., Anquetin, J., In Press. Virtual reconstruction
1345 of a Late Jurassic metriorhynchid skull from Switzerland and its use for scientific illustration and
1346 paleoart. MorphoMuseuM.
1347   Fara, E., Ouaja, M., Buffetaut, E., Srarfi, D., 2002. First occurrences of thalattosuchian
1348 crocodiles in the Middle and Upper Jurassic of Tunisia. Neues Jahrbuch fur Geologie und
1349 Palaontologie - Monatshefte 8, p. 465-476. 10.1127/njgpm/2002/2002/465.
1350   Fitzinger, L. J. F. J. 1843. Systema Reptilium. Fasciculus Primus, Amblyglossae.
1351 Braumüller et Seidel, Vienna.
1352   Foffa, D., Young, M.T., 2014. The cranial osteology of *Tyrannoneustes lythrodectikos*
1353 (Crocodylomorpha: Metriorhynchidae) from the Middle Jurassic of Europe. PeerJ 2, e608.

1354   Foffa, D., Young, M.T., Brusatte, S.L., Graham, M.R., Steel, L., 2017. A new
1355   metriorhynchid crocodylomorph from the Oxford Clay Formation (Middle Jurassic) of England,
1356   with implications for the origin and diversification of Geosaurini. Journal of Systematic
1357   Palaeontology 16, p. 1123–1143.
1358   Foffa, D., Young, M.T., Brusatte, S.L., 2018a. Filling the Corallian gap: New information
1359   on Late Jurassic marine reptile faunas from England. Acta Palaeontologica Polonica 63,
1360   10.4202/app.00455.2018.
1361   Foffa, D., Young, M.T., Stubbs, T.L., Dexter, K.G., Brusatte, S.L., 2018b. The long-term
1362   ecology and evolution of marine reptiles in a Jurassic seaway. Nature Ecology & Evolution 2, p.
1363   1548–1555. https://doi.org/10.1038/s41559-018-0656-6
1364   Foffa, D., Johnson, M. M., Young, M. T., Steel, L., & Brusatte, S. L., 2019. Revision of
1365   the Late Jurassic deep-water teleosauroid crocodylomorph *Teleosaurus megarhinus* Hulke, 1871
1366   and evidence of pelagic adaptations in Teleosauroidea. PeerJ, 7, e6646.
1367   Fraas, E., 1901. Die Meerkrokodile (Thalattosuchia n. g.) eine neue Sauriergruppe der
1368   Juraformation. Ahreshefte des Vereins für vaterländische Naturkunde in Württemberg 57, p. 409
1369   - 418
1370   Fraas, E., 1902. Die Meer-Crocodilier (Thalattosuchia) des oberen Jura unter specieller
1371   Berücksichtigung von *Dacosaurus* und *Geosaurus*. Palaeontographica 49, p. 1–71.
1372   Frey, B., Buchy M-C, Stinnesbeck W., Guadalupe López-Oliva J., 2002. *Geosaurus*
1373   *vignaudi* n.sp. (Crocodyliformes: Thalattosuchia), first evidence of metriorhynchid crocodilians
1374   in the Late Jurassic (Tithonian) of central-east Mexico (State of Puebla). Canadian Journal of
1375   Earth Sciences 39(10), p. 1467-1483. https://doi.org/10.1139/e02-060
1376   Gandola, R., Buffetaut, E., Monaghan, N., Dyke, G., 2006. Salt glands in the fossil
1377   crocodile Metriorhynchus. Journal of Vertebrate Paleontology 26, p. 1009–1010.
1378   Gasparini, Z., Iturralde-Vinent, M., 2001. Metriorhynchid crocodiles (Crocodyliformes)
1379   from the Oxfordian of Western Cuba. Neues Jahrbuch fur Geologie und Palaontologie -
1380   Monatshefte 2001, p. 534-542. 10.1127/njgpm/2001/2001/534.
1381   Geoffroy Saint-Hilaire, E. 1831. Recherches sur de grands sauriens trouvés à l'état fossile
1382   aux confins maritimes de la Basse-Normandie, attribués d'abord au Crocodile, puis déterminés
1383   sous les noms de *Teleosaurus* et *Steneosaurus*. Mémoires de l'Academie des sciences 12.
1384   George, I.D., Holliday, C.M., 2013. Trigeminal nerve morphology in *Alligator*
1385   *mississippiensis* and Its significance for Crocodyliform facial sensation and evolution. The
1386   Anatomical Record 296, p. 670–680.
1387   Goloboff, P.A., Catalano, S.A., 2016. TNT version 1.5, including a full implementation
1388   of phylogenetic morphometrics. Cladistics 32, p. 221–238.
1389   Goloboff, P.A., Farris, J.S., Nixon, K.C., 2008. TNT, a free program for phylogenetic
1390   analysis Cladistics 24, p. 774–786.
1391   Gower, D. J. 1999. The cranial and mandibular osteology of a new rauisuchian archosaur
1392   from the Middle Triassic of southern Germany. Stuttgarter Beiträge zur Naturkunde Serie B
1393   (Geologie und Paläontologie) 280, p. 1-49

1394   Grange, D.R., Benton, M.J., 1996. Kimmeridgian metriorhynchid crocodiles from
1395   England. Palaeontology. 39, p. 497-514

1396   Grigg, Gordon, Kirshner, D., 2015. Biology and Evolution of Crocodylians. CSIRO
1397   Publishing.

1398   Guignard. J.-P. & Weidmann. M., 1977. Nouveaux gisements de crocodiliens dans le
1399   Malm du Jura. Bulletin de la Société Vaudoise des Sciences Naturelles 73, p. 297-308

1400   Hay, O. P., 1930. Second Bibliography and Catalogue of the Fossil Vertebrata of North
1401   America, Vol II. Carnegie Institution of Washington Publication 390, Carnegie Institution of
1402   Washington, Washington, DC.

1403   Herrera Y., 2015. Metriorhynchidae (Crocodylomorpha: Thalattosuchia) from Upper
1404   Jurassic–Lower Cretaceous of Neuquén Basin (Argentina), with comments on the natural casts
1405   of the brain. In: M. Fernández, Y. Herrera (Eds.) Reptiles Extintos - Volumen en Homenaje a
1406   Zulma Gasparini. Publicación Electrónica de la Asociación Paleontológica Argentina 15(1), p.
1407   159–171.

1408   Herrera, Y., Fernández, M.S., Gasparini, Z., 2013. Postcranial skeleton *of Cricosaurus*
1409   *araucanensis* (Crocodyliformes: Thalattosuchia): morphology and palaeobiological insights 15.

1410   Herrera, Y., Gasparini, Z., & Fernández, M. S. 2015a. *Purranisaurus potens* Rusconi, an
1411   enigmatic metriorhynchid from the Late Jurassic–Early Cretaceous of the Neuquén Basin.
1412   Journal of Vertebrate Paleontology, 35(2), e904790.

1413   Herrera, Y., Fernández, M.S., Lamas, S.G., Campos, L., Talevi, M., Gasparini, Z., 2015b.
1414   Morphology of the sacral region and reproductive strategies of Metriorhynchidae : a counter-
1415   inductive approach. Earth and Environmental Science Transactions of The Royal Society of
1416   Edinburgh 106, p. 247–255. https://doi.org/10.1017/S1755691016000165

1417   Herrera, Y., Aiglstorfer, M., Bronzati, M., 2021a. A new species of *Cricosaurus*
1418   (Thalattosuchia: Crocodylomorpha) from southern Germany: the first three dimensionally
1419   preserved *Cricosaurus* skull from the Solnhofen Archipelago. Journal of Systematic
1420   Palaeontology 19(2), p. 145-167

1421   Herrera, Y., Fernández, M.S., Vennari, V.V., 2021b. *Cricosaurus* (Thalattosuchia,
1422   Metriorhynchidae) survival across the J/K boundary in the High Andes (Mendoza Province,
1423   Argentina). Cretaceous Research 118, 104673. https://doi.org/10.1016/j.cretres.2020.104673

1424   Holliday, C.M., Witmer, L.M., 2007. Archosaur adductor chamber evolution: Integration
1425   of musculoskeletal and topological criteria in jaw muscle homology. Journal of Morphology 268,
1426   p. 457–484. https://doi.org/10.1002/jmor.10524

1427   Holliday, C.M., Witmer, L.M., 2009. The epipterygoid of crocodyliforms and its
1428   significance for the evolution of the orbitotemporal region of eusuchians, Journal of Vertebrate
1429   Paleontology 29(3), p. 715-733, DOI: 10.1671/039.029.0330

1430   Iordansky, N.N., 1973. The skull of the Crocodilia. In Biology of the Reptilia 4 (Eds C
1431   Gans and TS Parsons), p. 201–260. Academic Press, New York

1432   Johnson, M., Young, M.T., Steel, L., Foffa, D., Smith, A., Hua, S., Havlik, P., Howlett,
1433   E., Dyke, G., 2017. Re-description of '*Steneosaurus*' *obtusidens* Andrews, 1909, an unusual

1434 macrophagous teleosaurid crocodylomorph from the Middle Jurassic of England. Zoological
1435 Journal of the Linnean Society 182, p.1-34. 10.1093/zoolinnean/zlx035.
1436   Johnson, M. M., Young, M. T., & Brusatte, S. L., 2020b. The phylogenetics of
1437 Teleosauroidea (Crocodylomorpha, Thalattosuchia) and implications for their ecology and
1438 evolution. PeerJ 8, e9808.
1439   Krebs, B., 1967. Zwei Sieneosaurus-Wirbel aus den Birmenstorfer Schichten (Ober-
1440 Oxford) vom «Weissen Graben» bei Mönthal (Kt. Aargau). Eclogae Geologicae Helvetiae 60, p.
1441 689-695.
1442   Le Mort, J., Martin, J.E., Picot, L., Hua, S., 2022. First description of the most complete
1443 *Metriorhynchus* aff. *superciliosus* (Thalattosuchia) specimen from the Callovian of the Vaches-
1444 Noires cliffs (Normandy, France) and limitations in the classification of Metriorhynchidae. In
1445 Annales de Paléontologie 108(3). Elsevier Masson.
1446   Leardi, J. M., Pol, D., & Clark, J. M., 2017. Detailed anatomy of the braincase of
1447 *Macelognathus vagans* Marsh, 1884 (Archosauria, Crocodylomorpha) using high resolution
1448 tomography and new insights on basal crocodylomorph phylogeny. PeerJ 5, e2801.
1449 https://doi.org/10.7717/peerj.2801
1450   Lepage, Y., Buffetaut, E., Hua, S., Martin, J.E., Tabouelle, J., 2008. Catalogue descriptif,
1451 anatomique, géologique et historique des fossiles présentés à l'exposition « Les Crocodiliens
1452 fossiles de Normandie » (6 novembre - 14 décembre 2008). Bulletin de la Société Géologique de
1453 Normandie et des Amis du Muséum du Havre 95(2), p. 5-152.
1454   Lydekker, R., 1889. On the remains and affinities of five genera of Mesozoic reptiles.
1455 Quarterly Journal of the Geological Society 45, p. 41-59.
1456 Maddison, W. P. and D.R. Maddison. 2019. Mesquite: a modular system for evolutionary
1457 analysis. Version 3.61 http://www.mesquiteproject.org
1458   Madzia, D., Sachs, S., Young, M. T., Lukeneder, A., Skupien, P., 2021. Evidence of two
1459 lineages of metriorhynchid crocodylomorphs in the Lower Cretaceous of the Czech Republic.
1460 Acta Palaeontologica Polonica 66(2).
1461   Martin, J.E., Vincent, P., Falconnet, J., 2015. The taxonomic content of *Machimosaurus*
1462 (Crocodylomorpha, Thalattosuchia). Comptes Rendus Palevol 14, p. 305– 310.
1463   Meyer, H. von, 1845. System der fossilen Saurier [Taxonomy of fossil saurians]. Neues
1464 Jahrbuch für Mineralogie, Geognosie, Geologie und PetrefaktenKunde. p. 278-285
1465   Martin, J. E. and Vincent, P., 2013. New remains of Machimosaurus hugii von Meyer,
1466 1837 (Crocodilia, Thalattosuchia) from the Kimmeridgian of Germany, Fossil Record, 16, p.
1467 179–196, https://doi.org/10.1002/mmng.201300009
1468   Marty, D., Hug, W., Iberg, A., Cavin, L., Meyer, C., Lockley, M., 2003. Preliminary
1469 Report on the Courtedoux Dinosaur Tracksite from the Kimmeridgian of Switzerland. Ichnos 10,
1470 p. 209–219. https://doi.org/10.1080/10420940390256212
1471   Massare, J.A., 1987. Tooth Morphology and Prey Preference of Mesozoic Marine
1472 Reptiles. Journal of Vertebrate Paleontology 7, p. 121–137.

Owen, R., 1883. On the Cranial and Vertebral characters of the Crocodilian Genus *Plesiosuchus*. Quarterly Journal of the Geological Society 40, p. 153-159

Parrilla-Bel, J., Young, M.T., Moreno-Azanza, M., Canudo, J. I., 2013. The first metriorhynchid crocodylomorph from the Middle Jurassic of Spain, with implications for evolution of the subclade Rhacheosaurini. PLoS ONE, 8:e54275. doi: 10.1371/journal.pone.0054275.

Parrilla-Bel, J., Canudo, J.I., 2015. Postcranial elements of "*Maledictosuchus riclaensis*" (Thalattosuchia) from the Middle Jurassic of Spain. Journal of Iberian Geology 41, p. 31–40. https://doi.org/10.5209/rev_JIGE.2015.v41.n1.48653

Pierce, S.E., Benton, M.J., 2006, *Pelagosaurus typus* Bronn, 1841 (Mesoeucrocodylia: Thalattosuchia) from the Upper Lias (Toarcian, Lower Jurassic) of Somerset, England, Journal of Vertebrate Paleontology 26(3), p. 621-635, DOI: 10.1671/0272-4634(2006)26[621:PTBMTF]2.0.CO;2

Pierce, S.E., Angielczyk, K.D. and Rayfield, E.J., 2009. Shape and mechanics in thalattosuchian (Crocodylomorpha) skulls: implications for feeding behaviour and niche partitioning. Journal of Anatomy 215, p. 555-576. https://doi.org/10.1111/j.1469-7580.2009.01137.x

Pochat-Cottilloux, Y., Martin, J. E., Amiot, R., Cubo, J., de Buffrénil, V., 2022. A survey of osteoderm histology and ornamentation among Crocodylomorpha: A new proxy to infer lifestyle? Journal of Morphology 284, e21542. https://doi.org/10.1002/jmor.21542

Pol, D., Gasparini, Z., 2009. Skull anatomy of *Dakosaurus andiniensis* (Thalattosuchia: Crocodylomorpha) and the phylogenetic position of Thalattosuchia. Journal of Systematic Palaeontology 7(2), p. 163–197.

Prasad, G.V.R., de Lapparent de Broin, F., 2002. Late Cretaceous crocodile remains from Naskal (India): comparisons and biogeographic affinities. Annales de Paléontologie 88, p. 19–71. https://doi.org/10.1016/S0753-3969(02)01036-4

Püntener C, Anquetin J, Billon-Bruyat J-P., 2020. New material of "Eurysternidae" (Thalassochelydia, Pan-Cryptodira) from the Kimmeridgian of the Swiss Jura Mountains. Palaeovertebrata 43:e2. DOI: 10.18563/pv.43.1.e2.

Quenstedt, F. A., 1856. Sonst und jetzt: populäre Vorträge über Geologie. Laupp

Rieppel, O., 1979. Ein *Geosaurus*-fragment (Reptilia, Thalattosuchia) aus dem oberen Malm von Evilard bei Biel.

Rieppel, O., 1981. Fossile Krokodilier aus dem Schweizer Jura. Eclogae Geologicae Helvetiae 74(3), p. 735-751.

Ronquist, F., Teslenko, M., van der Mark, P., Ayres, D.L., Darling, A., Höhna, S., Larget, B., Liu, L., Suchard, M.A., Huelsenbeck, J.P., 2012. MrBayes 3.2: Efficient Bayesian phylogenetic inference and model choice across a large model space. Systematic Biology 61, p. 539–542.

1511   Ruebenstahl, A.A., Klein, M.D., Yi, H., Xu, X., & Clark, J.M., 2022. Anatomy and
1512 relationships of the early diverging Crocodylomorphs Junggarsuchus sloani and Dibothrosuchus
1513 elaphros. The Anatomical Record 305(10), p. 2463– 2556. https://doi.org/10.1002/ar.24949
1514   Sachs, S., Young, M., Abel, P., Mallison, H., 2019. A new species of the metriorhynchid
1515 crocodylomorph *Cricosaurus* from the Upper Jurassic of southern Germany. Acta
1516 Palaeontologica Polonica 64. https://doi.org/10.4202/app.00541.2018
1517   Sachs, S., Young, M.T., Hornung, J.J., 2020. The enigma of *Enaliosuchus*, and a
1518 reassessment of the Lower Cretaceous fossil record of Metriorhynchidae, Cretaceous Research,
1519 114, 104479, ISSN 0195-6671, https://doi.org/10.1016/j.cretres.2020.104479.
1520   Sachs, S., Young, M., Abel, P., Mallison, H., 2021. A new species of *Cricosaurus*
1521 (Thalattosuchia, Metriorhynchidae) based upon a remarkably well-preserved skeleton from the
1522 Upper Jurassic of Germany. Palaeontologia Electronica. https://doi.org/10.26879/928
1523   Schaefer, K., 2012. Variabilité de la morphologie dentaire des crocodiliens marins
1524 (Thalattosuchia) du Kimméridgien d'Ajoie (Jura, Suisse). Mémoire de Master (non-publié),
1525 Université de Fribourg.
1526   Schaefer, K., Billon-Bruyat, J.-P., Hug, W.A., Friedli, V., Püntener, C., 2018. Vertébrés
1527 mésozoïques: crocodiliens. Catalogue du patrimoine paléontologique jurassien - A16.
1528   Schwab, J.A., Young, M.T., Walsh, S.A., Witmer, L.M., Herrera, Y., Brochu, C.A.,
1529 Butler, B.I., Brusatte, S.L., 2022. Ontogenetic variation in the crocodylian vestibular system.
1530 Journal of Anatomy 240, p. 821– 832. Available from: https://doi.org/10.1111/joa.13601
1531   Sebens, K.P., 1987. The Ecology of Indeterminate Growth in Animals 37.
1532   Spindler, F., R. Lauer, H. Tischlinger, and M. Mäuser. 2021. The integument of pelagic
1533 crocodylomorphs (Thalattosuchia: Metriorhynchidae). Palaeontologia Electronica 24:a25. doi:
1534 10.26879/1099.
1535   Vignaud, P. 1995. Les Thalattosuchia, crocodiles marins du Mesozoique: systematique
1536 phylogenetique, paleoecologie, biochronologie et implications paleogeographiques. Ph.D.
1537 dissertation, Universite de Poitiers, Poitiers, France,
1538   Vignaud, P., 1997. La morphologie dentaire des thalattosuchia (Crocodylia, Mesosuchia).
1539   von Arthaber, G., 1906. Beiträge zur kenntnis der organisation und der
1540 anpassungsercheinungen des genus *Metriorhynchus*.
1541   Wagner, J. A., 1858. Neue Beiträge zur Kenntniss der urweltlichen Fauna des
1542 lithographischen Schiefers: Saurier 8.
1543   Waskow, K., Grzegorczyk, D., Sander, P.M., 2018. The first record of *Tyrannoneustes*
1544 (Thalattosuchia: Metriorhynchidae): a complete skull from the Callovian (late Middle Jurassic)
1545 of Germany. PalZ 92, p. 457–480.
1546   Wilberg, E.W., 2012, Phylogenetic and morphometric assessment of the evolution of the
1547 longirostrine crocodylomorphs, The University of Iowa.
1548   Wilberg, E.W., Godoy, P.L., Griffiths, E.F., Turner, A.H. Benson, R.B., 2022. A new
1549 early diverging thalattosuchian (Crocodylomorpha) from the Early Jurassic (Pliensbachian) of

1550 Dorset, UK and implications for the origin and evolution of the group. Journal of Vertebrate
1551 Paleontology, p.e2161909.

1552 Wilkinson, L.E., Young, M.T., Benton, M.J., 2008. A new metriorhynchid crocodilian
1553 (Mesoeucrocodylia Thalattosuchia) from the Kimmeridgian (Upper Jurassic) of Wiltshire, UK.
1554 Palaeontology 51, p. 1307– 1333.

1555 Young M.T., Hua S., Steel L., Foffa D., Brusatte S.L., Thüring S., Mateus O., Ruiz-
1556 Omeñaca J.I., Havlik P., Lepage Y., De Andrade M.B., 2014a. Revision of the Late Jurassic
1557 teleosaurid genus Machimosaurus (Crocodylomorpha, Thalattosuchia) Royal Society Open
1558 Science 1, 140222 140222 http://doi.org/10.1098/rsos.140222

1559 Young, M.T., 2014b. Filling the 'Corallian Gap': re-description of a metriorhynchid
1560 crocodylomorph from the Oxfordian (Late Jurassic) of Headington, England. Historical Biology
1561 26, p. 80–90.

1562 Young, M.T., Andrade, M.B., 2009. What is *Geosaurus*? Redescription of *Geosaurus*
1563 *giganteus* (Thalattosuchia: Metriorhynchidae) from the Upper Jurassic of Bayern, Germany.
1564 Zoological Journal of the Linnean Society 157, p. 551–585.

1565 Young, M.T., Brusatte, S.L., Ruta, M., Andrade, M.B., 2010. The evolution of
1566 Metriorhynchoidea (Mesoeucrocodylia, Thalattosuchia): an integrated approach using geometric
1567 morphometrics, analysis of disparity, and biomechanics. Zoological Journal of the Linnean
1568 Society 158, p. 801–859.

1569 Young, M.T., Bell, M.A., Andrade, M.B., Brusatte, S.L., 2011. Body size estimation and
1570 evolution in metriorhynchid crocodylomorphs: implications for species diversification and niche
1571 partitioning. Zoological Journal of the Linnean Society 163(4), p. 1199–1216,
1572 https://doi.org/10.1111/j.1096-3642.2011.00734.x

1573 Young, M.T., Brusatte, S.L., Beatty, B.L., Andrade, M.B., Desojo, J.B., 2012a. Tooth-on-
1574 tooth interlocking occlusion suggests macrophagy in the Mesozoic marine crocodylomorph
1575 *Dakosaurus*. The Anatomical Record 295, p. 1147–1158.

1576 Young, M.T., Brusatte, S.L., Andrade, M.B., Desojo, J.B., Beatty, B.L., Steel, L.,
1577 Schoch, R.R., 2012b. The cranial osteology and feeding ecology of the metriorhynchid
1578 crocodylomorph genera *Dakosaurus* and *Plesiosuchus* from the Late Jurassic of Europe. PLOS
1579 ONE 7, 42.

1580 Young, M.T., Andrade, M.B., Brusatte, S.L., Sakamoto, M., Liston, J., 2013a. The oldest
1581 known metriorhynchid super-predator: a new genus and species from the Middle Jurassic of
1582 England, with implications for serration and mandibular evolution in predacious clades. Journal
1583 of Systematic Palaeontology 11, p. 475–513.

1584 Young, M.T., Andrade, M.B., Etches, S., Beatty, B.L., 2013b. A new metriorhynchid
1585 crocodylomorph from the Lower Kimmeridge Clay Formation (Late Jurassic) of England, with
1586 implications for the evolution of dermatocranium ornamentation in Geosaurini. Zoological
1587 Journal of the Linnean Society 169, p. 820–848.

1588   Young, M.T., Steel, L., Brusatte, S.L., Foffa, D., Lepage, Y., 2014. Tooth serration
1589   morphologies in the genus *Machimosaurus* (Crocodylomorpha, Thalattosuchia) from the Late
1590   Jurassic of Europe. Royal Society Open Science 1, 140269.
1591   Young, M.T., Foffa, D., Steel, L., Etches, S., 2019. Macroevolutionary trends in the
1592   genus *Torvoneustes* (Crocodylomorpha: Metriorhynchidae) and discovery of a giant specimen
1593   from the Late Jurassic of Kimmeridge, UK. Zoological Journal of the Linnean Society 189(2), p.
1594   483-493.
1595   Young, M.T., Brignon, A., Sachs, S., Hornung, J.J., Foffa, D., Kitson, J.J.N., Johnson,
1596   M.M., Steel, L., 2020a. Cutting the Gordian knot: a historical and taxonomic revision of the
1597   Jurassic crocodylomorph *Metriorhynchus*. Zoological Journal of the Linnean Society 192(2), p.
1598   510-553.
1599   Young, M.T., Sachs, S., Abel, P., Foffa, D., Herrera, Y., Kitson, J.J.N., 2020b.
1600   Convergent evolution and possible constraint in the posterodorsal retraction of the external nares
1601   in pelagic crocodylomorphs. Zoological Journal of the Linnean Society 189, p. 494- 520.

Figure 1

Geographical map of the Ajoie region, Canton of Jura, Switzerland.

The excavation site of MJSN BSY008-465 (BSY, Courtedoux–Bois de Sylleux) is indicated along the A16 Transjurane highway (in grey).
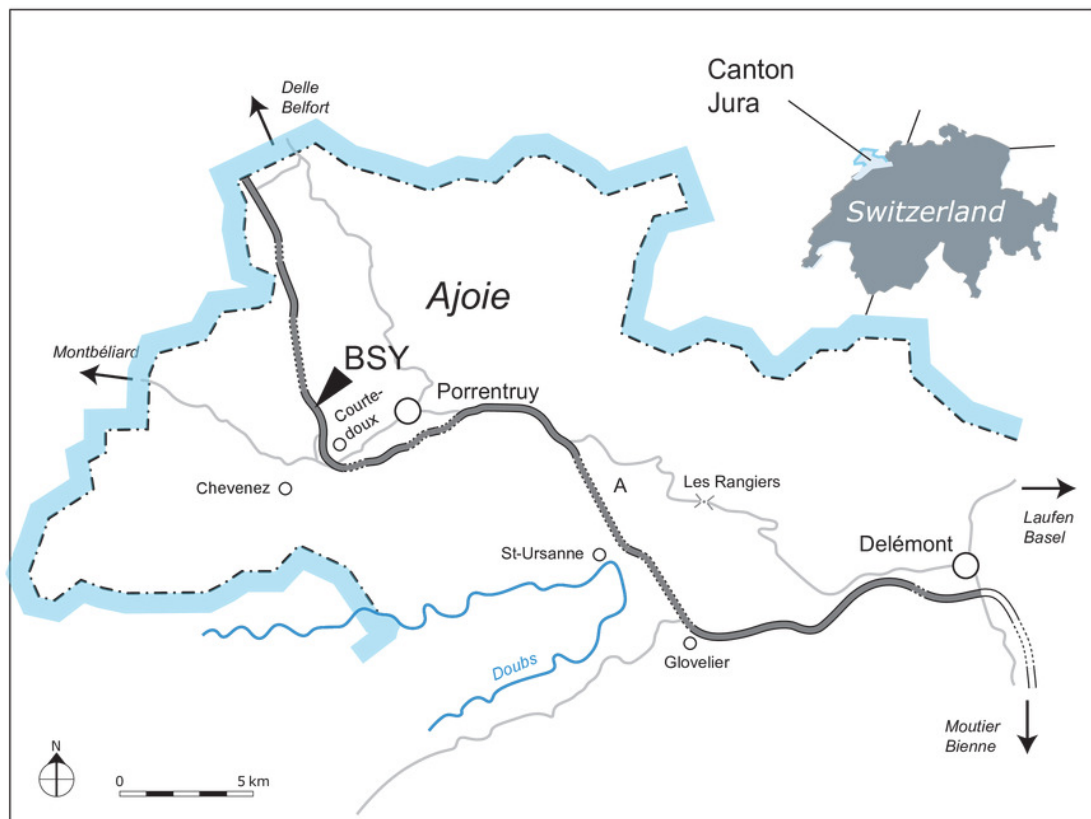
Figure 2

Taphonomical arrangement of the metriorhynchid skeleton MJSN BSY008-465.

(a) photograph of the skeleton still embedded in the limestone block (see text); (b) drawing of the bones in their taphonomical position.

50 cm
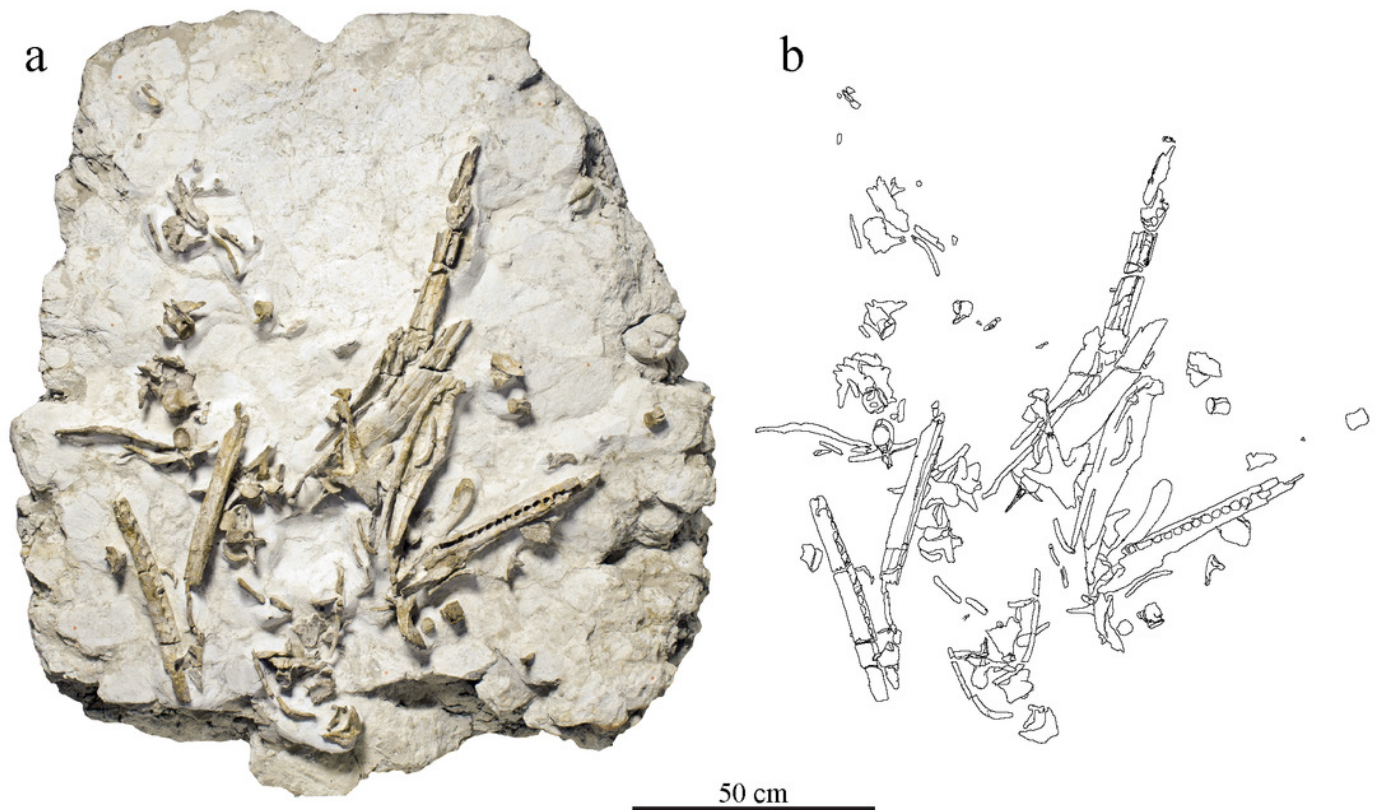
Figure 3

Stratigraphical section of the Reuchenette Formation in Ajoie, Canton of Jura, Switzerland, with a close-up on the Lower *Virgula* Marls.

MJSN BSY008-465 was found on the hardground level 4000 in the Lower *Virgula* Marls. The stratigraphical chart is derived from Comment *et al.* (2015) and Püntener *et al.* (2020).

Stage	Formation	Member	Bed	Ammonite zone	Lithology

Tithonien — Twannbach — Gigas

Autissio-dorensis

—?—

Upper Kimmeridgien — Reuchenette

Chevenez — Upper Virgula Marls — 150

Gray and White Limestones — Eudoxus

Coral Limestones — 9000 - 6000

Lower Virgula Marls

Mutabilis — 100 — 5600 / 1000

Courtedoux — Corbis Limestones — 980 - 605

600

500 / 495 / 300

Upper Pterocerian Limestones

Banné — Banné Marls — Cymodoce — 1690 B - 70 B

Lower Kimmeridgien — Vabenau

Upper Pterocerian Limestones

Creugenat Beds — 50

Thalassinoides Limestones — Baylei

—?—

Oxfordien — Courgenay — Cardium Limestones — 0m

Lower Virgula Marls — 6000 / 5600 / 5500 / 5400 / 5000 / 4500 / 4000 / 3500 / 3100 / 3000 / 10

BSY008-465

2900 / 2500 / 2450 / 2400 / 2100 / 2000 / 5

1900 / 1800 / 1700 / 1650 / 1500 / 1400 / 1300 / 1200 / 1100 / 1030 / 1000 / 0m

Corbis Limestones

Fossils
- Crocodilomorpha
- Dinosaur tracks
- Nautiloids
- Echinoderms
- Corals
- Nerineids
- Nanogyra
- Burrows

Lithology
- Indifferent limestone
- Sublithographic limestone
- Chalky limestone
- Bioclastic limestone
- Marly limestone
- Ooolithic limestone
- Granular limestone
- Marls
- Hardground

Figure 4

MJSN BSY008-465, holotype of *Torvoneustes jurensis* (Kimmeridgian, Porrentruy, Switzerland).

Scientific drawings of the reconstructed skull (a) and mandible (b) in dorsal and (c) lateral views. the remaining matrix is represented in yellow. Anterior is to the right. Abbreviations: **al**, alveolus; **an**, angular; **art**, articular; **cp**, coronoid process; **den**, dentary; **fr**, frontal; **mx**, maxilla; **na**, nasal; **pa**, parietal; **pmx**, premaxilla; **po**, postorbital; **prf**, prefrontal; **san,** surangular; **sdg,** surangulodentary groove; **sq**, squamosal; **spl**, splenial; **tc**, tooth crown.
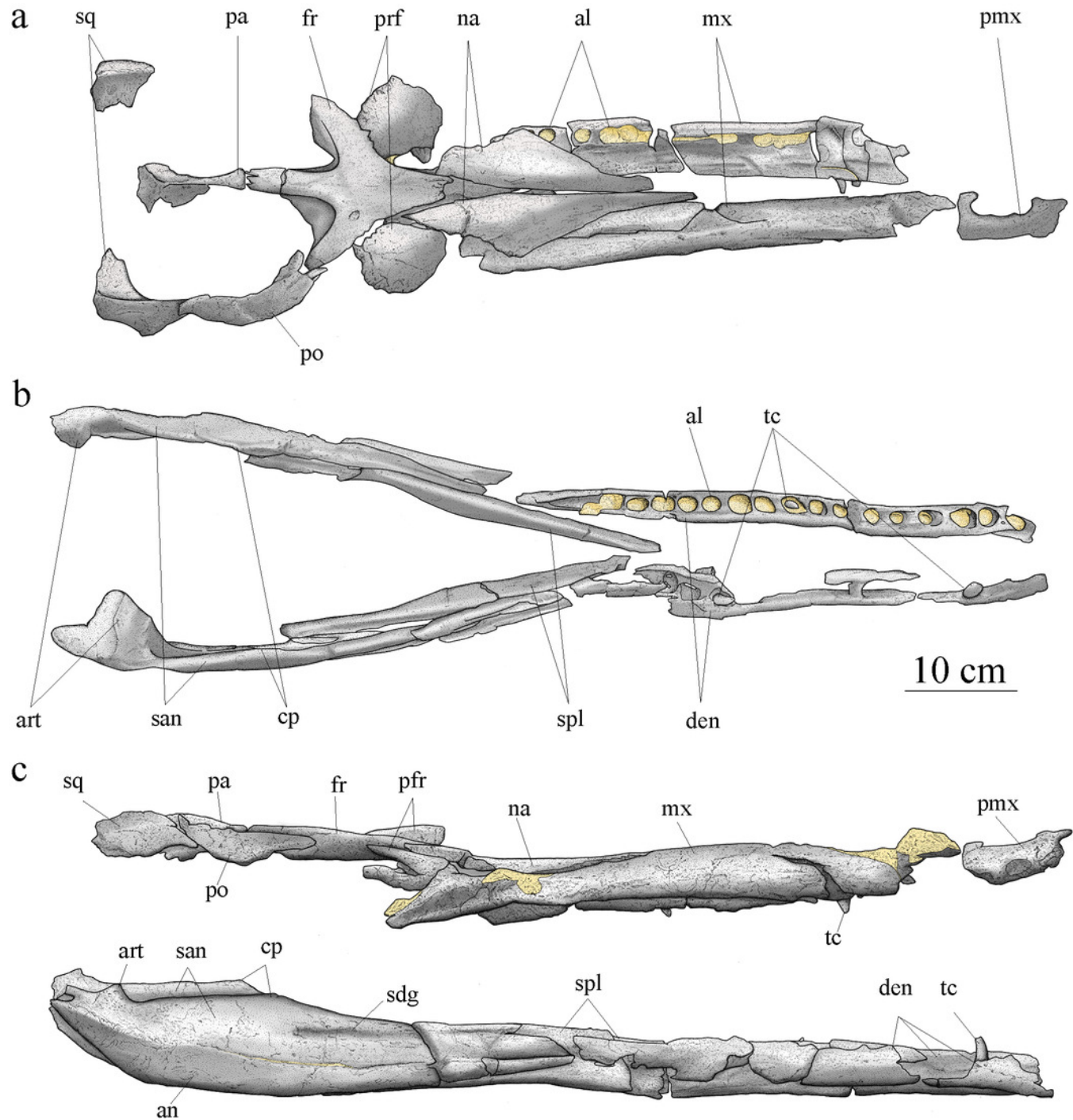
Figure 5

MJSN BSY008-465, holotype of *Torvoneustes jurensis* (Kimmeridgian, Porrentruy, Switzerland).

(a) right premaxilla, (b) right prefrontal, (c) Left nasal, and (d) right nasal in dorsal views. Anterior is to the right.
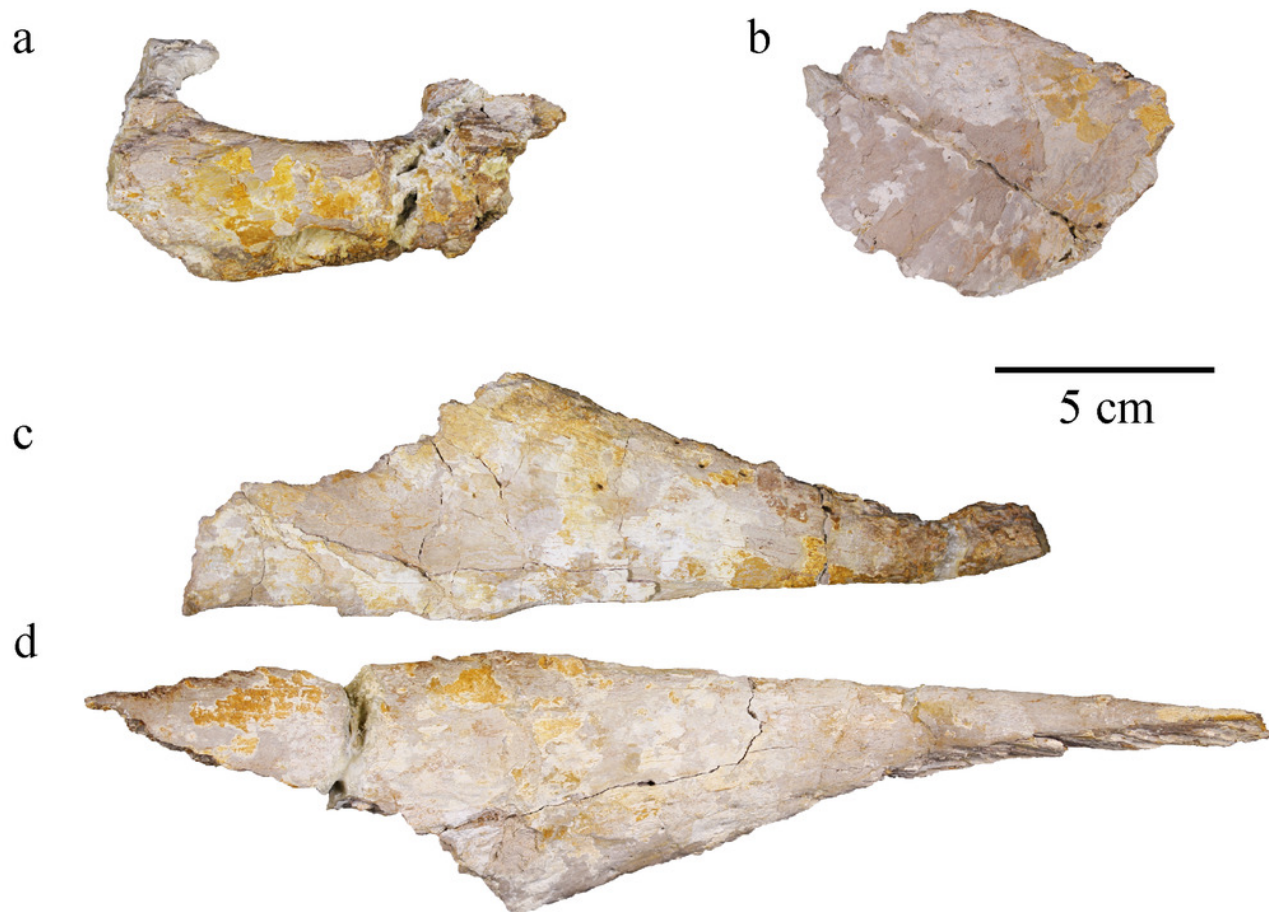
Figure 6

MJSN BSY008-465, holotype of *Torvoneustes jurensis* (Kimmeridgian, Porrentruy, Switzerland).

Photographs and scientific drawings of the right maxilla in (a, b) ventral and (c, d) lateral views. Anterior is to the right. Abbreviations: **al**, alveolus; **for**, foramen; **mx**, maxilla; **no**, notch; **pa**, palatine. Numbers indicate the preserved alveoli. Matrix is in yellow.
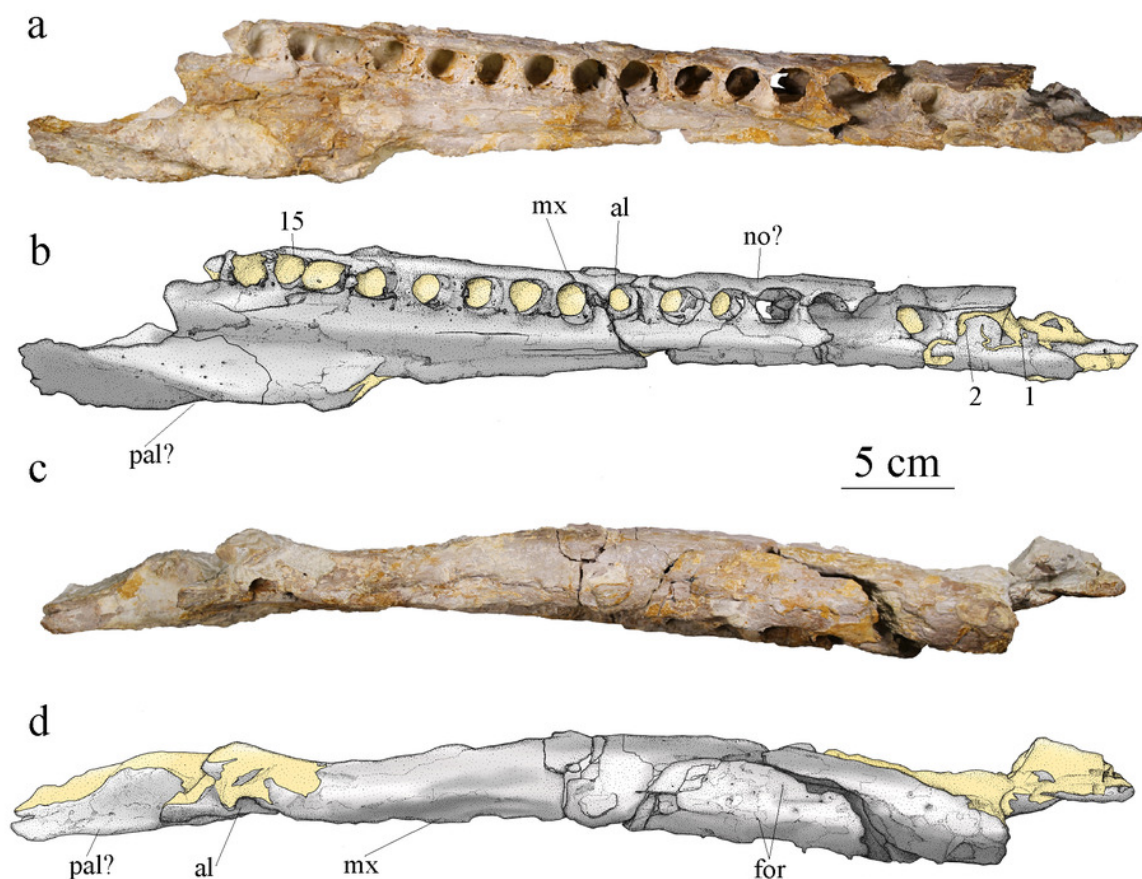
Figure 7

MJSN BSY008-465, holotype of *Torvoneustes jurensis* (Kimmeridgian, Porrentruy, Switzerland).

(a) Scientific drawing, (b) interpretative drawing and (c) photograph of the frontal and left prefrontal in dorsal view. The angle formed by the lateral contacts of the frontal with the prefrontal and nasal is indicated in (b). Abbreviation: **fr**, frontal; **if**, intertemporal flange; **prf**, prefrontal. Matrix is in yellow.
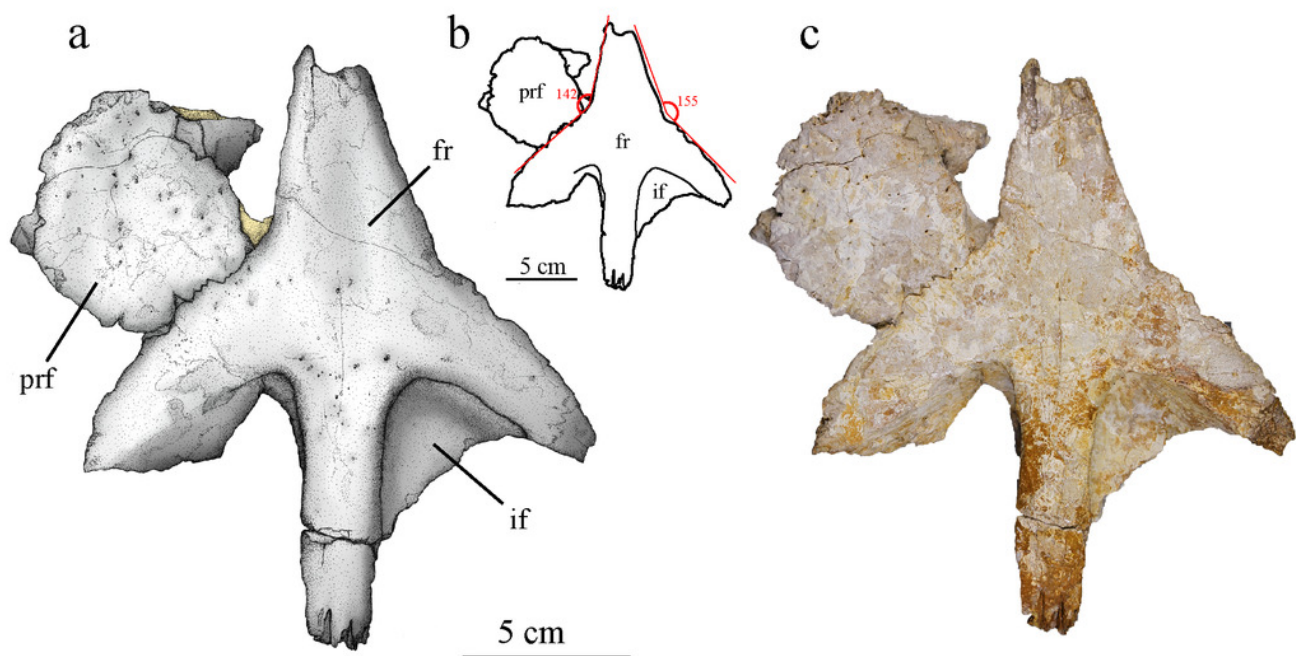
Figure 8

MJSN BSY008-465, holotype of *Torvoneustes jurensis* (Kimmeridgian, Porrentruy, Switzerland).

Posterior cranial elements with the right postorbital in (a) dorsal, (b) medial, and (c) lateral views; the parietal in (d) right lateral and (e) dorsal view; and the right squamosal in (f) dorsal view. Anterior to the right (except in b to the left). Abbreviations: **in**, incision; **sqfs**, squamosal flat surface.
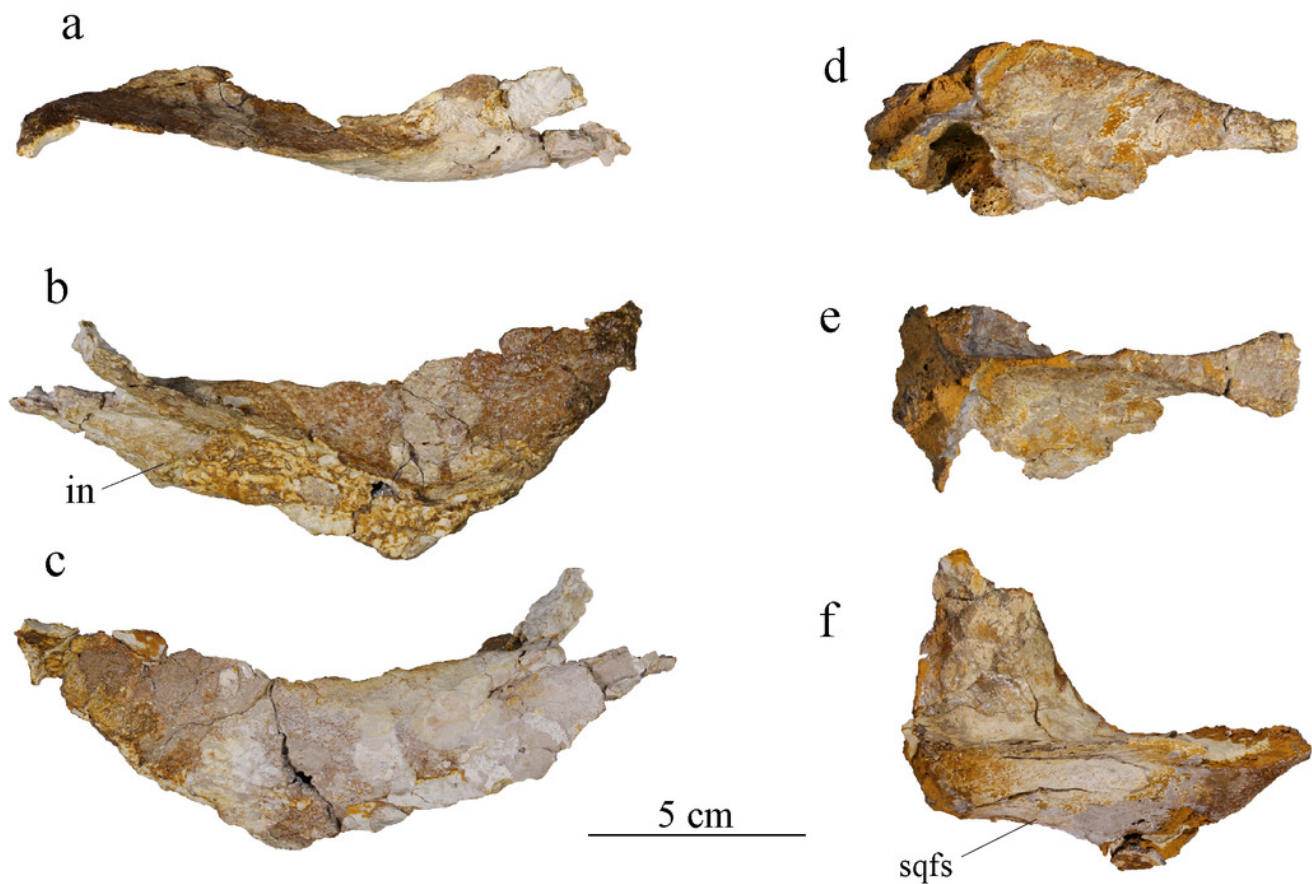
Figure 9

MJSN BSY008-465, holotype of *Torvoneustes jurensis* (Kimmeridgian, Porrentruy, Switzerland).

Photographs of the left dentary in (a) dorsal and (b) lateral views. Drawings of the left dentary in (c) dorsal and (d) lateral views. Anterior is to the left. Abbreviations: **al**, alveolus; **for**, foramen; **sdg**, surangulodentary groove; **tc**, tooth crown. Matrix is in yellow.
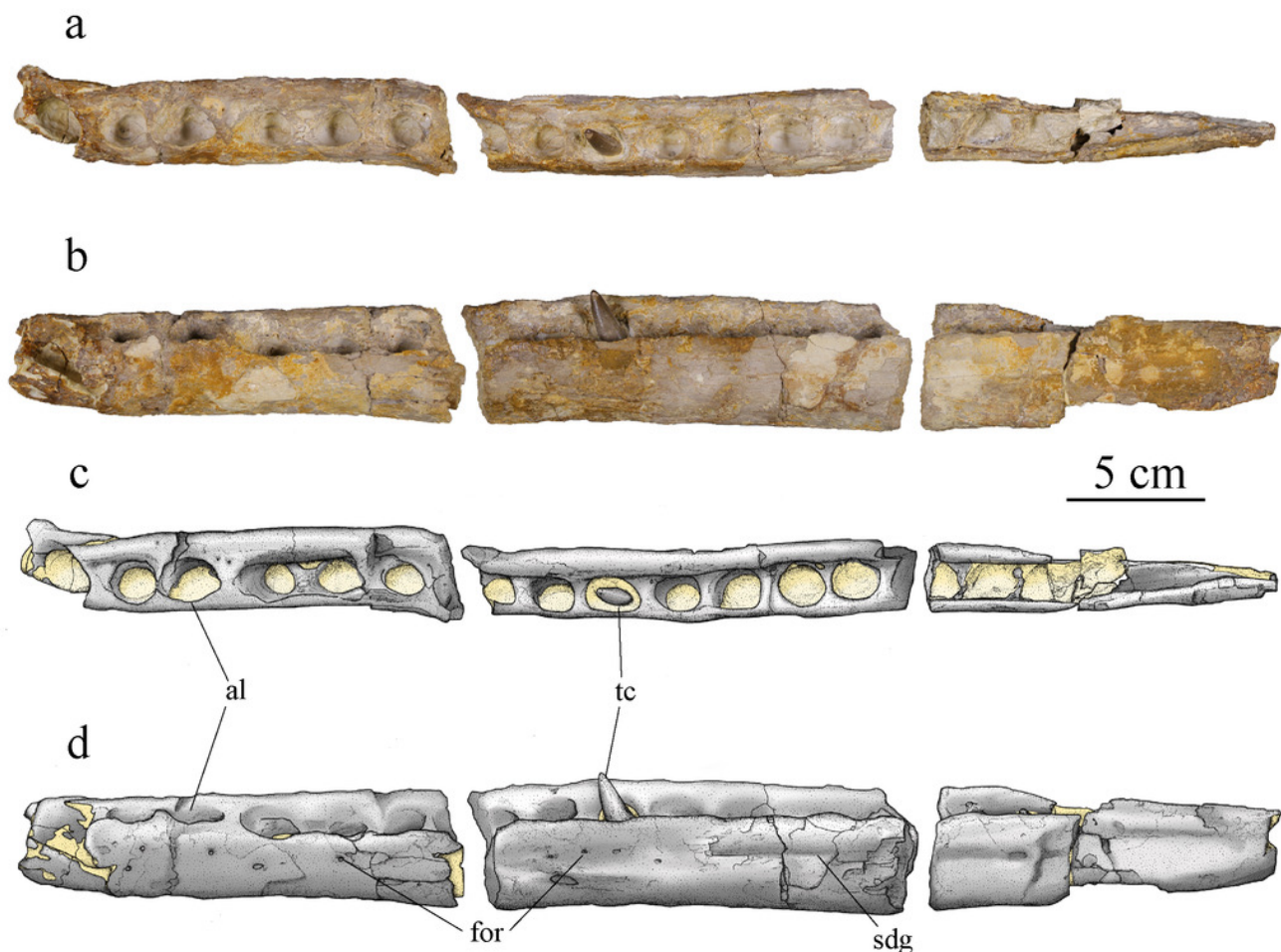
Figure 10

MJSN BSY008-465, holotype of *Torvoneustes jurensis* (Kimmeridgian, Porrentruy, Switzerland).

Photographs of the right splenial in (a) lateral, (b) medial, and (c) dorsal views. Photograph of the left splenial in (d) medial view. Abbreviations: **for**, foramen; **r**, ridge; **sym**, symphysis. Arrows point anteriorly and dashed lines show limits of the symphysis marks.

Figure 11

MJSN BSY008-465, holotype of *Torvoneustes jurensis* (Kimmeridgian, Porrentruy, Switzerland).

Photographs of the posterior part of the right ramus of the mandible in (a) medial, (b) dorsal, and (c) lateral views. Scientific drawings of the posterior part of the right ramus of the mandible in (d) medial, (e) dorsal, and (f) lateral views. Abbreviations: **an**, angular; **art**, articular; **cp**, coronoid process; **for**, foramen; **gf**, glenoid fossa; **pra**, prearticular; **ret**, retroarticular process; **san**, surangular; **sdg**, surangulodentary groove. Matrix is in yellow.
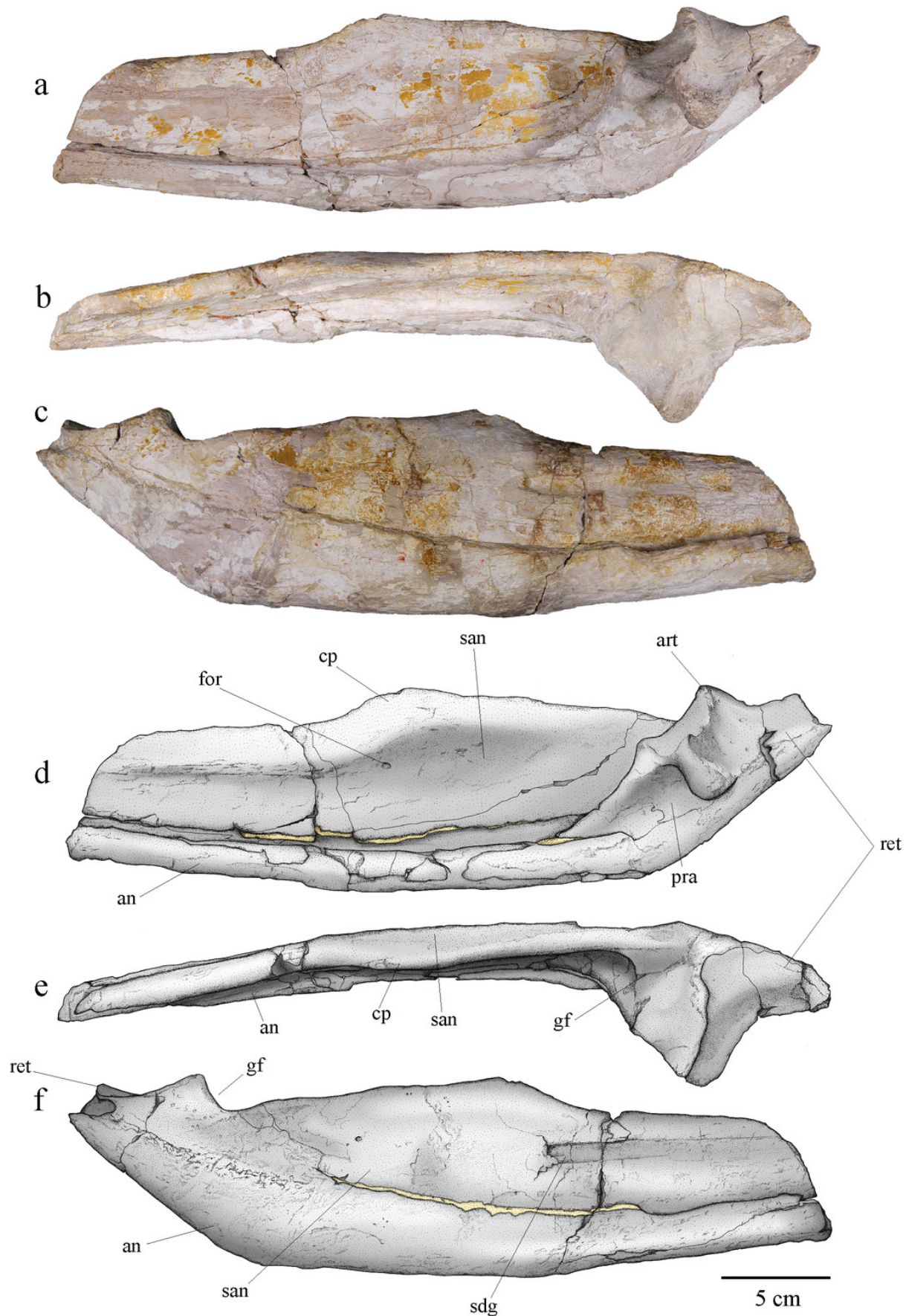
Figure 12

MJSN BSY008-465, holotype of *Torvoneustes jurensis* (Kimmeridgian, Porrentruy, Switzerland).

Two of the best-preserved isolated teeth in (a) lateral and (b) probably anterior views.

Abbreviations: **c**, crown; **ca**, carina; **r**, root.
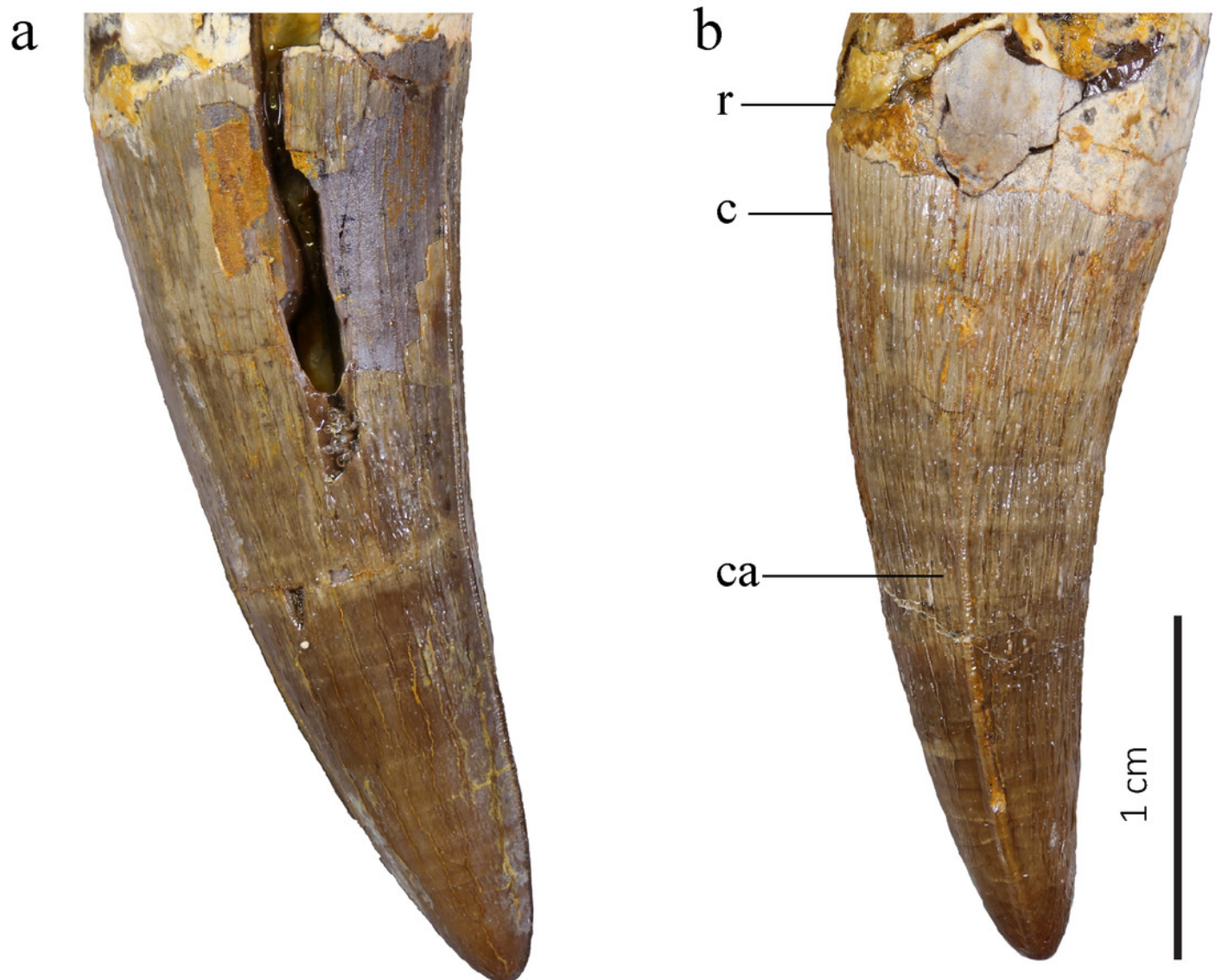
Figure 13

MJSN BSY008-465, holotype of *Torvoneustes jurensis* (Kimmeridgian, Porrentruy, Switzerland).

Microscopic photographs of MJSN BSY008-465 teeth. (a, b) mid-upper tooth crown; (c) tooth apex; (d) tooth base. **ib**, inflated base; **fd**, false denticle and **td**, true denticle.
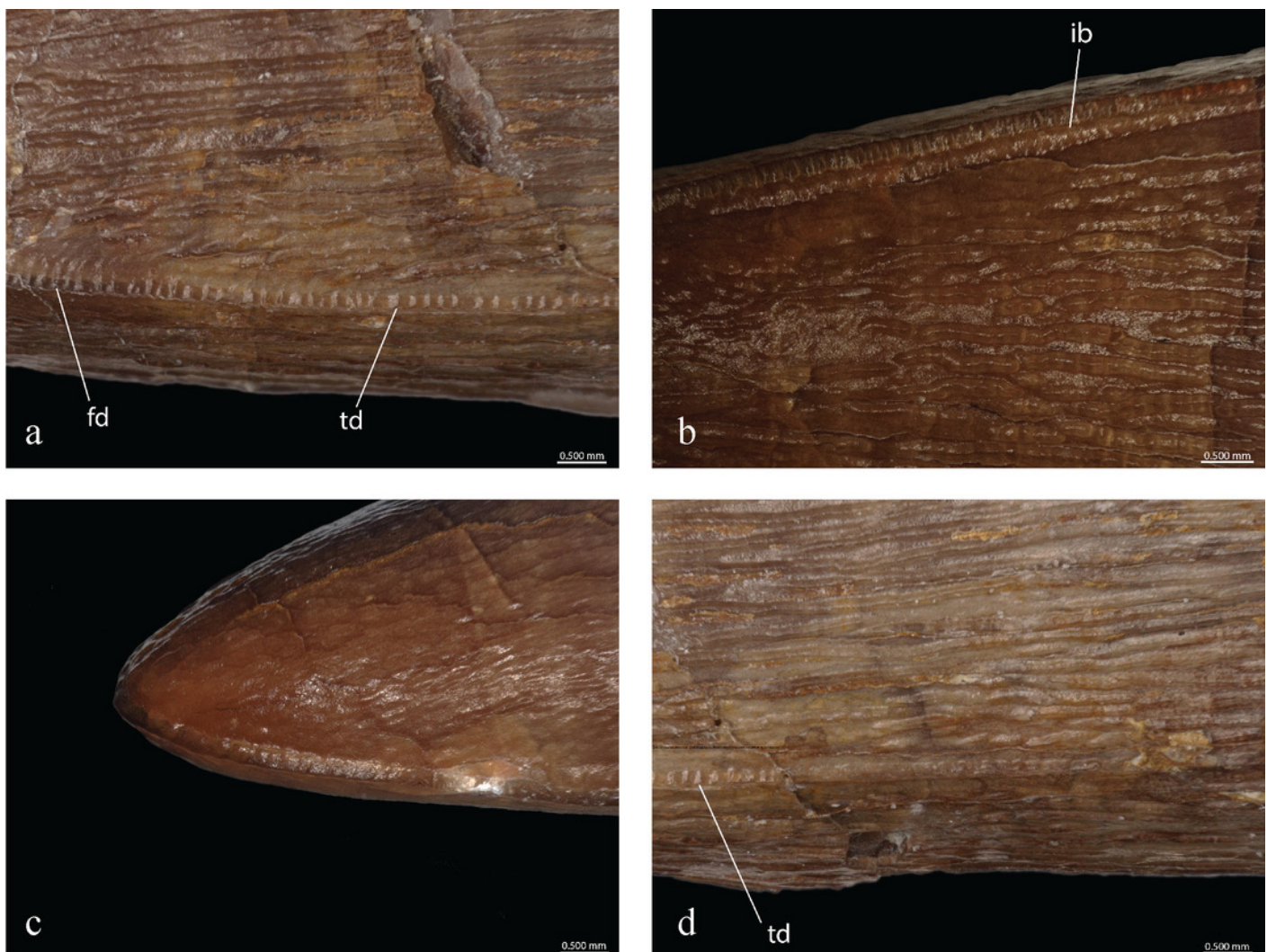
Figure 14

MJSN BSY008-465, holotype of *Torvoneustes jurensis* (Kimmeridgian, Porrentruy, Switzerland).

Cervical vertebra in (a) anterior and (b) right lateral views; dorsal vertebra in (c) anterior and (d) right lateral views; anterior caudal vertebra in (e) anterior and (f) right lateral views; Posterior caudal vertebrae in (g) anterior and (h) right lateral views. Abbreviations: **di**, diapophysis; **pa**, parapophysis; **prz**, prezygapophysis; **pz**, postzygapophysis.
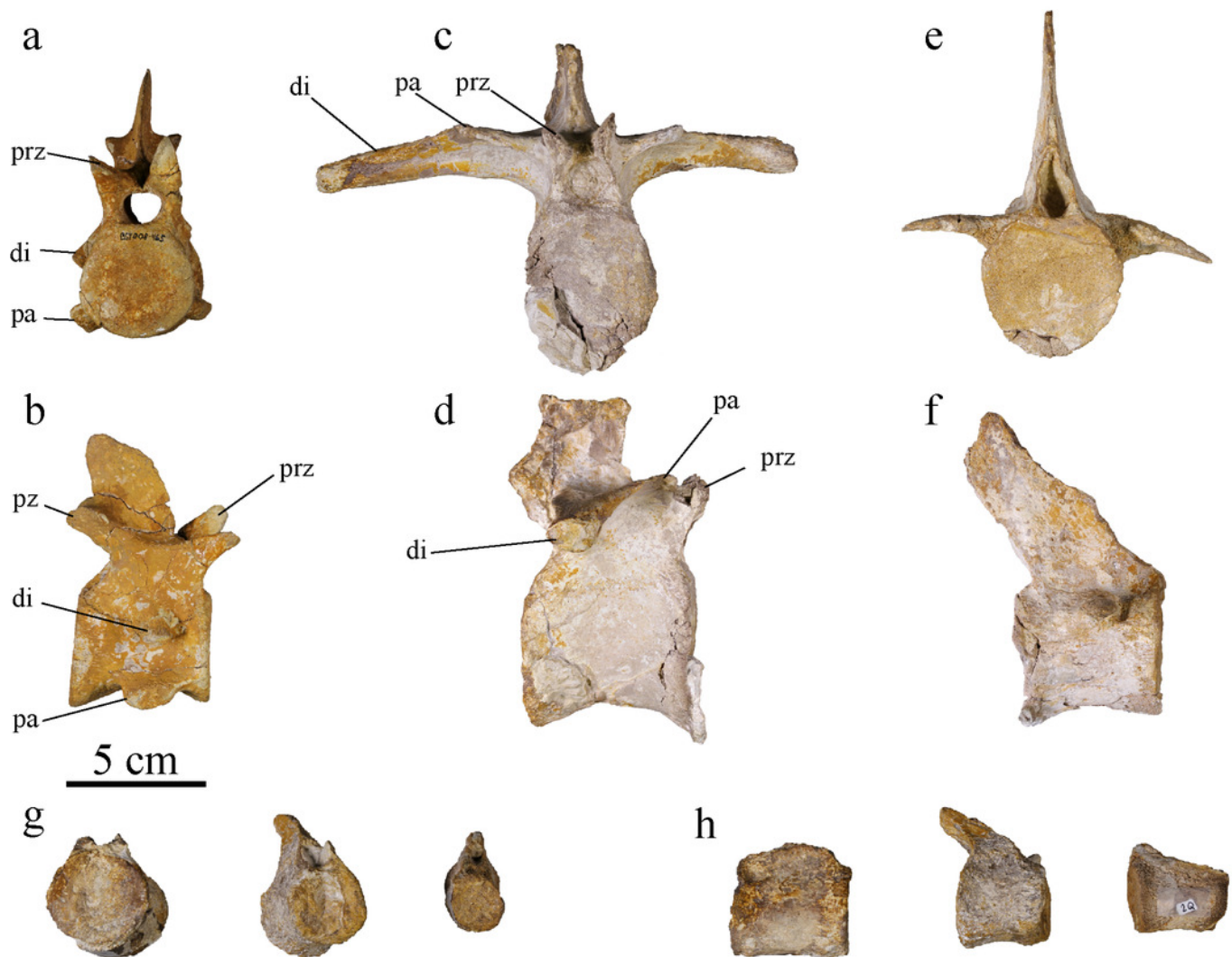
Figure 15

MJSN BSY008-465, holotype of *Torvoneustes jurensis* (Kimmeridgian, Porrentruy, Switzerland).

(a-c) cervical ribs, (d,e) dorsal ribs; chevron in (f) dorsal and (g) lateral views (anterior to the top).
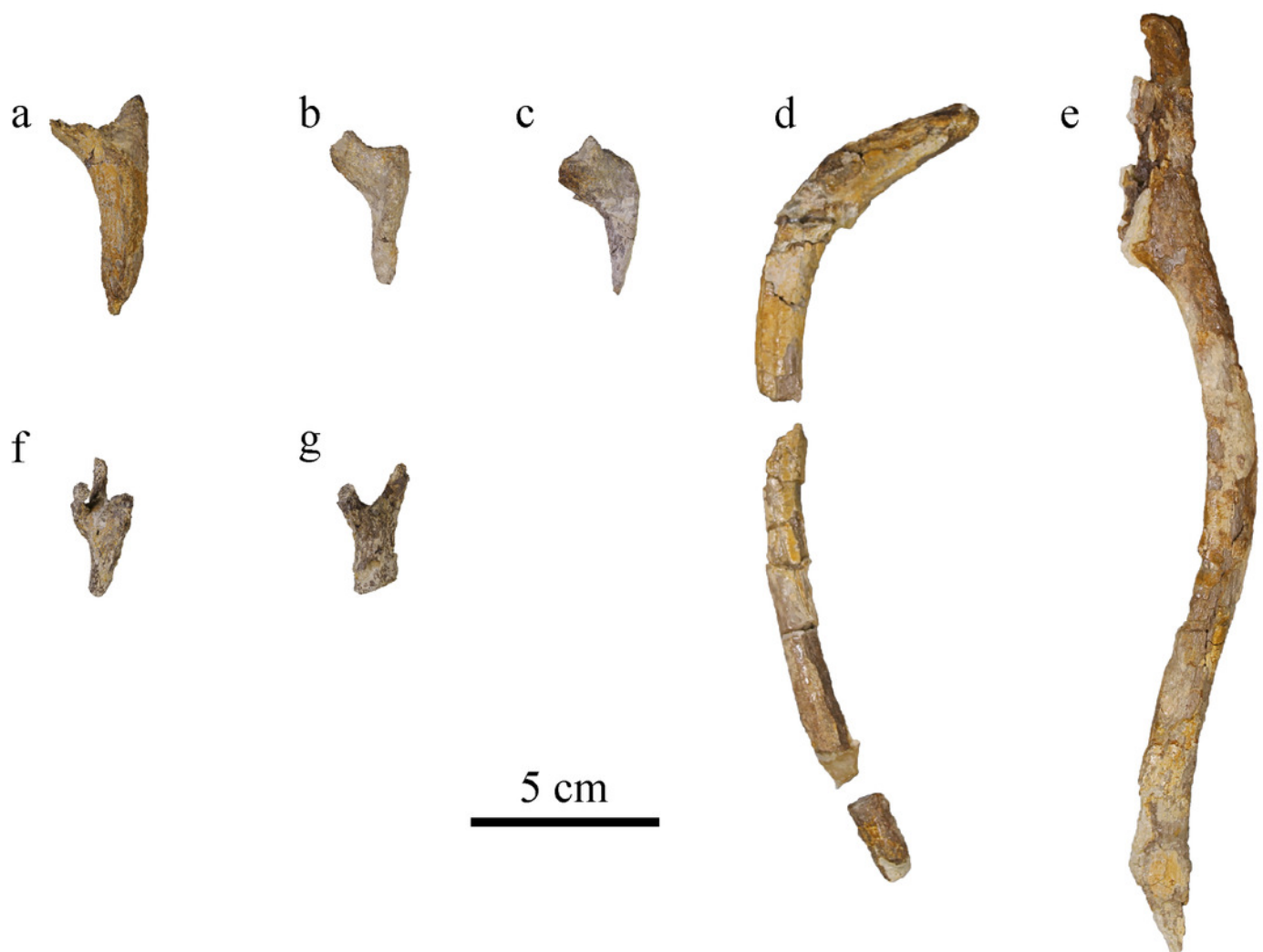
Figure 16

MJSN BSY008-465, holotype of *Torvoneustes jurensis* (Kimmeridgian, Porrentruy, Switzerland).

Right femur in (a) medial and (b) lateral views; (c) left ischium in lateral view; (d) right fibula in lateral view.
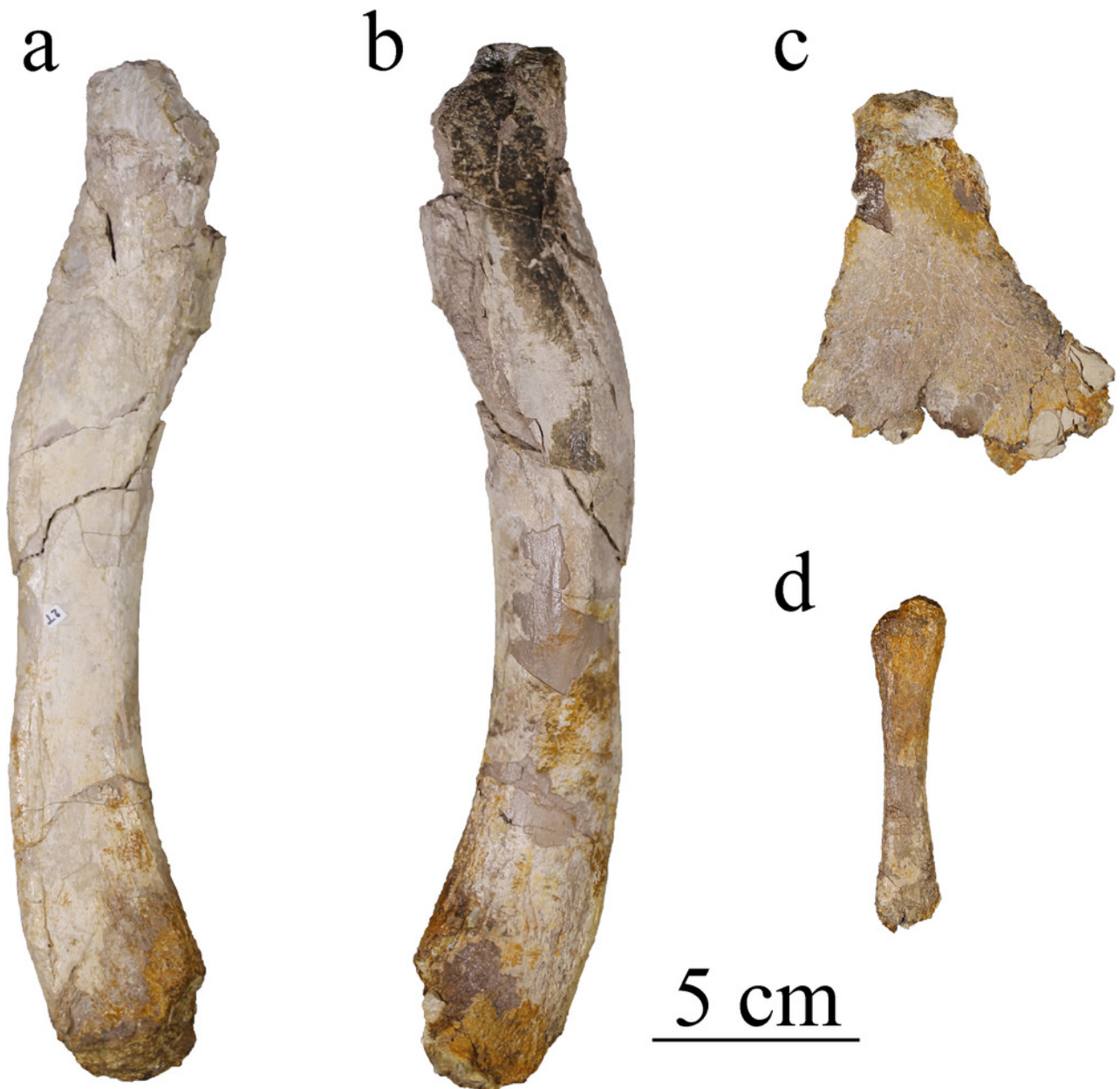
Figure 17

Phylogenetic placement of MJSN BSY008-465 (*Torvoneustes jurensis* sp. nov.) within Geosaurinae in the parsimony analyses.

(a) strict consensus topology for the unweighted analysis; (b) strict consensus topology for the strongly downweighted analyses (k = 1 and k = 3), (c) strict consensus topology for the moderately downweighted analyses (k = 7 and k = 10); (d) strict consensus topology for the moderately to weakly downweighted analyses (k = 15, k = 20 and k = 50). Numbers indicate clades: 1. Geosaurinae, 2. Geosaurini, 3. E-clade. Complete strict consensus trees are provided in Supplementary material 3.

a

b

c

d
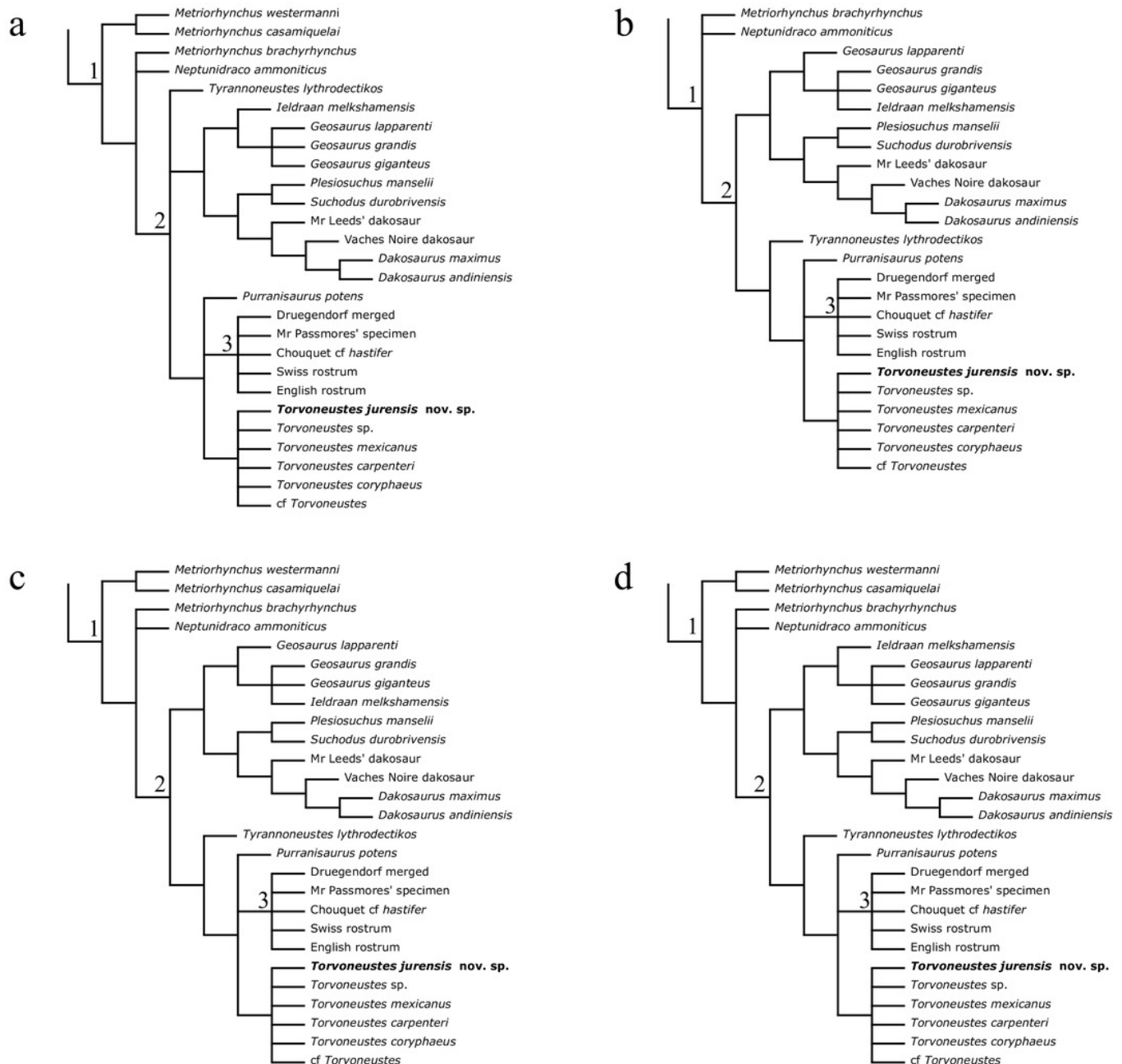
Figure 18

Phylogenetic placement of MJSN BSY008-465 (*Torvoneustes jurensis* sp. nov.) within Geosaurinae after pruning of unstable taxa.

(a) maximum agreement subtree for the unweighted analysis; (b) maximum agreement subtree for the strongly downweighted analyses (k = 1 and k = 3); (c) maximum agreement subtree for the moderately downweighted analyses (k = 7 and k = 10); (d) maximum agreement subtree for the moderately to weakly downweighted analyses (k = 15, k = 20 and k = 50). Numbers indicate clades: 1. Geosaurinae, 2. Geosaurini, 3. E- clade. Complete pruned consensus trees are provided in Supplementary material 4.
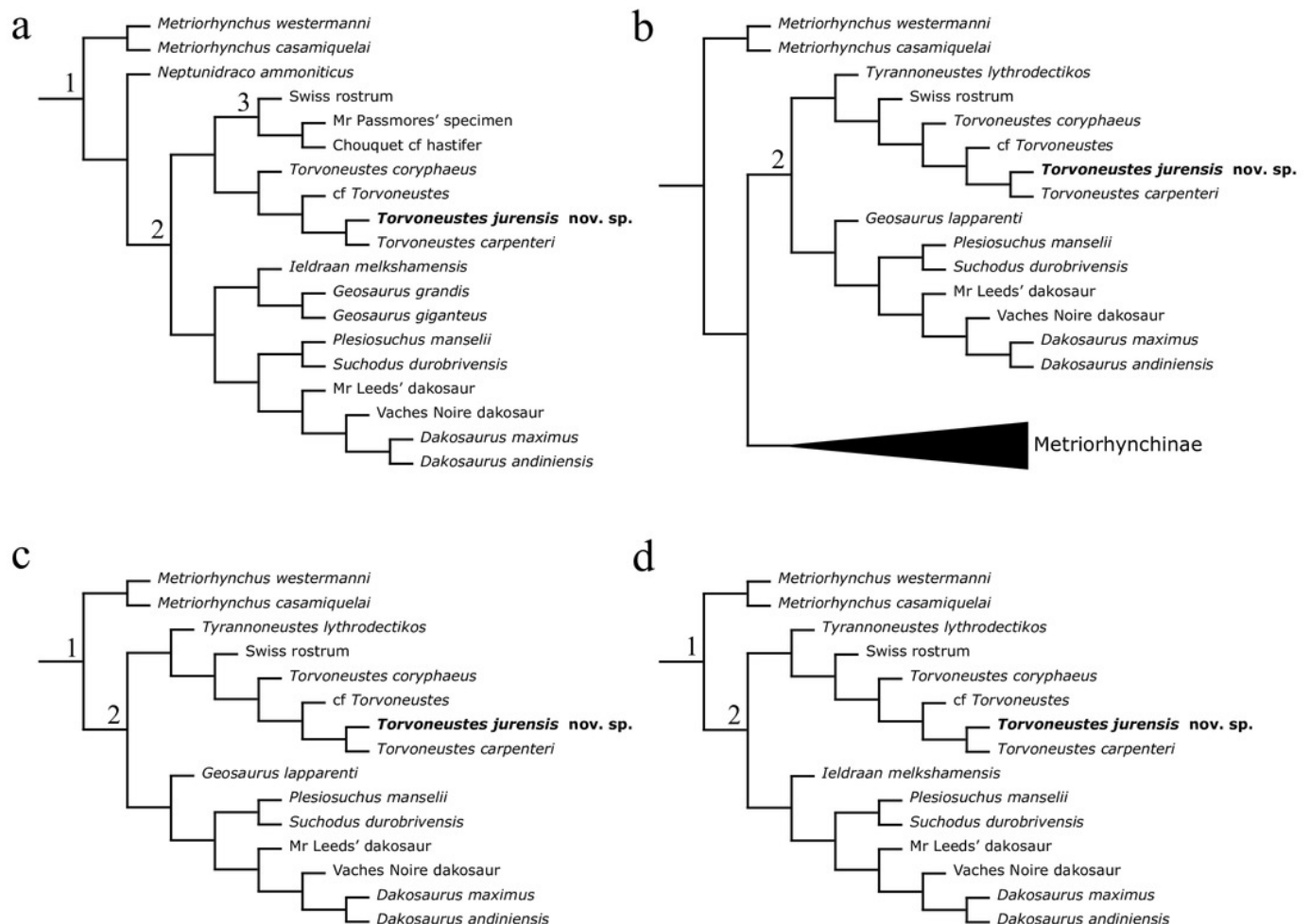
Figure 19

Phylogenetic placement of MJSN BSY008-465 (*Torvoneustes jurensis* sp. nov) within Metriorhynchidae in the Bayesian analysis.

Numbers in red represent node support values. Numbers on the tree branches indicate clades: 1. Metriorhynchidae, 2. Geosaurinae and 3. Geosaurini. Complete tree is provided in Supplementary material 5.
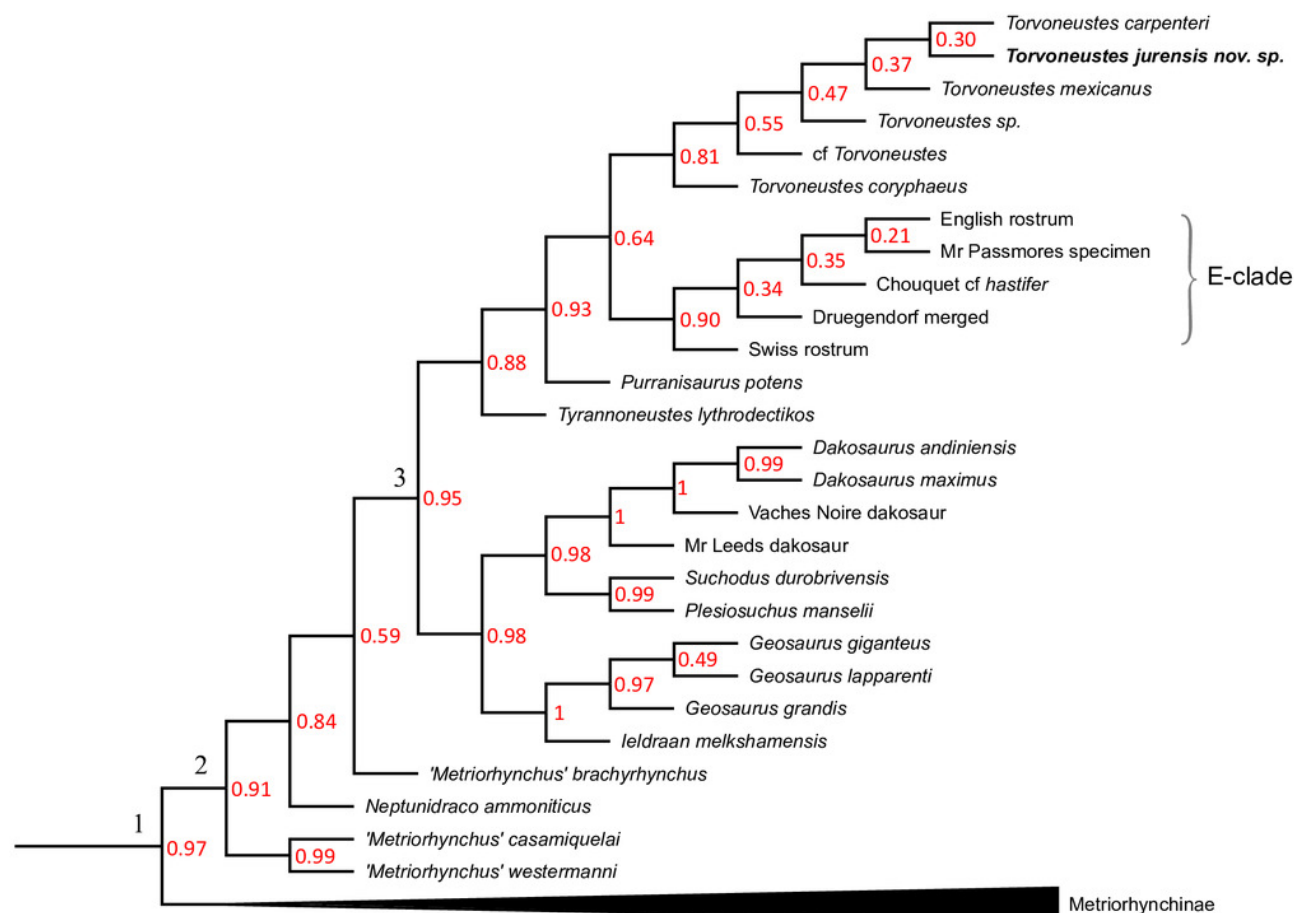
Figure 20

Life reconstruction of Torvoneustes jurensis MJSN BSY008-465 in the Kimmeridgian environnement of Jura.

Artwork by SDSO.
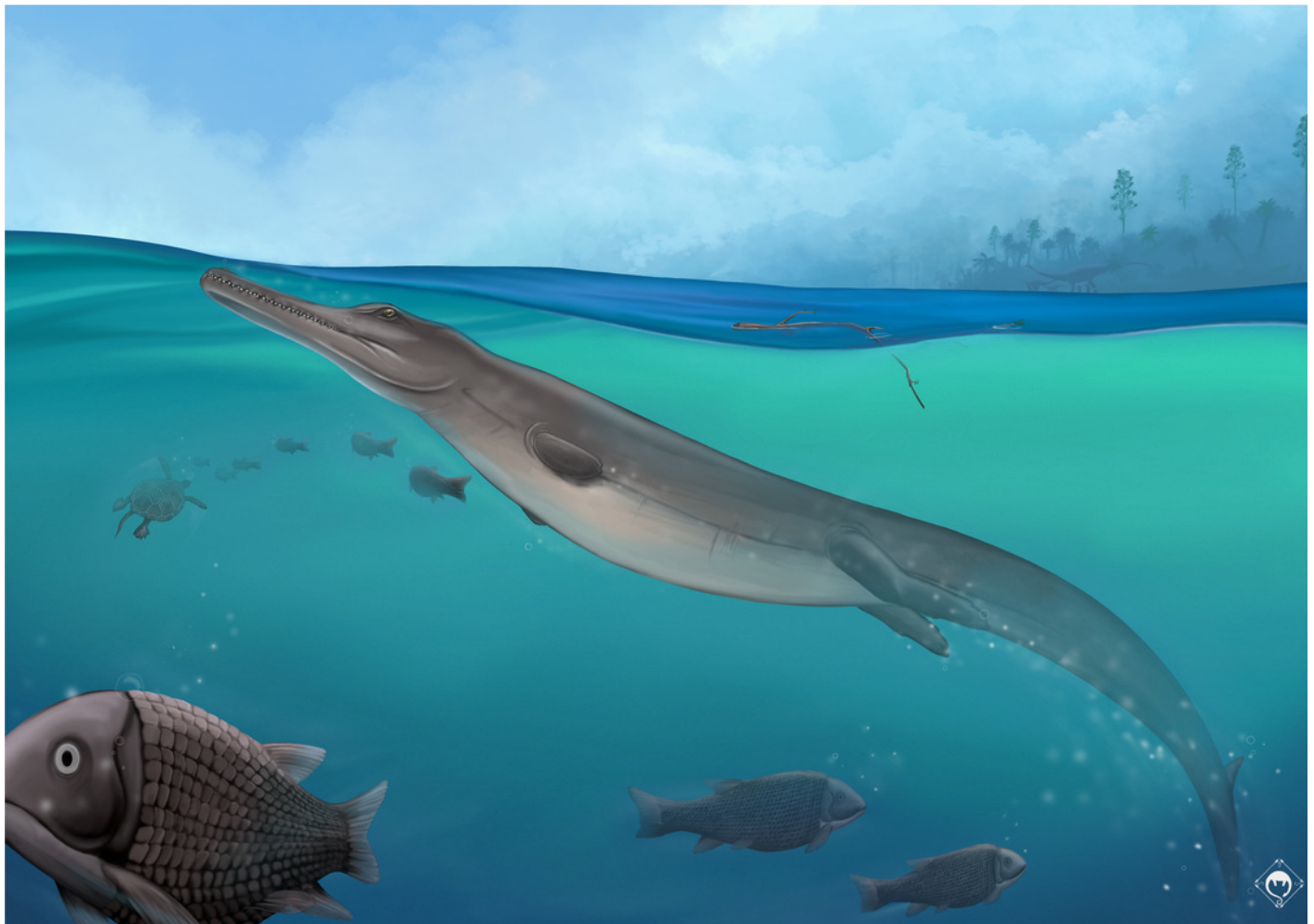
Overview of the Kimmeridgian-Lower Tithonian metriorhynchids species and a few of their dental characteristics.

Gracilineustes acutus is excluded from the table due to the lack of information, the specimen was lost during WW2. The same goes for *Rhacheosaurus gracilis* NHMUK PV R 3948 for whom the teeth or alveoli are indistinguishable, while *Rhacheosaurus* cf *gracilis* LF 2426 skull is not entirely preserved. Therein the distinction between "true ziphodont" and "false ziphodont" condition as defined by Young *et al.*, 2010 is not specified. The estimated tooth count is from the referred articles; the denticle density for *D. maximus* and *Geo. grandis* from Andrade *et al.*, 2010 and for *To. mexicanus* from Barrientos-Lara *et al.*, 2016.

		Species	Age	Country	Teeth ornamentation	Carinae	Denticules	Ziphodonty	Denticules density (number of denticle/5mm)	Maxillary tooth count (absolute)	Maxillary tooth count (estimated)	Dentary tooth count (absolute)	Dentary tooth count (estimated)	Specimen description
		Cricosaurus suevicus (Fraas, 1901, 1902, SMNS 9808)	Upper Kimmeridgian	Germany	Smooth	Yes, faint	No	/	/	26		24		Complete specimen in limestone
		Cricosaurus albersdoerferi (Sachs *et al.*, 2021, BMMS-BK 1-2)	Upper Kimmeridgian	Germany	Smooth	Yes, faint	No	/	/	23	23+	22	22+	Complete specimen in limestone
		Cricosaurus elegans (Wagner, 1852, BSPG AS I 504)	Lower Tithonian	Germany	Smooth	Yes, faint	No							Skull in limestone
		Cricosaurus bambergensis (Sachs *et al.*, 2019, NKMB-P-Watt14/274)	Upper Kimmeridgian	Germany	Smooth	Yes, faint	No	/	/	23	23+	18+	18+	Complete specimen in limestone
		Cricosaurus rauhuti (Herrera *et al.*, 2021, SNSB-BSPG 1973 I 195)	Lower Tithonian	Germany	Well-spaced, low longitudinal ridges	Yes, at least unicarenate	No	/	/	/	/	/	/	Incomplete skull
		Maledictosuchus nuyiviianan (Barrientos-Lara *et al.*, 2018, IGM 4863)	Kimmeridgian	Mexico	Smooth labial side. discontinuous low apicobasal ridges on the lingual surface	Yes	No	/	/	17	26?	/	/	Incomplete skull
Metriorhynchinae	Rhacheosaurini	*Cricosaurus' saltillensis* (Buchy *et al.*, 2013, MUDE CPC 487)	Lower Tithonian	Mexico	faint apicobasally aligned subparallel ridges	Yes, faint	No	/	/	12	17	15	~15?	Disarticulated skull
		Metriorhynchus palpebrosus (Phillips, 1871, Grange & Benton, 1996,	Lower Tithonian	United Kingdom	?	?	?	?	?	25 (OUMNH J.29823)-27	/	14	14+	Skull. No teeth remaining

		(OUMNH J.29823)												
		Me. Geoffroyii (Me. Brevirostris) (Young *et al.*, 2020; MHNG V-2232)	Lower Kimmeridgian	France	?	?	?	?	?	14	20+? (half of the rostrum is easily missing)	/	/	Anterior half of the rostrum, no teeth remaining
		Metriorhynchus' cf *hastifer* (Chouquet cf '*hastifer*',Lepage *et al.,* 2008, Eudes-Deslongchamps, 1867)	Kimmeridgian	France	Conspicuous apicobasal ridges	Yes	?	?		20?	20+?	/	/	complete skull
		Dakosaurus maximus (Young *et al.*, 2012, SMNS 8203)	Upper Kimmeridgian	Germany	Overall smooth	Yes, prominent	Yes	Macro	16-18	13		12		Incomplete skull
		Plesiosuchus manselii (Young *et al*., 2012, NHMUK PV OR40103)	Upper Kimmeridgian	United Kingdom	Low relief apicobasal ridges	Yes, prominent	Yes	Micro	?	14	14 to 18	13		Incomplete skull
		Geosaurus giganteus (Young & Andrade, 2009, NHM R.1229, NHM 37020)	Lower Tithonian	Germany	Overall smooth	Yes, prominent	Yes	Micro	?	12 (NHM 37020)	12+	7 (NHM 37020)	7+	NHM R.1229 : middle portion of the skull and mandible, deformed. NHM 37020 : skull and mandible in limestone.
		Geosaurus grandis (Young et al., 2012, BSPG AS-VI-1)	Lower Tithonian	Germany	Smooth	Yes, prominent	Yes	Micro	28,1	14				
Geosaurinae	Geosaurini	*Torvoneustes carpenteri* (Grange & Benton, 1996, BRSMG Ce17365)	Upper Kimmeridgian	United Kingdom	Conspicuous apicobasal ridges	Yes, prominent	Yes	Micro	?	11	14	/	/	Heavily crushed , incomplete skull

		Torvoneustes coryphaeus (Young *et al.*, 2013, MJML K1863)	Lower Kimmeridgian	United Kingdom	Conspicuous apicobasal ridges	Yes, prominent	Yes	Micro	?	11	17-19	/	/	Incomplete skull, half of the rostrum missing
		Torvoneustes mexicanus (Barrientos-Lara *et al.*, 2016, IGM 9026)	Kimmeridgian	Mexico	Conspicuous apicobasal ridges	Yes, prominent	Yes	Micro	30	5		4		Fragmentary rostrum
		MJSN BSY008-465	Upper Kimmeridgian	Switzerland	Conspicuous apicobasal ridges	Yes, prominent	Yes	Micro	30-40	15	Up to 21	16	Up to 17	Disarticulated skull

Descriptive statistics of the cladograms resulting from the parsimony analysis.

In the unweighted analysis, the number of Most Parsimonious Cladograms is higher than the storage capacity (20 000).

K	Number of MPCs	Length	CI	RI	RC	HI
-		2417	0,334	0,803	0,268	0,666
1	297	2072	0,389	0,845	0,329	0,611
3	297	2065	0,391	0,846	0,331	0,609
7	99	2044	0,395	0,848	0,335	0,605
10	99	2044	0,395	0,848	0,335	0,605
15	33	2034	0,397	0,85	0,337	0,603
20	33	2033	0,397	0,85	0,337	0,603
50	33	2033	0,397	0,85	0,337	0,603

Comparison of cranial features within the genus *Torvoneustes.*

Comparison of cranial features within the genus *Torvoneustes*. Comparative table of currently named species of *Torvoneustes* and their diagnostic cranial features identified in To. jurensis. False serration definition and denticle density methodology follow Andrade *et al.*, 2010 (see description for more details). BS: Base length.

	Skull ornamentation	Frontal	Distinct angle at the frontal-prefrontal-nasal contact	Tooth count per maxilla (estimated)	Teeth morphology	False serration	Denticles size	Denticles density (#denticules/5mm)
Torvoneustes carpenteri (Grange & Benton, 1996; Wilkinson *et al.*, 2008)	Smooth with ornamentation on the maxillae	Does not reach the anterior end of the prefrontal	No	14	Robust, blunt apex	Yes	Irregular in size. BS: 120-220 μm	-
Torvoneustes coryphaeus (Young *et al.*, 2013b)	Ornamented	Reach the anterior end of the prefrontal	No	17-19	Robust, blunt apex	No	-	-
Torvoneustes mexicanus (Barrientos-Lara et al., 2016)	-	-	-	-	Slender, sharp apex	Yes	Regular in size. BS: 142 μm	30
Torvoneustes jurensis sp. nov.	Smooth	Reach the anterior end of the prefrontal	Yes	Up to 18	Slender, sharp apex	Yes	Irregular in size. BS: 120-200 μm	30-40